# A Mechanistic Understanding of Vagus Nerve Stimulation Therapy: Investigating the Effects of Parasympathetic Modulation on Cardiac Dynamics

A Dissertation
SUBMITTED TO THE FACULTY OF
UNIVERSITY OF MINNESOTA
BY

Steven Wallace Lee

IN PARTIAL FULFILLMENT OF THE REQUIREMENTS
FOR THE DEGREE OF
DOCTOR OF PHILOSOPHY

Advisor: Dr. Alena Talkachova

March 2018

# ACKNOWLEDGEMENTS

First and foremost, I would like to thank my PhD advisor, Dr. Alena Talkachova. She gave me freedom to explore my own ideas and encouraged me to be creative. At the same time, she was available for long discussions which have inevitably helped me improve my analytical and scientific skills. I am also extremely grateful for having Dr. Matthew Johnson, Dr. John Osborn, and Dr. Bruce KenKnight as members of my dissertation committee. In addition to their willingness to read through this dissertation, I extremely appreciate their feedbacks, insights, and lending their areas of expertise towards my project. In particular, I thank Dr. KenKnight and Dr. Osborn for their involvement in my early PhD training and in mutual research projects. And I thank Dr. Johnson for agreeing to serve as Chair of this committee and the many 'impromptu' discussions we have had at Nils Hasselmo which have challenged me to think critically. Hence, this dissertation is a product of my encounters and conversations with all four committee members.

Second, I would like to thank the National Heart, Lung, and Blood Institute of the NIH for providing a three year pre-doctoral fellowship to support my PhD studies. And although I had to decline their two year pre-doctoral fellowship, I also appreciate the American Heart Association for their confidence in my project and offered to fund my studies.

Third, I have to thank my wonderful lab mates: the 'Talkachovians'. Previous lab members which included Dr. Ramjay Viswewaran, Dr. Xueyi (Thomas) Xie, Joseph Ippolito, Virendra Kakade, Dr. Ning Wei, and Dr. Stephen McyIntire for being great

mentors during the early stages of my PhD. In particular, Thomas for being such a great friend, collaborator, and confidant. Furthermore, I like to thank members who joined around the same I did: Shivaram Pogai Arunachalam, Elizabeth Annoni, Christopher Johnson, and Kanchan Kulkarni. It is because of each and every one of you that many times I was able to find the 'inner strength' to continue and persevere with my experiments. Especially Kanchan Kulkarni for being the best possible "partner-in-crime:" our work dynamic has been so intellectually stimulating and productive, and I am grateful to have you both as a colleague and personal friend. To the newest members, Vasanth Ravikumar and Preethy Parthiban, seeing that both of you are so focused and diligent has been highly motivating and inspiring and I wish you all the best in your future endeavors. I would also like to thank my collaborators over the years: Dr. Mary G. Garry and Dr. Qinglu Li for their discussion and support with both the chronic VNS + ventricular project and inflammatory project; Dr. Kevin Wickman and Allison Anderson for not only supplying their transgenic mice but being available for fruitful discussions; and Pilar Ariza-Guzman for being such a great friend, and if it were not for your patience, dedication, and surgical expertise, I would not have been able to complete the VNS and $M_2R$-$I_{KACh}$ project on-time and obtain such high-quality recordings.

Finally, I thank all of my other colleagues and friends at the University of Minnesota for making my PhD experience enjoyable and fulfilling. A special thanks to Anh La, Ghaidan Shamsan, Allison Siehr, Supriya Thathachary, Edgar Peña, Lazarina (Inka) Gyoneva, Kevin Mohsenian, Kianna Elahi-Gedwillo, Rachel Edwards, and Rohit

Dhume for always being there for emotional support and it is always fun to spend time with you all outside our lab benches.

# DEDICATION

I dedicate this PhD dissertation to both my parents, Kin and Fong, and sister, Vivian. All of you have supported me throughout my life, always believed in my abilities, and encouraged me to always persevere even when the times get tough. All of you have given me the drive needed to complete this dissertation.

# ABSTRACT

Vagus nerve stimulation (VNS) is a neuromodulatory approach that involves delivering electrical impulses to the vagus nerve to modulate the autonomic nervous system. In addition to being FDA-approved for use in epilepsy and depression, a plethora of both experimental and clinical studies also supports the potential of VNS to treat cardiovascular diseases. While promising, the precise mechanism by which this therapy exerts its cardioprotective effects are not well-established.

The central dogma states that vagus nerves primarily innervate the atria with very minimal to no innervation into the ventricles. Based on this concept, parasympathetic system activation by VNS should not significantly affect ventricular properties. This is not the case, however, as VNS has been extensively shown to exert marked anti-arrhythmic effects in the ventricles. Furthermore, this supposition that there is minimal vagal innervation into the ventricular myocardium has been challenged by a series of immunohistochemical, histological, and western blot experiments. The first aim of my dissertation was to investigate the potential for a direct effect of long-term VNS on ventricular electrophysiology and test the hypothesis that VNS induces electrical remodeling of the ventricles to render the therapy's reported anti-arrhythmic effects. Secondly, I then examined the direct contributions of the $M_2$ muscarinic receptor activated potassium channel ($M_2R$-$I_{KACh}$) in mediating the chronotropic effects of VNS. For this second aim, I applied VNS on several transgenic mice that lack the $I_{KACh}$ channel constitutively, and selectively in the atria or the ventricles. Thirdly, there still does not exist a universally accepted published prospective VNS paradigm, which further highlights the

complexity of parameter optimization. This work introduced an innovative concept of incorporating stochasticity when stimulating the vagus nerve (stochastic VNS, S-VNS) and I evaluated the effects of S-VNS on acute heart rate (HR) dynamics in comparison to traditional, periodic VNS. Collectively, the work performed in this thesis contribute to the mechanistic understanding of VNS therapy, in particular to the fundamental role of the parasympathetic nervous system in ventricular electrophysiology, and facilitate the optimization and improvement of VNS efficacy.

# TABLE OF CONTENTS

# LIST OF FIGURES

# LIST OF ABBREVIATIONS

| | |
|---|---|
| 2D | Two dimensional |
| μ | Action potential duration heterogeneity |
| $\Delta HR_{ON}$ | Relative change in heart Rate |
| ACh | Acetylcholine |
| AChE | Acetylcholinesterase |
| AF | Atrial fibrillation |
| APD | Action potential duration |
| $APD^{5\%}$ | $5^{th}$ Percentile of the APD distribution |
| $APD^{50\%}$ | $50^{th}$ Percentile of the APD distribution |
| $APD^{95\%}$ | $95^{th}$ Percentile of the APD distribution |
| $APD_{50}$ | Action potential duration at 50% repolarization |
| $APD_{80}$ | Action potential duration at 80% repolarization |
| ANTHEM-HF | Autonomic Neural Regulation Therapy to Enhance Myocardial Function in Heart Failure |
| AV | Atrioventricular |
| BCL | Basic cycle length |
| $Ca^{2+}$ | Calcium |
| cAMP | Cyclic adenosine monophosphate |
| CCD | Charge-coupled device |
| CCh | Carbachol |
| CHAT | Choline acetyltransferase |
| CNS | Central nervous system |
| CV | Conduction velocity |
| Cx-43 | Connexin-43 |
| DMN | Dorsal motor nucleus |
| ECG | Electrocardiogram |
| EF | Ejection fraction |

| | |
|---|---|
| ENCORE | Extension Study of Neural Regulation therapy on Myocardial Function in Heart Failure |
| eNOS | Endothelial nitric oxide synthase |
| FDA | Food Drug and Administration |
| FREQ | Frequency |
| GIRK | G protein-coupled inwardly-rectifying potassium channels |
| HF | Heart failure |
| HR | Heart rate |
| $HR_{ON}$ | Mean heart rate during **ON** period of vagus nerve stimulation |
| $HR_{POST}$ | Mean heart rate during **POST** period of vagus nerve stimulation |
| $HR_{PRE}$ | Mean heart rate during **PRE** period of vagus nerve stimulation |
| HTN | Hypertension |
| HRV | Heart rate variability |
| $I_{KACh}$ | Acetylcholine-activated inward-rectifying potassium channel |
| iNOS | Inducible nitric oxide synthase |
| I/R | Ischemia-reperfusion |
| INOVATE-HF | Increase of Vagal Tone in Chronic Heart Failure |
| LAD | Left anterior descending coronary artery |
| LV | Left ventricle |
| LVEDV | Left ventricular end diastolic volume |
| LVESV | Left ventricular end systolic volume |
| $M_2R$ | $M_2$ muscarinic receptor |
| MI | Myocardial infarction |
| MLC2v | Ventricular isoform of the myosin light chain 2 |
| NCX1 | Sodium calcium exchanger |
| NE | Norepinephrine |
| NECTAR-HF | Neural Cardiac Therapy for Heart Failure Study |
| nNOS | Neuronal nitric oxide synthase |
| NTS | Nucleus tractus solitarius |
| OCT | Optical coherence tomography |

| | |
|---|---|
| PAC | Premature Atrial Complex |
| PRC | Phase response curves |
| P-VNS | Periodic vagus nerve stimulation |
| RA | Right atrium |
| RyR2 | Ryanodine receptor 2 |
| SA | Sinoatrial |
| SERCA | Sarcoplasmic reticulum $Ca^{2+}$ ATPase |
| SGX | Bilateral stellate ganglionectomy |
| SLN | Sarcolipin |
| STOCH | Stochasticity |
| S-VNS | Stochastic vagus nerve stimulation |
| TTC | Tetrazolium chloride |
| RV | Right ventricle |
| VF | Ventricular fibrillation |
| VNI | Vagus nerve isolation |
| VNS | Vagus nerve stimulation |
| VT | Ventricular tachycardia |

# CHAPTER 1 INTRODUCTION

## 1.1 Neuromodulation Therapy: An Emerging Field

Neuromodulation is one of the most rapidly growing fields in medicine today that encompasses a wide range of implantable or noninvasive interventional approaches to treat neurological and other nervous system disorders. This therapy involves altering the central or peripheral nervous systems, either electrically or chemically, to inhibit, excite, and/or modify the neural activity to achieve therapeutic outcomes (Krames et al., 2009).

To date, a plethora of neuromodulation techniques have been utilized to treat movement disorders, epilepsy, psychiatric disorders, chronic pain, addiction, and others (Krames et al., 2009). Some examples of these therapies include but not limited to deep brain stimulation, transcranial direct current stimulation, spinal cord stimulation, and vagus nerve stimulation (VNS). For my thesis research, I used VNS and investigated the therapy's effects on the dynamics of the heart using animal models.

## 1.2 General Physiology of the Heart

The heart is a muscle that facilitates blood flow through the vascular system to supply nutrients throughout the body and to re-oxygenate blood via pulmonary circulation. The heart consists of four chambers as shown in **Fig. 1.1**. The left and right atria are the two chambers that receive blood while the left and right ventricles pump blood out of the heart. The left side of the heart is responsible for distributing oxygenated blood throughout the body; whereas, the right side receives the deoxygenated blood from the body and pump it to the lungs in order for the lungs to get re-oxygenated.

.

### 1.2.1 The Electrical Conduction System of the Heart

In order for the heart to function properly, it needs to contract and relax in a coordinated fashion. The mechanical contractions of the heart are triggered by electrical waves of excitation propagating through the cardiac tissue. In healthy hearts, the electrical impulses originate in the heart's own natural pacemaker, the sinoatrial (SA) node in the right atrium. From the SA node, the electrical impulse excites the atria and causes it to contract. Then, after a short delay to allow enough time for the ventricles to fill up, the electrical wave travels through the atrioventricular (AV) node, which serves as the electrical connection between the atria and the ventricles, to the Purkinje fibers via the Bundle of His. Finally, the Purkinje fibers will carry the electrical wave to the ventricles causing them to contract. A representation of the anatomy of the electrical conduction system in the heart is shown in **Fig. 1.2**.

The contraction of the heart is a phenomenon that is brought about by a well-timed summation of single cardiomyocyte contractions. The contraction of each myocyte is triggered by the electrical wave of excitation that originates from the SA node. Each time a myocyte is triggered, the properties of transmembrane ion channels (e.g. sodium, potassium, calcium…) change and a complex movement of ions in and out of the cell takes place, thereby causing a cyclic change in the membrane potential. This sequence of changes in the membrane potential is known as the action potential. The action potential of one myocyte will act as the stimulus to surrounding cells though gap junctions and diffusion, thus, eliciting an action potential in downstream cells in the conduction system. This process is repeated until the electrical signal propagates through the entire heart causing

the whole heart to contract. **Fig. 1.2** also shows the shape of the action potential of the SA node and cardiomyocytes, and are represented along with respective resting potentials and different phases.

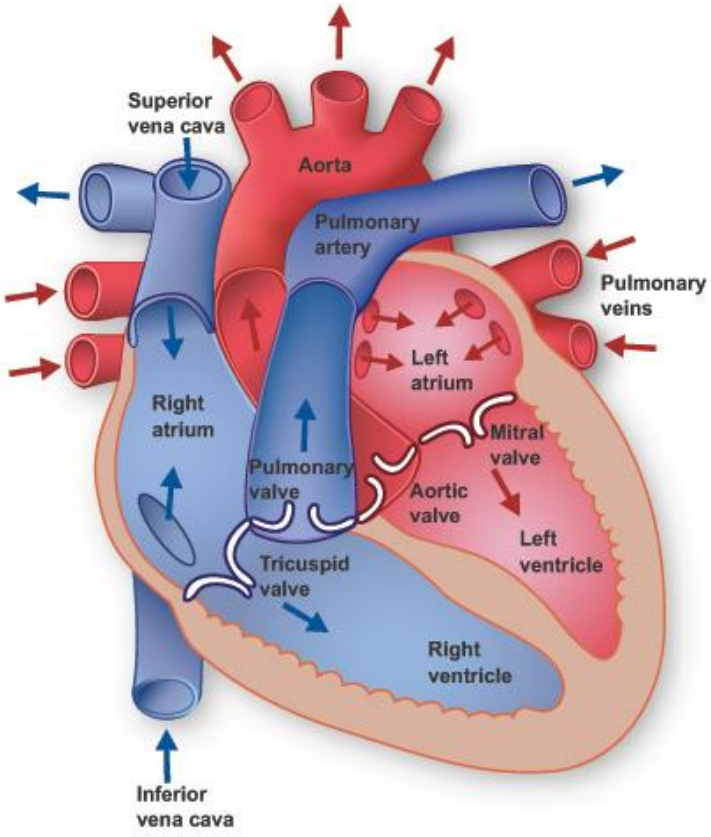


***Figure 1.1: Schematic illustration of the heart.*** From (Texas Heart Institute, 2016) .

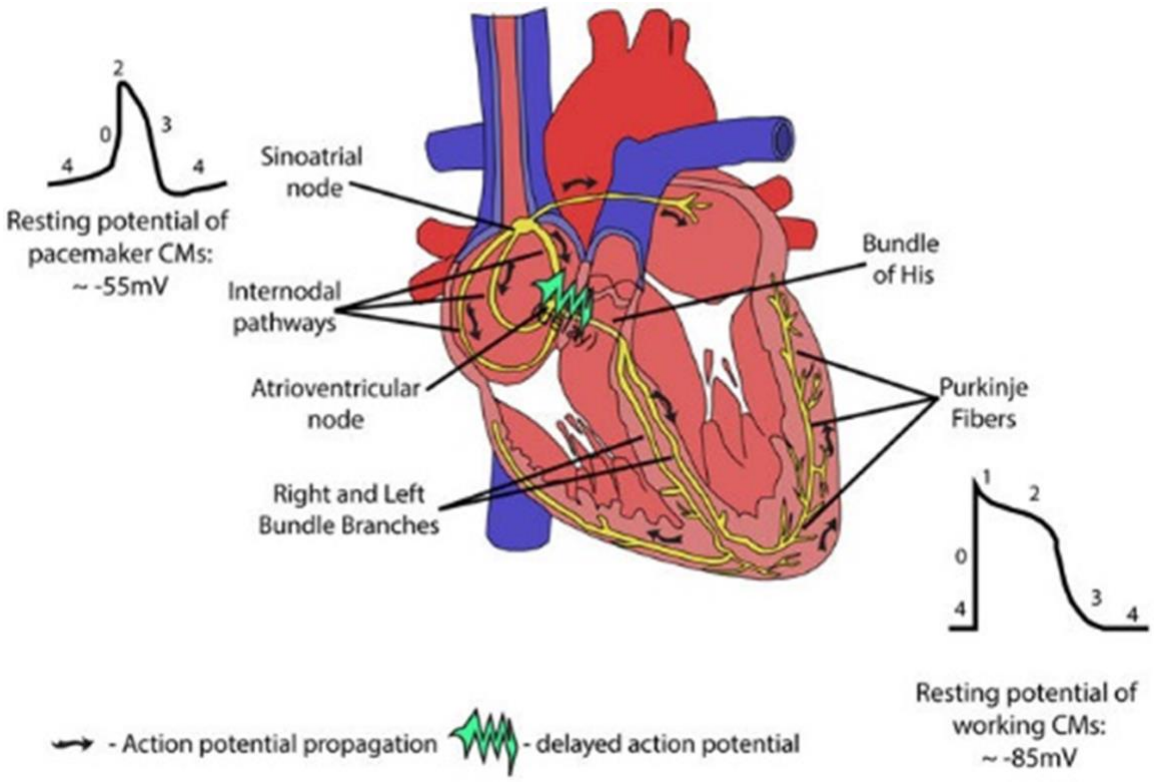


***Figure 1.2: Schematic diagram of the electrical conduction system.*** Here summarizes the electrical conduction in the heart and the cardiac action potentials of SA node cells and other myocytes showing the different phases (Monteiro et al., 2017).

## 1.3 The Cardiac Autonomic Nervous System

Neurons have a soma, axon (or nerve fibers), and a nerve terminal where neurotransmitters are released from vesicles to receptors. Clusters of soma in the central nervous system are called nuclei; whereas, those located in the autonomic nervous system are called ganglia. The autonomic nervous system is part of the peripheral system that regulates visceral functions such as HR, blood pressure, and digestion to ensure the stability of the body's internal environment. It has two main subdivisions: the sympathetic and parasympathetic nervous systems. Both of these systems function automatically and subconsciously in an involuntary manner (Bush et al., 2016).

The sympathetic nervous system is associated with the "fight-or-flight' response of the body in cases of stress or danger. Whereas, the parasympathetic nervous system promotes all of the body's internal responses that are associated with a relaxed state ("rest-and-digest"). Hence, the sympathetic and parasympathetic branches have traditionally been regarded as acting in an antagonistic manner (Gordan et al., 2015; McCorry, 2007). Specifically, in terms of the heart, the sympathetic nervous system provides excitatory stimulation, resulting in positive inotropic (contractility), dromotropic (conduction), and chronotropic (heart rate) effects. In contrast, the parasympathetic nervous system opposes the effects of the sympathetic by providing inhibitory effects (McCorry, 2007).

## 1.4 The Extrinsic Cardiac Autonomic Nervous System

The autonomic control of the heart is complex and may be divided into two components: extrinsic and intrinsic (Ardell et al., 2015; Armour et al., 1997; Park and Cho, 2014). I will first discuss about the extrinsic cardiac autonomic nervous system which consists of fibers mediating connections between the heart and the nervous system (Park and Cho, 2014; Shen and Zipes, 2014). An overview of the cardiac innervation is shown in **Fig. 1.3**.

Both divisions of the autonomic nervous system require two neurons in order to transmit efferent information from the central nervous system to peripheral organ systems: preganglionic and postganglionic. As the name suggest, preganglionic fibers refer to those that precedes the ganglia, and post-ganglionic fibers are fibers that arise from the ganglia itself and come in contact with an effector organ such as the heart. In general, the sympathetic preganglionic fibers are short, but the postganglionic fibers are long.

Conversely, in the parasympathetic nervous system, the preganglionic fibers are long and the postganglionic fibers are short (Gordan et al., 2015; McCorry, 2007). In addition to efferent fibers, there are also afferent autonomic fibers that project sensory information about the state of the body to the brainstem and higher centers (Gordan et al., 2015). These afferent signals arise from the renal nerves of the kidneys, baroreceptors located in blood vessels, carotid bodies located on the external carotid arteries, and ganglionated plexi (Linz et al., 2014).

In order to control the function of the heart, both the sympathetic and parasympathetic system releases neurotransmitters that interact with receptor sites on cardiomyocytes. Regardless of which division, all preganglionic fibers are cholinergic, meaning that these fibers use acetylcholine (ACh) as the neurotransmitter. To induce the excitatory and inhibitory effects on the heart, the sympathetic system releases norepinephrine (NE) while the parasympathetic system releases ACh from their postsynaptic neurons, respectively.

### 1.4.1 Sympathetic Innervation of the Heart

Sympathetic innervation of the heart arises from the thoracolumbar segments of the spinal cord, specifically from $T_1$ to $L_2$, bilaterally. The pre-ganglionic sympathetic fibers originate in the lateral gray matter of the spinal cord and synapse with the post-ganglionic sympathetic neurons either in the cervical or the thoracic ganglia of the sympathetic chain located along the side of the viscera column (i.e., paravertebral ganglia) (Gordan et al., 2015). From the sympathetic chain, the post-ganglionic fibers then innervate both the atrial and ventricular myocardium (Triposkiadis et al., 2009).

As mentioned previously, a majority of the postganglionic fibers of the sympathetic system are adrenergic since they release NE which then bind to adrenergic receptors. There are two types of adrenergic receptors: $\alpha$ and $\beta$. In the cardiovascular system, there are $\alpha_1$, $\alpha_2$, $\beta_1$, and $\beta_2$. $\beta_1$ receptors are the predominant receptor type in number and function (McCorry, 2007). Activation of these adrenergic receptors by NE initiates a cascade of signaling pathways via the G protein subunit alpha complexes ($G_\alpha$), leading to the activation of adenyl cyclase and subsequently increased calcium influx (Harvey, 2012; Linz et al., 2014).

### 1.4.2 Parasympathetic Innervation of the Heart and the Vagus Nerve

The vagus nerve, or also known as the tenth cranial nerve, is the longest of the twelve cranial nerves in the human body. Originating in the medulla oblongata, the vagus nerve is composed of roughly 80% afferent and 20% efferent fibers (Howland, 2014; Seki et al., 2014; Vonck et al., 2007). The vagus nerve consists of approximately 75% of all parasympathetic fibers (McCorry, 2007). The nerve fibers of the vagus can be classified into A, B, or C types, and each has activation properties that are distinctly different (AgostoniI et al., 1957; Byku and Mann, 2016; Castoro et al., 2011). Type A (diameter, 5 – 20 μm) and Type B (diameter, 1 – 3 μm) are large, myelinated fibers and have high conduction velocities; whereas, Type C (diameter, 0.2 - 2 μm) are the smallest, unmyelinated, and have the slowest conduction velocities (Castoro et al., 2011). In general, Type A fibers, especially those that are above 12 μm, provide efferent motor control of the laryngeal muscles, while Types B and C fibers provide autonomic control of the heart (Yoo et al., 2016).

In general, the afferent sensory fibers transmit information via the nodose ganglion and synapse in the nucleus tractus solitarius (NTS) of the brainstem (Kapa et al., 2016). From there, the NTS provides connection to the dorsal motor nucleus (DMN) of the vagus and the nucleus ambiguus, where the efferent preganglionic parasympathetic fibers to the heart originate (Kapa et al., 2016). These efferent preganglionic fibers do not directly innervate the heart but rather synapse within the intrinsic cardiac ganglia that primarily lies on the ventral and dorsal fat pads of the heart. From these fat pads, the postganglionic efferent parasympathetic fibers then heavily innervate the SA and AV nodes and sparsely into the ventricular myocardium (Kapa et al., 2016). This concept of sparse parasympathetic innervation in the ventricles, however, has since been challenged (see Section 1.8 for more details).

ACh is the predominant neurotransmitter from the parasympathetic nervous system, in both the preganglionic and postganglionic neurons. ACh can bind to two types of receptors: nicotinic receptors and muscarinic receptors. Nicotinic receptors produce rapid, excitatory responses and are located at the synapses between the preganglionic and postganglionic neurons. Muscarinic receptors are located in the postganglionic neurons of the heart and compared to nicotinic receptors, the responses are slower in comparison. In terms of the parasympathetic control of the heart, the muscarinic $M_2$ receptors are the primary mediators (Heller Brown and Laiken, 2012). Activation of the $M_2$ receptors will slow pacemaker depolarization and the sinus rate via the pertussis toxin-sensitive $G_{\alpha i/o}$ proteins to inhibit adenyl cyclase, reduce cyclic adenosine monophosphate (cAMP), and open the $I_{KACh}$ channel (Harvey, 2012; Liang et al., 2014; Wydeven et al., 2014).

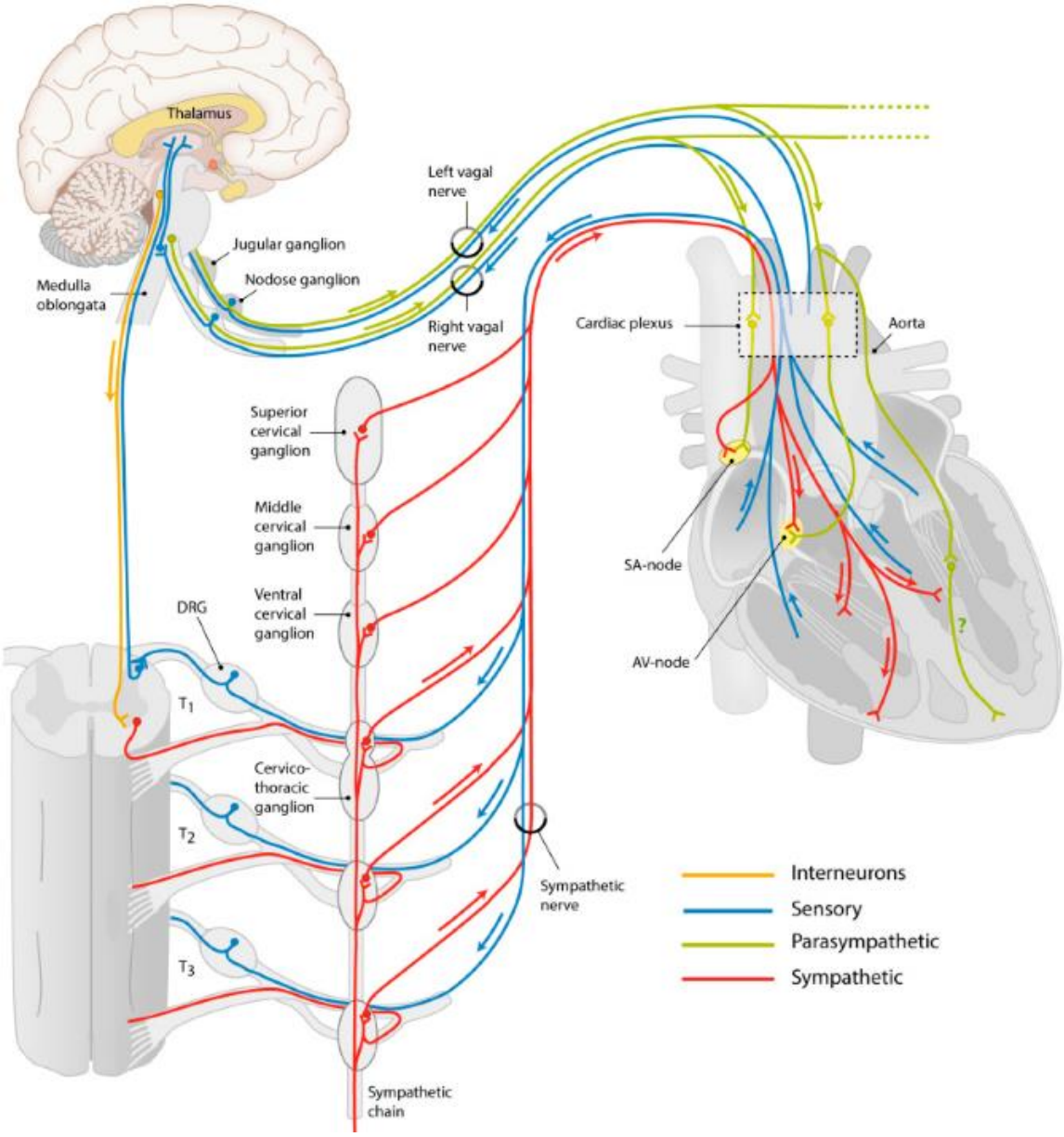


***Figure 1.3: Overview of the cardiac innervation by the autonomic nervous system.*** Figure adapted from (Végh et al., 2016).

## 1.5 The Intrinsic Cardiac Autonomic Nervous System

Briefly, the intrinsic cardiac nervous system is a complex neural network that is comprised of ganglionated cardiac plexuses that is mainly embedded within the epicardial fat on the surfaces of the atria (i.e., SA and AV nodes and the pulmonary vein-left atrium) and ventricles (i.e., primarily located at the origins of the several major cardiac blood vessels) (Linz et al., 2014; Shen and Zipes, 2014). These ganglia contain local circuit neurons that can respond and maintain beat-to-beat control of cardiac function. These ganglionated plexus can act as integration centers that regulate the interaction between the extrinsic and intrinsic cardiac nervous system via modulating the activity of the other through efferent and afferent connections. Or the intrinsic cardiac system may act entirely independent from the influences of the central or peripheral nervous system components (Ardell et al., 2015; Kapa et al., 2016).

## 1.6 VNS Therapy

VNS is a neuromodulatory treatment that stimulates the vagus nerve. The therapy consists of an implanted pacemaker-like pulse generator and a nerve stimulation electrode that delivers mild electrical impulses to the patient's vagus nerve. A thin thread-like flexible wire, attached to the generator, runs under the skin to the vagus nerve. **Fig. 1.4** describes the VNS system.

### 1.6.1 FDA-approved Treatment for Epilepsy and Treatment-Resistant Depression

Since the late 19$^{th}$ century, VNS has been used as a therapy to treat epilepsy (Yuan and Silberstein, 2016b). In fact, early animal studies demonstrated that VNS was able to alter the activity of the brain, suppress seizures and tremors, and induce an extended period

of seizure inhibition post-VNS. With these successes, human trials were then conducted and significant seizure reduction in patients diagnosed with intractable epilepsy was demonstrated (Ben-Menachem et al.; Penry and Dean, 1990; Uthman et al., 1993). The United States Food and Drug Administration (FDA) then approved the use of VNS to treat intractable epilepsy in 1997 (O'Reardon et al., 2006). In addition, it was observed that epileptic patients who underwent VNS treatment showed mood improvements (Elger et al., 2000). Hence, Rush et al conducted an open trial using VNS to treat adult outpatients with nonpsychotic, treatment-resistant major depressive or bipolar disorders (Rush et al., 2000). The results from this study suggest that VNS has antidepressant effects, and the FDA approved the use of VNS for treatment-resistant depression in 2005 (O'Reardon et al., 2006; Rush et al., 2000). In addition to its antidepressant and antiepileptic effects, electrical stimulation of the vagus nerve has also been proposed to be able to treat other medical diseases such as obesity, headaches, and gastric motility disorders (Akdemir and Benditt, 2016; Yuan and Silberstein, 2016a).

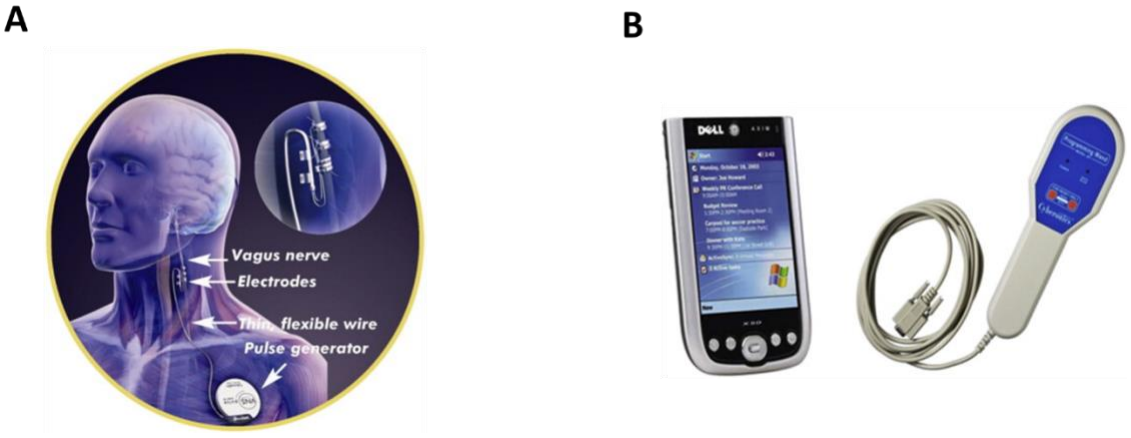


***Figure 1.4: Illustration of the VNS system.*** **(A)** VNS pulse generator implanted with lead wrapped around patient's vagus nerve and **(B)** handheld programmer and wand to communicate with the pulse generator via telemetry to noninvasively program, retrieve data, and perform device diagnostics. Figure adapted from (Dicarlo et al., 2013).

### 1.6.2 Potential to Treat Cardiovascular Diseases

According to the American Heart Association, cardiovascular diseases remains to be the leading cause of death in the USA, accounting for nearly 801,000 deaths in the USA alone (Benjamin et al., 2017). While pharmacotherapy and mechanical devices have improved clinical outcomes, the morbidity and mortality rates of heart failure (HF) still remains high (Swedberg et al., 2008). Currently, the only approach to conclusively treat HF patients is heart transplantation. This therapy, however, has risks and limitations: its invasiveness, cost, and the limited number of donor organs available (Bernstein and Srivastava, 2012). As a result, there is a huge need for new approaches and more effective cardiovascular therapies.

The pathophysiology of HF and other cardiovascular diseases such as hypertension and myocardial infarction (MI) are often associated with neurohormonal activation of the sympathetic nervous system and withdrawal of the parasympathetic system. In the early stages of HF, activation of the sympathetic nervous system serves as a compensatory physiological response for the heart to induce positive inotropic and chronotropic effects to meet the increased physiologic and metabolic demands. However, this excessive upregulation of the sympathetic nervous system will eventually contribute to the progression and pathogenesis of HF.

Over the past decades, VNS has been extensively studied as a potential therapy for HF. Here, the aim of the therapy is to modulate the parasympathetic activity in order to reestablish the cardiac autonomic balance in response to the increased sympathetic tone seen in cardiac diseases (De Ferrari et al., 2011; Klein and Ferrari, 2010; Li et al., 2004).

The therapeutic effects have been investigated in several animal models, and they suggest chronic VNS might have significant positive effects in the failing heart.

First, preclinical results from Li et al have shown that HF rats treated with VNS showed significant improvements in LV hemodynamics and decreased mortality from 50% to 14% (Li et al., 2004). Furthermore, it was also demonstrated in a high-rate ventricular pacing HF canine model that the animals receiving VNS treatment had significantly lower LV end-diastolic and systolic volumes and higher LV ejection fraction (Zhang et al., 2009b). In addition to its hemodynamic effects, VNS has also been shown to be able to attenuate LV remodeling associated with HF (Liu et al., 1997). Furthermore, VNS has also been shown to exhibit anti-arrhythmic (De Ferrari and Schwartz, 2011; Schwartz and De Ferrari, 2009; Wu and Lu, 2011) and anti-inflammatory (Borovikova et al., 2000; Calvillo et al., 2011; Mihaylova et al., 2012; Yamakawa et al., 2013) effects.

Based on the encouraging results of the preclinical studies, a number of clinical studies have been conducted (Gold et al., 2015). One such clinical study was the ANTHEM-HF and its subsequent extension study (ENCORE) which have yielded favorable and encouraging results as VNS patients showed significant improvements in LV structure and function, decreased HF symptom expression and decreased T-wave alternans, which is a measure of electrical instability (Gold et al., 2015; Nearing et al., 2016; Premchand et al., 2014, 2015).

Furthermore, VNS is also a promising alternative approach to current treatments of cardiovascular diseases (e.g., oral medication and ablative therapies) because as mentioned previously, the vagus nerve directly innervates the heart allowing VNS to potentially

provide a stronger and quicker response. Furthermore, it is notable that, relative to adjusting medication levels, the effects of VNS can be much more quickly adjusted by changing stimulation parameters. In other words, VNS provides the advantage of higher spatiotemporal precision and reversibility that is absent from oral medications and other invasive approaches (Johnson et al., 2013).

## 1.7 Mechanisms Underlying the Beneficial Effects of VNS Remains to be Further Elucidated

In spite of the above-mentioned studies demonstrating the therapeutic potential of VNS, the precise mechanisms of this therapy are not well-established. A variety of mechanisms by which VNS exerts its cardioprotective effects have been proposed and are supported by animal studies, including:

- HR reduction leading to improvements in LV function by reducing cardiac workload (Klein and Ferrari, 2010; Sabbah, 2011);
- Inhibition of proinflammatory cytokine release, through activation of the α7 nicotinic ACh receptor, and thereby prevent cardiac tissue injury and cell death (Borovikova et al., 2000; Calvillo et al., 2011; Mihaylova et al., 2012; Yamakawa et al., 2013);
- Normalization of nitric oxide signaling (NOS) pathway, specifically improve expression of endothelial (eNOS) and normalize the expressions of induced (iNOS) and neuronal (nNOS) in the HF-induced myocardium (Kalla et al., 2016; Sabbah, 2011); and

- Preservation of connexin-43 (Cx-43) which are protein molecules that form gap junctions. Intercellular electrical coupling mainly occurs through gap junctions and during cardiac diseases (Gutstein et al., 2001; Jiang et al., 2008; Lerner et al., 2000; Papp et al., 2007), it has been shown that the amount and distribution of Cx-43 are significantly altered (Ando et al., 2005; Wu and Lu, 2011).

While these proposed mechanisms may be able to partially explain the beneficial effects of VNS, it is yet to be explained how stimulating the vagus nerve can induce anti-arrhythmic actions in the ventricles. Hence, ***one of the main objectives of my thesis work was to further improve our understanding of how the parasympathetic branch influences ventricular physiology. This is especially crucial since now there are emerging evidences suggesting significant innervation of the vagus into the ventricles than what was initially perceived.***

## 1.8 'Realities' of the Cardiac Parasympathetic Innervation into the Heart

The myocardium is innervated by both sympathetic and parasympathetic nerves. The dogma of physiology teaching states that there are significant innervation of the sympathetic postganglionic nerves into the atria, SA and AV nodes, and the ventricles; whereas, the parasympathetic postganglionic nerves are limited to only the atria, and if any, very sparse innervations into the ventricles. As a result, it was initially postulated that there should minimal to no direct influence of the parasympathetic branch on ventricular

performance (Coote, 2013; Jungen et al., 2017; Végh et al., 2016). This supposition, however, has recently been challenged by several studies.

### 1.8.1 Histochemical Evidences

In the early 1950s and 1960s, the laboratory of Koelle and Kanovasky & Roots developed a thiocholine staining method to identify acetylcholinesterase (AChE), which is the enzyme responsible for hydrolyzing ACh (Karnovsky and Roots, 1964; Koelle, 1955). As a result of this staining method, several researchers have shown that there are indeed parasympathetic innervation into the ventricles of several species such as rats, pigs, humans, canine, and cats (Coote, 2013; Jacobowitz et al., 1967; Kent et al., 1974; Taggart et al., 2011; Ulphani et al., 2010; Zang et al., 2005).

In addition to staining for AChE, parasympathetic distribution into ventricles was also confirmed using immunohistochemical method for choline acetyltransferase (CHAT) (Coote, 2013; Pauza et al., 2013; Yasuhara et al., 2007). CHAT is an enzyme that catalyzes the transfer of an acetyl group from acetyl-CoA to choline, synthesizing ACh (Oda, 1999).

### 1.8.2 Microdialysis and Molecular (Muscarinic) Evidences

Evidence of postganglionic parasympathetic innervation in the ventricular myocardium may also be assessed by measuring ACh concentrations released during cervical VNS. Using microdialysis technique, several researchers have shown in both mice and cats that electrical stimulation of the vagus nerve increased ACh from postganglionic vagal nerve terminals in the ventricle. Whereas, transection or pharmacological blockade of the vagal nerve postganglionic terminal prevented the effect of VNS on ACh release (Akiyama and Yamazaki, 2001; Kawada et al., 2001; Zhan et al., 2013).

Muscarinic receptors are one of the primary binding sites for ACh, and they are expressed in the postganglionic terminals of the heart. The muscarinic $M_2$ subtype receptors are the primary mediators in parasympathetic regulation of the heart (Heller Brown and Laiken, 2012). Using RT-PCR and western blotting techniques, expressions of the $M_2$ and other muscarinic receptor subtypes have been identified in the ventricles in various species, although it is significantly lower than what is expressed in the atria (Krejcí and Tucek, 2002; Wang et al., 2001; Zang et al., 2005).

## 1.9 Research Objectives and Organization of Thesis

As mentioned thus far, in spite of several studies demonstrating the therapeutic potential of VNS to treat cardiac diseases, the mechanism of action of VNS remains unclear. One of many reasons for this is due to the myriad of experimental factors and stimulation parameters used in studies; thus, making probing the physiological mechanism of action of VNS extremely challenging to understand. This is because VNS can have different effects depending on the parameters and level of stimulation used. Furthermore, it was widely believed that the parasympathetic system had minimal to no influence on ventricular physiology since the postganglionic vagus nerve only sparsely innervates the ventricles, However, an abundance of histological and experimental studies have since argued this supposition.

*Hence, the focus of my research is as follows: First, I investigated the effects of VNS on the electrophysiological properties of the ventricles in order to gain a better understanding and determine whether ventricles may play a role in the therapeutic mechanisms of VNS. Second, I used novel genetic mouse lines to further investigate the*

*role of $M_2$ receptors in mediating the chronotropic effects of VNS. Third, I developed and investigated a novel stimulation paradigm to electrically stimulate the vagus nerve in order to further optimize and improve VNS efficacy.* **The overall aim of this dissertation is to improve our knowledge of VNS and to elucidate the mechanism of action in order to further optimize and improve VNS efficacy.** The thesis is divided into the following chapters:

**Chapter 2** describes the study used to demonstrate the therapeutic effects of VNS in a chronic MI rat model. In this study, I looked into the electrophysiological changes induced by long-term VNS in the atria of MI hearts. Through this study, I investigated and gained a better understanding of how both chronic MI and VNS affected the atria, especially since there is significant vagal fiber innervation into the atrium and it remains unclear how chronic ventricular MI affects atrial properties. Details of the experimental investigations performed and the results are also provided.

Due to the emergence of evidences supporting significant parasympathetic innervation and possibly more influence on ventricular physiology than what was initially perceived, **Chapter 3** discusses the research study performed to investigate the effects of stimulating the vagus nerve of healthy rats when the autonomic nervous system is in balance. It details the use of optical imaging techniques to compare the ventricular electrophysiological properties between VNS-treated and non-treated hearts. Furthermore, testing in normal, healthy controls is essential to understanding the mechanism of VNS and evaluate any potential negative effects the therapy may have without the interferences of other confounding factors.

After showing that VNS modifies both atrial and ventricular electrophysiological properties in **Chapters 2** and **3**, respectively, in the whole-heart level, **Chapter 4** investigates from a molecular standpoint. Specifically, **Chapter 4** details the application of VNS on novel transgenic mouse lines that lack the $M_2R$-$I_{KACh}$ signaling pathway constitutively, and selectively in the atria/SA node or ventricles. The goal of the study was to distinguish the specific role of cardiac $I_{KACh}$ in mediating the chronotropic effects of acute VNS on the heart. To our knowledge, this study is the first to probe the direct link between VNS and $M_2R$-$I_{KACh}$ channel in a tissue-specific area of the heart (i.e. atria and the ventricles) *in-vivo*.

There still does not exist a universally accepted published prospective VNS paradigm, which further highlights the importance and complexity of parameter optimization. To further optimize and improve VNS efficacy, **Chapter 5** describes an investigative study performed to evaluate the effects of incorporating stochasticity when stimulating the vagus nerve (stochastic VNS) on acute heart rate (HR) dynamics. The effect of stochastic VNS was evaluated in rats by comparing the acute HR and HR variability (HRV) responses to standard, periodic VNS.

**Chapter 6** summarizes the work completed as part of this dissertation by highlighting the major findings and discussing the possible future directions for this research.

# CHAPTER 2 EFFECTS OF VNS ON ATRIAL ELECTROPHYSIOLOGICAL PROPERTIES

**(Published)**

X. Xie*, S.W. Lee*, C. Johnson, J. Ippolito, B.H. KenKnight, and E.G. Tolkacheva, "Intermittent Vagal Nerve Stimulation Alters the Electrophysiological Properties of Atrium in the Myocardial Infarction Rat Model," Conf Proc IEEE Eng Med Biol Soc. 2014; 2014: pages 1575-1578. **[*Authors contributed equally to the study]**

## 2.1 Chapter Synopsis

Intermittent vagal nerve stimulation (VNS) has emerged as a potential therapy to treat cardiovascular diseases by delivering electrical stimulation to the vagus nerves. The purpose of this study was to investigate the electrophysiological changes in the atrium resulting from long-term intermittent VNS therapy in the chronic myocardial infarction (MI) rat model. MI was induced via left anterior descending coronary artery (LAD) ligation in male Sprague-Dawley rats, randomized into two groups: MI (implanted with nonfunctional VNS stimulators) and MI-VNS (implanted with functional VNS stimulators and received chronic intermittent VNS treatment) groups. Further, a sham group was used as control in which MI was not performed and received nonfunctional VNS stimulators. At 12 weeks, optical mapping of right atrium (RA) of sinus rhythm was performed. Our results demonstrated that chronic MI changed the electrical properties of the atrium action potentials and resulted in reduced action potential duration at 50% ($APD_{50}$) and 80%

($APD_{80}$) repolarization. Chronic right cervical VNS restored the APD back to healthy heart APD values. Additionally, APD heterogeneity index increased as a result of the chronic MI. Chronic VNS was not found to alter this increase. By calculating PR intervals from weekly ECG recordings of anaesthetized rats, we demonstrated that chronic MI and intermittent VNS did not affect the AV conduction time from the atria to the ventricles. From our study, we conclude the MI decreased the APD and increased APD spatial dispersion. VNS increased the APD back to healthy normal values but did change the APD spatial dispersion and the electrical conduction in the RA.

## 2.2 Introduction

Myocardial infarction (MI) is the most common cause of heart failure (HF) (Coronel et al., 2013; Klocke et al., 2007). Current therapies designed to treat MI patients include conventional pharmacological and mechanical device-based interventions. While these approaches have improved the prognosis of patients with MI, the mortality rate still remains high (Swedberg et al., 2008).

As mentioned previously, VNS is an adjunctive procedure involving the stimulation of the vagus nerve with electrical impulses and is currently used clinically to treat intractable epilepsy and treatment-resistant depression (Ghanem and Early, 2006; Groves and Brown, 2005). Recently, modulation of nerve activity through cardiac VNS has emerged as a potential therapy for cardiovascular diseases (De Ferrari et al., 2011). It has been shown that chronic VNS can inhibit sudden cardiac death (Vanoli et al., 1991) and markedly suppress arrhythmias (Li et al., 2004) in MI animal models. Peripheral cardiac nerve stimulation can also modify atrial and ventricular contractile functions (Brack et al., 2011; Kunze, 1972). It

has been reported that chronic VNS may improve left ventricular function and the quality of life in chronic HF patients with severe systolic dysfunction (De Ferrari et al., 2011).

It is well known that parasympathetic vagal nerves extensively innervate the atria. The vagus nerve (parasympathetic) system communicates with the heart through the intracardiac ganglia, which are divided into the sinoatrial (SA) and atrioventricular (AV) nodes (Sampaio et al., 2003). It is thought that VNS might have a significant effect on atrial electrophysiological properties due to dense vagal innervations. However, the effects of chronic VNS on the atrium remain unclear. Additionally, there are controversial findings on whether VNS is linked to atrial fibrillation (AF). Specifically, VNS has been shown to shorten the duration of action potential (APD) in atrial myocytes and reduce the atrial absolute refractory period, facilitating the induction of AF by a single atrial ectopic beat and the presence of multiple reentrant circuits coexisting in the atrial myocardium (Chen and Tan, 2007; Zhang and Mazgalev, 2011). Furthermore, animal studies involving vagal denervation have suggested that VNS may be proarrhythmic (Lemola et al., 2008; Schauerte et al., 2000). Nonetheless, there are also studies that have shown that VNS can inhibit spontaneous activities of isolated cardiac myocytes from rabbit pulmonary veins (Chen et al., 2002a) and canine superior vena cava (Chen et al., 2002b). In addition, it has been shown that the use of phenylephrine to enhance the vagal tone suppresses focal AF originating in the pulmonary veins in patients (Tai et al., 2000; Zhang and Mazgalev, 2011). Low-level VNS has also been implemented in ambulatory dogs to reduce atrial tachy-arrhythmias (Shen et al., 2011). Therefore, further investigations are required to determine the exact role of VNS on the electrophysiological properties of atria.

The objective of this study was to use high resolution optical mapping techniques to evaluate the changes in atrial electrophysiology due to chronic intermittent VNS in a chronic MI rat model. We aimed to identify whether these changes might potentially promote or inhibit the creation of substrates for atrial arrhythmias. To our knowledge, this is the first study to characterize the electrophysiological changes in the atria in MI rat hearts after treatment with long-term VNS.

## 2.3 Materials and Methods

### 2.3.1 MI Rat Model

All experiments conformed to the Guide for the Care and Use of Laboratory Animals (NIH publication No. 85-23, revised 1996) and the University of Minnesota guidelines regulating the care and use of animals.

Male Sprague-Dawley rats (n=6, 250-300g, Charles River Laboratories, Wilmington, MA) were randomized into three groups: Sham (n=2), MI (n=2), and MI-VNS (n=2). Sham rats underwent open chest and cervical sham surgeries only, while MI was induced in both MI and MI-VNS rat hearts. The MI was created through permanent ligation of the left anterior descending coronary artery (LAD) in the MI and MI-VNS groups. Rats were anesthetized with Isoflurane (3%) during the open chest MI surgeries. Rats were intubated with a ventilator (Model 683, Harvard Apparatus) and body temperature was maintained at 37°C throughout the surgeries. LAD surgery was performed by ligation of the proximal LAD artery with 6-0 silk sutures. Full LAD occlusion was visually confirmed

when the myocardium of the left ventricle changed color to a pale blue, reflecting the lack of oxygenated blood flow into the region.

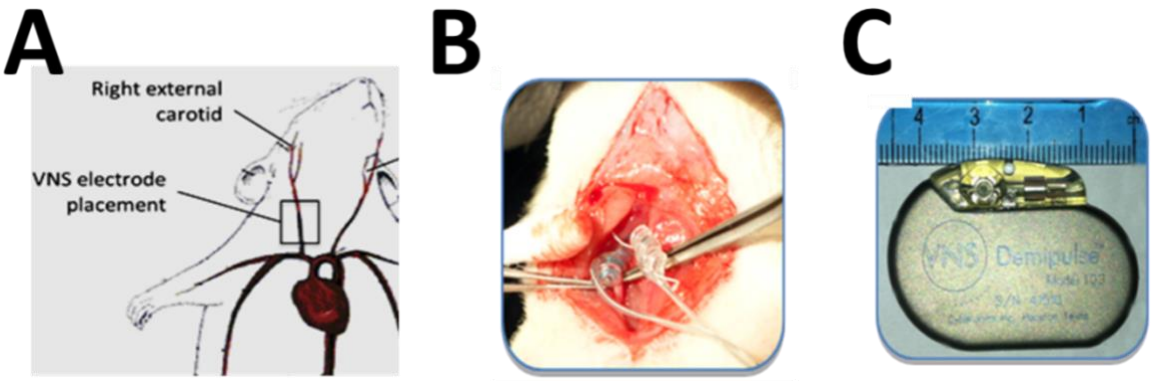


***Figure 2.1: Surgical Implantation of VNS in Rats.*** **A)** VNS lead placement around the cervical vagus nerve and carotid artery bundle. **B)** Placement of the helical bipolar leads. **C)** Cyberonics 105 Vagal Nerve Stimulator.

### 2.3.2 VNS Stimulator Implantation

Immediately after MI surgery, VNS stimulators (**Fig. 2.1(c)**, Cyberonics Model 103, Houston TX) were implanted subcutaneously on the lower back of the rats. Active and non-functional VNS stimulators were implanted in MI-VNS and MI rats, respectively. The bipolar cuff electrodes were coiled around the bundle of right cervical vagus nerve and carotid artery as shown in **Fig. 2.1(b)**. Intermittent VNS was given to the MI-VNS rats for 12 weeks. Parameters of VNS stimulation were defined as in previous literature (Li et al., 2004): stimulation frequency of 20 Hz; pulse width of 500 microseconds; and stimulation current of 1 mA; duty cycle of roughly 12% (7 second ON every 1 minute).

### 2.3.3 ECG Recordings

ECG recording was performed as described previously (Ippolito et al., 2014). Briefly, ECG recordings was performed in all rats weekly for approximately 20 minutes per animal using the iWorx IX-ECG-12 recording system, while rats were lightly anesthetized with 2% Isoflurane. Custom-made program in Matlab was written to calculate

PR intervals and heart rate (HR) from anaesthetized rats' ECG data. For each week and for each rat, mean PR intervals were calculated over 20 minutes of ECG recording. HR was derived from the first 2 minutes of the ECG during which the effects of anesthesia were minimal.

### 2.3.4 High-Resolution Optical Mapping

At week 12, rat hearts were extracted. The aorta was quickly cannulated and perfused in a retrograde manner using Langendorff-perfusion system with warm (37±1ºC) oxygenated Tyrode's solution. A dose of 0.01 ml of the fluorescent voltage-sensitive dye di-4-ANEPPS (10 μmol/L) was administered to the right atrium (RA) directly. Two diode continuous lasers (532 nm, SDL-532-1000 T, Shanghai Dream Lasers Tech., Shanghai, China) were used for excitation, and the fluorescence signal was recorded from the RA surface by fast (1000 frames per second) 14-bit resolution, 80x80 pixels resolution camera (Little Joe, RedShirt Imaging, SciMeasure). The field of view was approximately 6 x 6 mm (**Fig. 2.2(a)**). After stabilization (~30 minutes), optical mapping movies of the whole RA were acquired during sinus rhythm.

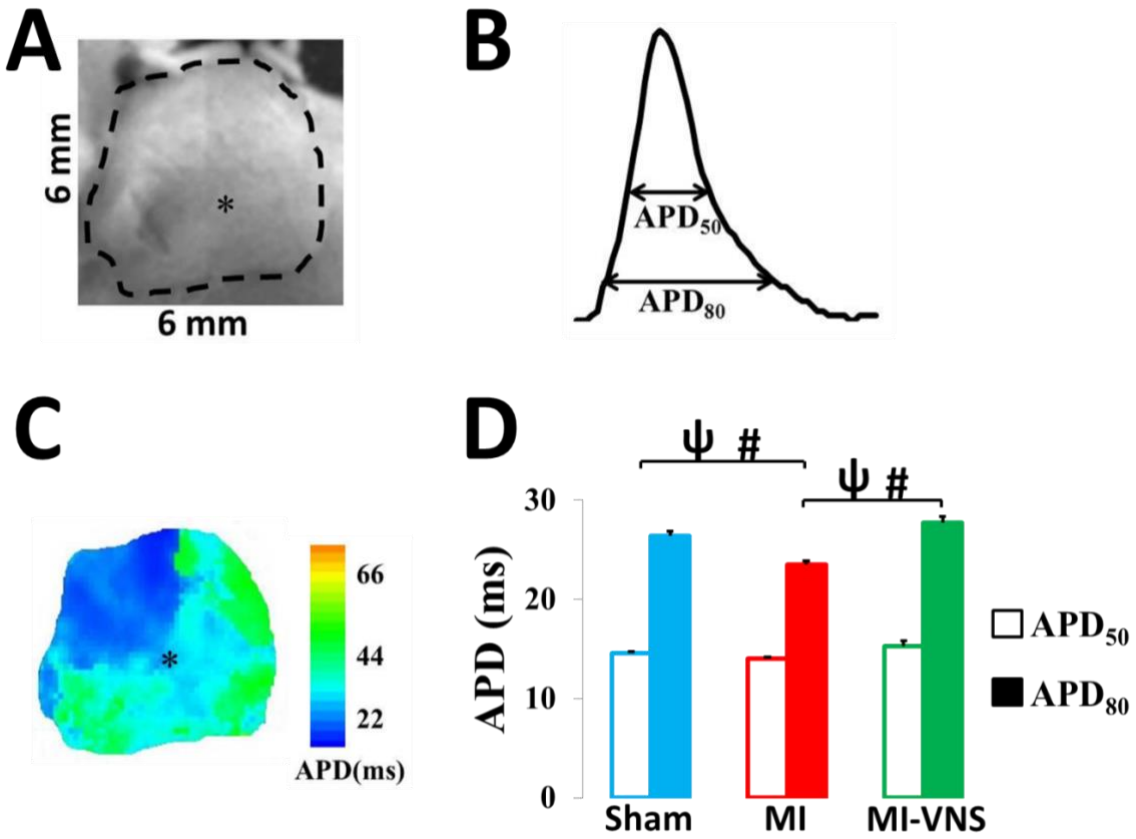


***Figure 2.2: Measurements of Atrial APD.*** **A)** Optical mapping field of view (indicated by dashed lines) of RA. **B)** A typical action potential trace from pixel marked as "*" of the RA demonstrating $APD_{50}$ and $APD_{80}$. **C)** Corresponding 2D $APD_{80}$ maps to **A)**. **D)** Mean values for $APD_{50}$ (open bars) and $APD_{80}$ (filled bars). ψ represents statistical difference between $APD_{50}$ and # represents statistical difference between $APD_{80}$ ($p < 0.05$).

### 2.3.5 Data Analysis

We analyzed 12 sinus rhythm responses from each rat, for all three groups. Sinus rhythm APD was measured at both 50% ($APD_{50}$) and 80% ($APD_{80}$) repolarization (**Fig. 2.2(b)**), and two-dimensional (2D) APD maps (**Fig. 2.2(c)**) were constructed to reveal the spatial distribution of APDs on the RA surfaces of the heart. The APD heterogeneity, μ, was calculated as described previously (Mironov et al., 2008):

$$\mu = \frac{(\mathrm{APD}^{95\%} - \mathrm{APD}^{5\%})}{\mathrm{APD}^{50\%}} \quad (1)$$

where $\mathrm{APD}^{95\%}$ and $\mathrm{APD}^{5\%}$ represent the 95th and 5th percentiles of the APD distribution, respectively, and $\mathrm{APD}^{50\%}$ is the median APD distribution.

Mean APD and μ were calculated as the following. For each rat, we first calculated mean APD and μ from a single sinus rhythm across the entire RA. Then, we performed averaging of these mean APD and μ values for all 12 sinus rhythm responses. Data are presented as means ± standard error of the mean. Statistical comparisons among the 3 groups were performed using an ANOVA statistical test. $P < 0.05$ was considered to be statistically significant.

## 2.4 Results

### 2.4.1 Effect of VNS on APD and Spatial Heterogeneity

**Fig. 2.2(d)** shows mean values for $APD_{50}$ (open bars) and $APD_{80}$ (filled bars) of Sham (blue), MI (red), and MI-VNS (green) rats during sinus rhythm. Note that MI significantly reduced both $APD_{50}$ and $APD_{80}$ ($p<0.05$) of RA. However, this reduction of APD at both levels of repolarization was restored upon chronic intermittent VNS stimulation back to Sham (healthy) level.

**Fig. 2.3(a)** shows representative sinus rhythm traces as well as examples of 2D $APD_{80}$ maps for Sham, MI and MI-VNS rats. Note the enhanced spatial dispersion of APD during sinus rhythm for both MI and MI-VNS rats. We quantified these data by calculating mean μ values separately for both $APD_{50}$ (open bars) and $APD_{80}$ (filled bars). **Fig. 2.3(b,c)**

indicate that MI significantly increased μ in RA ($p<0.05$), but was not reduced with chronic intermittent VNS.

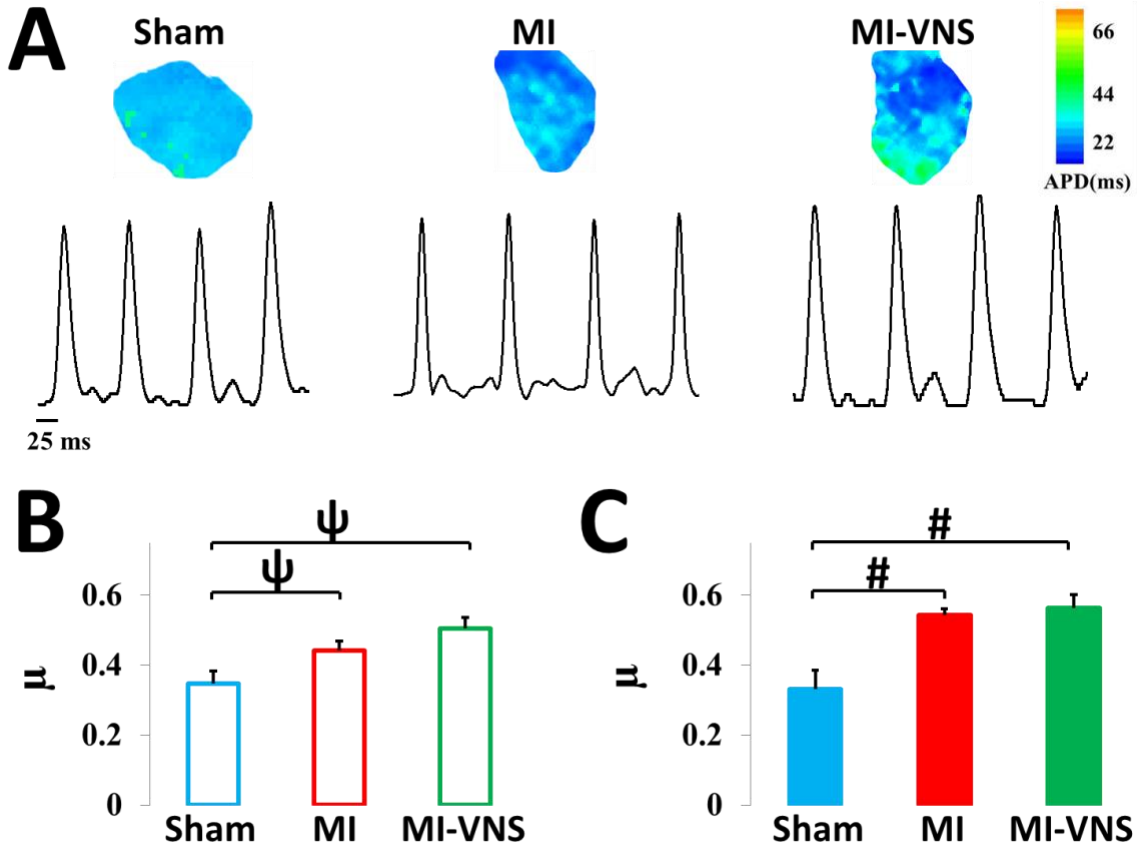


***Figure 2.3: Measurements of Atrial μ.*** **A)** Typical samples of 2D APD maps and representative sinus rhythm action potential traces (from pixel marked as "*") from all three groups. Mean spatial heterogeneity index μ afor **B)** $APD_{50}$ (open bars) and **C)** $APD_{80}$ (filled bars) are shown for Sham, MI and MIa-VNS groups. ψ represents statistical difference between $APD_{50}$ and # represents statistical difference between $APD_{80}$, $p<0.05$.

## 2.4.2 Effect of VNS on PR Interval and HR

To investigate whether VNS affects the electrical conduction time from atria to ventricles, we calculated PR intervals from weekly ECG recordings of anaesthetized rats. Average data in **Fig. 2.4(a)** illustrates the absence of any differences in PR intervals of

Sham (blue), MI (red) and MI-VNS (green) ECG recording over the duration of study. In addition, as seen in **Fig. 2.4(b)**, our chronic VNS treatment did not induce any significant changes in HR of the anaesthetized rats.

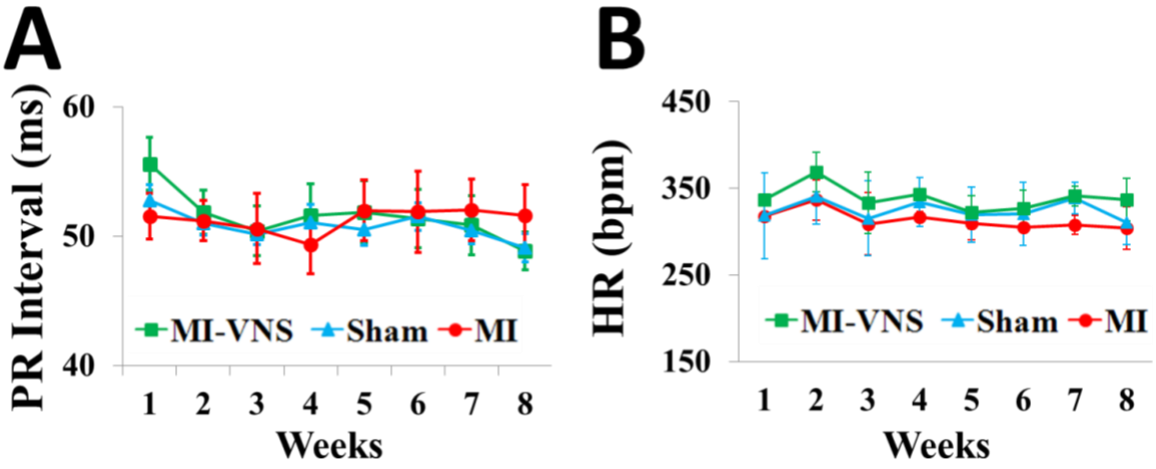


***Figure 2.4: Effect of VNS on PR Interval and HR.*** **A)** Mean PR interval over 8 weeks of study for Sham (blue), MI (red) and MI-VNS (green) hearts. **B)** Mean weekly HR over 8 weeks of study for Sham (blue), MI (red), and MI-VNS (green).

## 2.5 Conclusions and Discussion

In this study, we investigated the long-term effects of both MI and intermittent VNS on the electrophysiological properties of the atrium in a MI rat model. The main findings of our study are as follows: 1) chronic MI decreased APD and the VNS restored the APD values during sinus rhythm in rat heart RA. On the other hand, 2) VNS had no effect on APD heterogeneity that was increased due to chronic MI. Finally, 3) neither chronic MI nor intermittent VNS affected the AV conduction system in the heart.

There are only few studies on the effects of chronic MI on atrial electrophysiology. Previous studies showed inconsistent changes in atrial action potential morphology in cardiovascular diseases: APD was increased (Yeh et al., 2008), shortened (Sridhar et al., 2009), or unchanged (Li et al., 2000). MI-induced HF is often associated with AF (Miyauchi

et al., 2003) and our study showed that MI decreases both atrial $APD_{50}$ and $APD_{80}$ during sinus rhythm. The shortening of the atrial APD could potentially provide substrates for atrial arrhythmias since reduction in APD can shorten the wavelength of re-entry (the product of both APD and conduction velocity) and increase the number of wavelets during AF (Nattel, 2002; Zhang and Mazgalev, 2011). On the other hand, chronic VNS increased both the $APD_{50}$ and $APD_{80}$ values and restored them back to the healthy animal values, which can be a potentially anti-arrhythmic effect.

Our results also indicate that MI increased the spatial APD heterogeneity in the RA. However, VNS did not reduce the heterogeneity of the MI hearts towards healthy values. This result may explain the reported conflicting results regarding the anti-arrhythmic effects in the whole heart induced by the VNS. The increased spatial heterogeneity of APD is known to be one of the contributing factors to arrhythmogenesis (Mironov et al., 2008). This indicates that the reported anti-arrhythmic effects of VNS in the whole heart level are less likely related with the APD spatial heterogeneity in the RA.

The PR interval is one of the many important parameters used to identify cardiovascular diseases. It can be used as an indication of unfavorable alteration in the electrical system of the heart. An abnormal PR interval is often associated with SA nodal and or AV nodal blocks. Our PR interval results showed that both MI and VNS did not affect the PR intervals among the three groups of rats. This could indicate that there were no SA nodal and/or AV nodal disturbances.

The potential benefits of chronic VNS are now being evaluated in human subjects diagnosed with chronic, symptomatic HF (Dicarlo et al., 2013). Previously, data from a

small pilot study suggested that VNS alters the natural history of HF (De Ferrari et al., 2011). Large, multi-center, controlled clinical studies are underway and should provide additional insights regarding the safety and efficacy of this new therapy for treatment of chronic HF.

A limitation of this study was the limited sample size. Another limitation was the use of general anesthesia to perform ECG recordings from the rats. While it is known that anesthesia changes the HR (RR interval) of animals in comparison to conscious animal ECG recordings, we believe that changes to the PR interval are minimal.

# CHAPTER 3 EFFECTS OF VNS ON VENTRICULAR ELECTROPHYSIOLOGICAL PROPERTIES

**(Published)**

S.W. Lee, Q. Li, I. Libbus, X. Xie, B.H. KenKnight, M.G. Garry, and E.G. Tolkacheva, "Chronic cyclic vagus nerve stimulation has beneficial electrophysiological effects on healthy hearts in the absence of autonomic imbalance." Physiol Rep. 2016 May;4(9). pii: e12786. doi: 10.14814/phy2.12786)

## 3.1 Chapter Synopsis

Cardiovascular disease degrades regulatory function of the autonomic nervous system. Cyclic vagus nerve stimulation (VNS) is an already FDA-approved therapy for drug-resistant epilepsy and depression and has been shown to normalize autonomic function and improve objective measures of heart function and subjective measures of heart failure symptoms. However, it remains unclear whether VNS may induce negative effects in patients with potentially healthy hearts where VNS can be used for epileptic patients. Hence, this study aims to investigate the effects of VNS on the hearts of healthy rats with normal autonomic balance. Sprague-Dawley rats were implanted with stimulators and randomized to either Sham or VNS groups. Rats in VNS group received 10 weeks of chronic intermittent VNS via stimulation of the right cervical vagus nerve. Echocardiography was performed at Baseline (prior to VNS), Week 2, and Week 9. After 10 weeks, high-resolution optical mapping was performed in *ex vivo* perfused hearts to

evaluate the electrophysiological remodeling that occurs in the heart as a result of the VNS therapy. Chronic VNS modified the electrophysiological properties of healthy rat hearts by reducing the action potential duration at 50% ($APD_{50}$) and 80% ($APD_{80}$) repolarization. Chronic VNS also affected the restitution properties of the heart at the $APD_{50}$ level and increased myocardial conduction velocity (CV). VNS did not induce any significant changes to ventricular ejection fraction (EF) and spatial dispersion of APD, thus indicating that VNS did not negatively affect cardiac function. VNS also reduced the susceptibility to ventricular arrhythmias (ventricular fibrillation [VF] and ventricular tachycardia [VT]) during programmed electrical stimulation. Chronic application of cyclic VNS induces changes to the electrophysiological properties of healthy rat hearts. The observed decrease in APD and increase in CV suggest that the beneficial effects of VNS do not require the presence of existing autonomic imbalance.

## 3.2 Introduction

Vagus nerve stimulation (VNS) is an approved clinical therapy for drug-refractory epilepsy and depression, and more than 130,000 VNS therapy systems have been implanted since 1995 (Shuchman, 2007). In the past decade, several pre-clinical and clinical studies have demonstrated the beneficial effects of VNS on cardiovascular diseases via parasympathetic nervous system activity modulation (Beaumont et al., 2015; De Ferrari and Schwartz, 2011; Sabbah, 2011).

The autonomic nervous system consists of two distinct branches: the parasympathetic and sympathetic nervous systems. The balance between the two systems plays a significant role in regulating cardiovascular functions and specifically, the

coordination of the electro-mechanical function of the heart, leading to optimized cardiac output under a variety of environmental and metabolic stressors. Heart diseases such as chronic heart failure (HF) and hypertension (HTN) are associated with autonomic dysregulation characterized by a sustained increase of sympathetic drive and withdrawal of parasympathetic activity (Bibevski and Dunlap, 2011; Schwartz and De Ferrari, 2011). VNS has emerged as a promising therapy to treat cardiovascular diseases by its proposed mechanism to correct this autonomic imbalance (Annoni et al., 2015; Beaumont et al., 2015; De Ferrari and Schwartz, 2011; Li et al., 2004; Premchand et al., 2015; Schwartz and De Ferrari, 2009; Xie et al., 2014).

Nonetheless, despite the extensive research and advances that have been made in recent years to support the concept of electrical VNS as a therapeutic approach, very little is known about the effects of chronic VNS on healthy hearts. While it has always been known that parasympathetic vagal nerve fibers densely innervate the atria and the sinoatrial (SA) and atrioventricular (AV) nodes, it was initially believed by many that vagal fibers only sparsely innervate the ventricles (Coote, 2013). However, other studies have challenged this supposition and suggest that the vagal fibers in fact play a greater role in ventricular function than initially believed (Armour et al., 1997; Coote, 2013; Randall et al., 2003; Ulphani et al., 2010).

As a result of this finding, it is important to gain a better understanding and fully characterize how stimulating the vagus nerve may affect the normal heart when the autonomic nervous system is in balance. In addition, as applies to any novel therapy, testing in normal, healthy controls is essential to understanding the mechanisms of action of VNS.

Most importantly, it makes it feasible to evaluate any potential negative effects the therapy may have without the interferences of other confounding factors. Moreover, VNS is FDA-approved to treat epileptic patients; however, the electrophysiological side effects of VNS on their potentially healthy hearts are not well characterized. Hence, the main objective of this novel study is to investigate the effects of chronic, intermittent VNS on the electrophysiological properties of healthy rat hearts.

## 3.3 Materials and Methods

### 3.3.1 Animal Preparation

All animal experiments were approved by the University of Minnesota Animal Care and Use Committee and were conducted in accordance with both the Institutional and National Institute of Health Guidelines for the Care and Use of Laboratory Animals.

Male Sprague-Dawley rats (n=9, 250-300 grams, Charles River Laboratories, Wilmington, MA) were randomized into two groups: Sham (n=6) and VNS (n=3). Sham group animals were implanted with non-functional vagus nerve stimulators, and VNS group animals were implanted with functional vagus nerve stimulators (Demipulse Model 103, Cyberonics Inc., Houston, TX, USA). All animals were maintained and monitored for a total of 10 weeks. Rats were placed in a quiet, temperature- and humidity-controlled room with a 12:12 hour light-dark cycle. Food and water were available ad libitum.

### 3.3.2 VNS Stimulator Implantation

The VNS pulse generator (Demipulse Model 103, Cyberonics, Inc., Houston, USA) was implanted subcutaneously on the lower back of the rats as described previously (Annoni et al., 2015; Xie et al., 2014). During the surgery, rats were anaesthetized with Isoflurane (5% for induction; 2% or 3.5% for maintenance) in oxygen (2 L/min for

induction, 1 L/min for maintenance). The rats' body temperature was maintained at 37°C on a temperature-controlled surgical table. Briefly, the back and the neck of the rat were shaved, and the right cervical vagus nerve and common carotid artery bundle were isolated from the surrounding tissue through a small incision on the neck. The custom 1.5 mm diameter helical lead bipolar cuff electrodes were placed around the carotid artery bundle containing the vagus nerve. The therapy group received continuous cyclic low-level VNS for 10 weeks. Low-level VNS parameters were set as follows: stimulation frequency of 20 Hz, pulse width of 500 μsec, and stimulation current of 1.0 mA. The pulse generator was programmed to deliver continuously cyclic VNS: 7 seconds ON and 66 seconds OFF. The effectiveness of VNS and its effect on acute and chronic changes in heart rate have been evaluated in previous studies (Annoni et al., 2015; Xie et al., 2014).

### 3.3.3 Echocardiography

Echocardiography was performed in VNS (n=3) and Sham (n=2) rats prior to VNS implantation surgery (Baseline), two weeks after surgery (Week 2), and one week prior to sacrifice (Week 9). Anesthesia was induced with 2% isoflurane gas in 100% oxygen, and transthoracic echocardiography (VisualSonics, VEVO-770 with 700-Series RMV Scanhead Probe, Toronto, Canada) was performed. Echocardiographic M-mode images of the left ventricle (LV) were obtained using a parasternal short-axis view at the middle of papillary muscle level. Left ventricular end diastolic (LVEDV) and systolic (LVESV) volumes were measured and used to calculate the percentage of LV ejection fraction (EF), an index of LV function, for each animal using the following equation: EF = ((LVEDV-LVESV) / LVEDV) x 100%.

### 3.3.4 High-Resolution Optical Mapping

At the end of 10 weeks, VNS (n=3) and Sham (n=4) rats were euthanized and hearts quickly extracted through a thoracotomy. Immediately upon removal, the hearts were immersed in cold cardioplegic solution (in mM: glucose 280, KCl 13.44, $NaHCO_3$ 12.6, and mannitol 34). The aorta was then quickly cannulated and perfused (retrograde) with warm (37±1°C) oxygenated Tyrode's solution (in mM: NaCl 130, $CaCl_2$ 1.8, KCl 4, $MgCl_2$ 1.0, $NaH_2PO_4$ 1.2, $NaHCO_3$ 24, glucose 5.5, and pH 7.4). The hearts were immersed in a chamber and superfused with the same Tyrode's solution.

After 30 minutes of stabilization, voltage-sensitive dye (di-4-ANEPPS, 5µg/mL; Molecular Probes, USA) was added to the perfusate. Two 532 nm diode continuous green lasers (SDL-532-1000 T, Shanghai Dream Lasers Tech, Shanghai, China) were used to illuminate both the right ventricles (RV) and LV surfaces of the heart. Fluorescence signals from more than 80% of total ventricular surface were captured with two 12-bit charge-coupled device (CCD) cameras (DALSA, Waterloo, Canada), that ran synchronously at 600 frames per second with 64 x 64 pixel resolutions. Blebbistatin (10 - 15 µM) was added to the Tyrode's solution to stop heart contractions and reduce motion artifacts (Smith et al., 2012).

Hearts were paced periodically. An external stimuli (5 ms duration, twice the activation threshold) were applied to the base of the RV at progressively decreasing basic cycle length (BCL) from 200 ms in steps of 20 ms until BCL reached 80 ms; or until ventricular tachycardia (VT) or fibrillation (VF) was initiated (Annoni et al., 2015). If and only when VF/VT was not induced during periodic pacing, a burst pacing protocol was used. At each BCL, 40 stimuli were applied to reach steady state. Optical mapping movies

were recorded at steady state of each pacing BCL from both LV and RV epicardial surfaces of the heart. The background fluorescence was subtracted from each frame, and spatial (3 x 3 pixels) and temporal (5 pixels) convolution filters were used.

### 3.3.5 Data Analysis

Both LV and RV optical mapping movies were used for data analysis. No significant differences were found between data from the two ventricles, and therefore, data was pooled for analysis.

*Action Potential Duration Measurements*. Optical action potential duration was measured at both 50% and 80% repolarization ($APD_{50}$ and $APD_{80}$, respectively), and two-dimensional (2D) APD maps were constructed to reveal the spatial distribution of APDs on the epicardial surface of the heart. Mean APD was obtained at different BCLs by averaging APDs from all pixels.

*Conduction Velocity Measurements.* Local conduction velocity (CV) was calculated as described previously (Annoni et al., 2015; Smith et al., 2012). Specifically, the distributions of activation times (measured at $(dV/dt)_{max}$) for the spatial regions of 5 x 5 pixels were fitted with the plane, and gradients of activation times $g_x$ and $g_y$ were calculated for each plane along the x and y axes, respectively. The magnitude of the local CV was calculated for each pixel as $(g_x^2 + g_y^2)^{-1/2}$.

*APD Heterogeneity Measurements.* The spatial dispersion of APD or dispersion of repolarization at both 50% and 80% repolarization was estimated based on the heterogeneity index, μ (Annoni et al., 2015; Smith et al., 2012):

$$\mu = \frac{(\mathrm{APD}^{95\%} - \mathrm{APD}^{5\%})}{\mathrm{APD}^{50\%}} \quad (1)$$

where $APD^{95\%}$ and $APD^{5\%}$ represent the $95^{th}$ percentile and $5^{th}$ percentiles of the APD distribution, respectively, and $APD^{50\%}$ is the median of APD distribution.

### 3.3.6 Statistical Analysis

All data are presented as means ± standard errors of the mean. Statistical comparisons of APD, μ, and echocardiography data between Sham and VNS groups were performed using one-way ANOVA test (Origin Software, Northampton, MA, USA). Statistical comparison of echocardiographic assessment among Baseline, Week 2, and Week 9 were performed using a paired Student's t-test. Comparison of CV were performed using a paired t-test. Values of $p < 0.05$ were considered to be statistically significant.

## 3.4 Results

### 3.4.1 Echocardiographic Assessments of Long-Term VNS

To determine both the *in vivo* acute and chronic effects of VNS on cardiac performance in the healthy animals, LV function was assessed using echocardiography at both Weeks 2 and 9 after VNS implantation. As presented in **Fig. 3.1**, VNS rats exhibited similar EF as compared to Sham rats throughout the duration of the study. Furthermore, EF did not change significantly over time in both Sham and VNS rats. Measurements of fractional shortening were also made, and no significant differences were observed (data not shown).

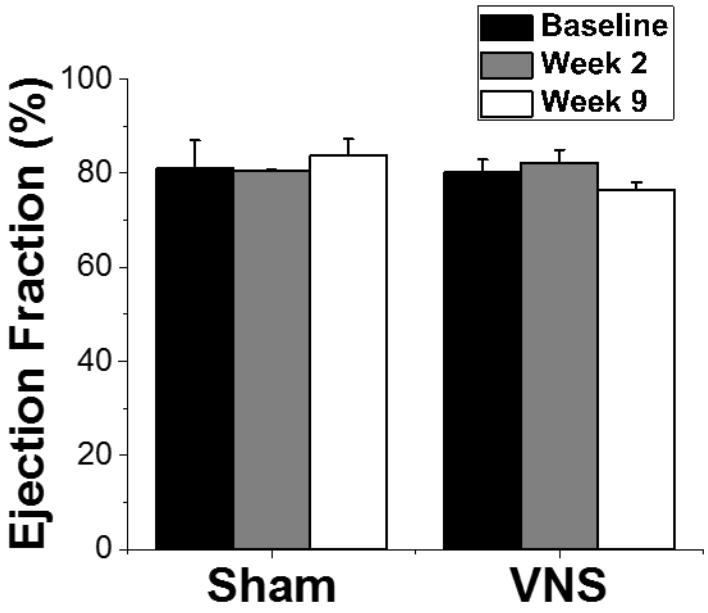


***Figure 3.1: Effects of long term intermittent VNS on left ventricular (LV) function.*** Mean ejection fraction (EF) (%) measurements from Sham and VNS rats for Baseline, Week 2, and Week 9.

### 3.4.2 Effect of VNS on Ventricular APD

*Ex vivo* optical mapping was used to probe action potential conduction and restitution dynamics in order to determine how long-term intermittent VNS modulates the basic electrophysiological properties of the healthy myocardium. Changes in APD were measured during periodic pacing at gradually decremented BCLs. **Fig. 3.2(a,b)** (top panels) show examples of 2D $APD_{80}$ and $APD_{50}$ maps, respectively, obtained at a BCL of 200 ms and 100 ms for both Sham and VNS-treated rats. The lower panels show corresponding traces of action potentials from a representative single pixel. **Fig. 3.2(a)** bottom panel compares VNS versus Sham traces at the same BCLs. APD from the VNS group is shorter than APD of the Sham group for BCL 200 ms, but not for 100 ms. **Fig. 3.2(b)** compares both VNS and Sham action potential traces that were recorded at different BCLs.

The change in APD of all VNS and Sham rats is shown in **Fig. 3.3(a)** for different BCLs. At higher BCLs (between 200 ms and 120 ms), the APDs of VNS rats (both $APD_{50}$ and $APD_{80}$) were significantly lower than those of Sham rats. For instance, at BCL 200 ms, the $APD_{80}$ and $APD_{50}$ values for Sham rats were 70.69 ± 0.34 ms and 45.39 ± 0.84 ms, respectively. After VNS treatment, the $APD_{80}$ and $APD_{50}$ values of VNS rats were both significantly ($p<0.05$) reduced to 60.12 ± 2.16 ms and 29.81 ± 1.59 ms, respectively. This APD shortening effect disappeared at lower BCLs (between 100 ms and 80 ms). At BCL 100 ms, the $APD_{80}$ values for Sham and VNS rats were 63.98 ± 1.82 ms and 61.87 ± 0.22 ms (p=NS), respectively. Furthermore, the $APD_{50}$ values for Sham and VNS rats were and 42.89 ± 1.42 ms and 37.22 ± 0.28 ms (p=NS).

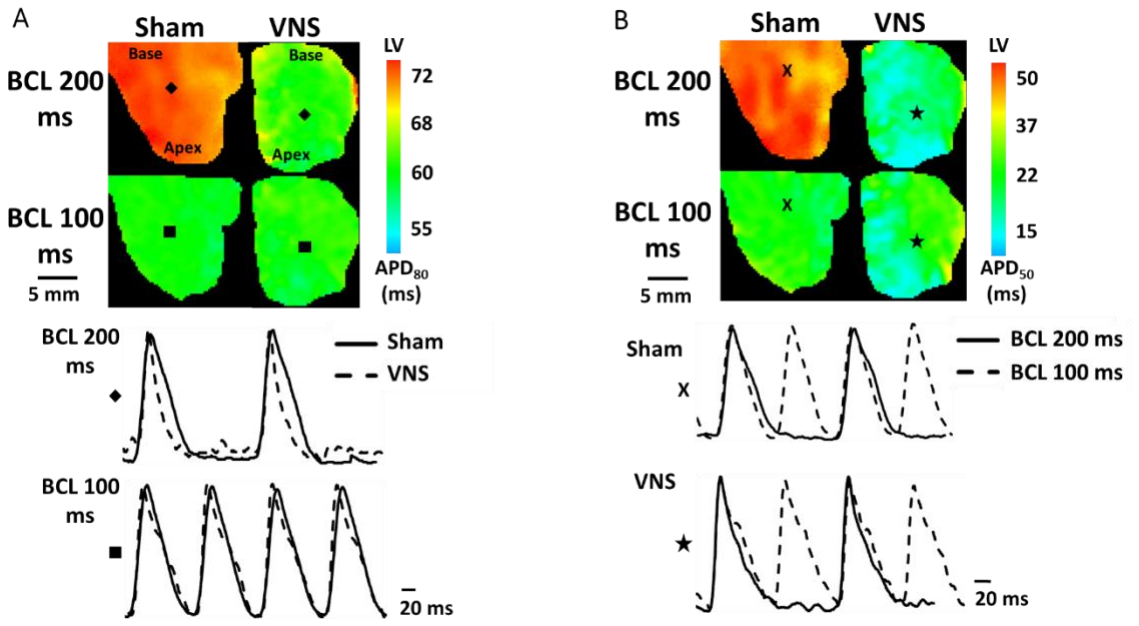


***Figure 3.2: Representative right ventricular (LV) action potential duration (APD) maps at basic cycle length (BCL) = 200 ms and 100 ms.*** **A)** Examples of $APD_{80}$ maps with action potential traces from pixels "◆" and "■" for BCLs = 200 ms and 100 ms, respectively. **B)** Examples of $APD_{50}$ maps with representative action potential traces from pixels "✕" and "★" for Sham and VNS, respectively.

### 3.4.3 Effect of VNS on Ventricular APD Restitution Properties

Calculation of the restitution properties of the heart (i.e. the change of APD as BCL decreases) showed that the APD of VNS rats (both $APD_{80}$ and $APD_{50}$) did not monotonically decrease as BCL decreased, in contrast to APDs of Sham rats (**Fig. 3.3.(a)**). Therefore, it was not feasible to fit the VNS data to a single curve and accurately calculate the slope of restitution curve for VNS rats, and we used an alternative approach, in which APD values at different BCLs were normalized to the APD value at BCL 200 ms for each individual rat. The mean normalized APD data for both Sham and VNS rats for $APD_{80}$ and $APD_{50}$ are shown in **Fig. 3.3(b,c)**, respectively. Note that $APD_{80}$ decreased as BCL decreases, showing normal restitution properties, both for VNS and Sham rats. However, the behavior of $APD_{50}$ is different: the monotonic decrease of APD was observed for Sham,

but a biphasic change of APD, with initial increase and subsequent decrease, was observed in VNS rats. These data suggests that VNS affects the dynamic behavior of the heart for $APD_{50}$, but not for $APD_{80}$.

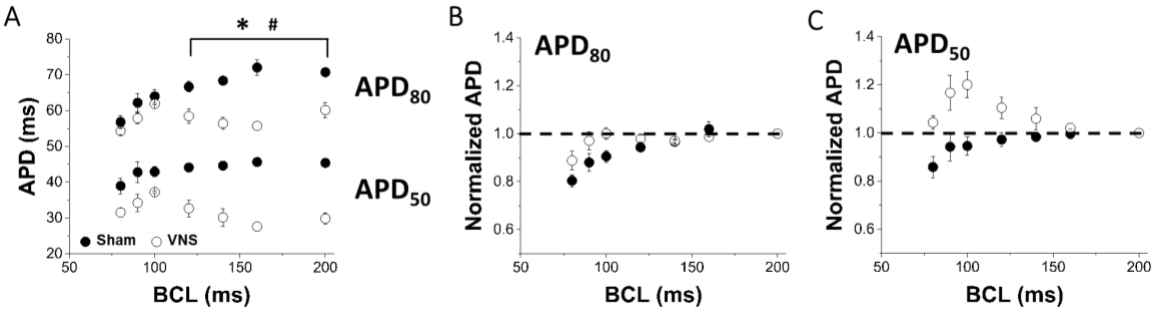


***Figure 3.3: Effects of long term intermittent VNS on APD.*** **A)** Mean $APD_{50}$ and $APD_{80}$ values for both Sham and VNS at different BCLs. Normalized **B)** $APD_{80}$ and **C)** $APD_{50}$ values to BCL 200. *, # Statistical significance ($p < 0.05$) between Sham and VNS for $APD_{80}$ and $APD_{50}$, respectively.

### 3.4.4 Effect of VNS on μ and CV

To determine whether VNS affected the spatial dispersion of APD, we calculated the heterogeneity index μ at different BCL values for both $APD_{50}$ and $APD_{80}$. The μ values calculated for BCL 200 ms and 100 ms are shown in **Fig. 3.4(a,b)**, demonstrating no significant differences in μ values between VNS and Sham at different BCLs. The values are similar for other BCLs (data not shown).

To investigate the effect of VNS on action potential propagation in the ventricular myocardium surfaces, we constructed activation time maps illustrating action potential propagation for both Sham and VNS groups at various BCLs. Representative examples of 2D activation time maps at BCL 100 ms is shown in **Fig. 3.5(b)**. These maps show normal propagation in both VNS and Sham rats. **Fig. 3.5(a)** shows mean CV data at different BCLs. Chronic VNS significantly increased the mean CV of impulse propagation in the ventricles for all BCL ($p<0.05$). Specifically, by 23% for BCL 200 ms (from 0.676 ± 0.024 m/s to 0.830 ± 0.039 m/s) and by 31% for BCL 100 ms (from 0.604 ± 0.026 m/s to 0.792 ± 0.045 m/s).

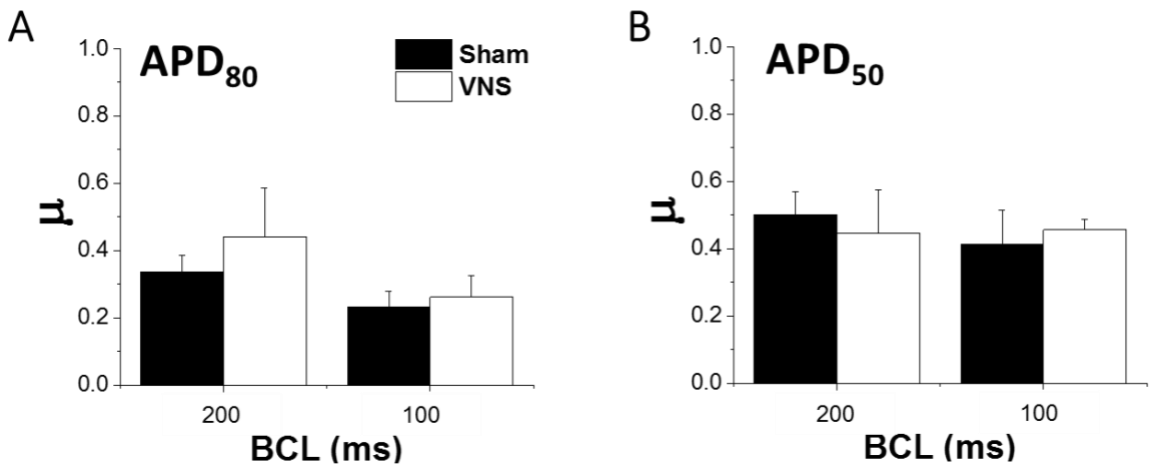


***Figure 3.4: Effects of VNS on spatial dispersion of APD (μ).*** Mean μ values for **A)** $APD_{80}$ and **B)** $APD_{50}$ for BCLs = 200 ms and 100 ms.

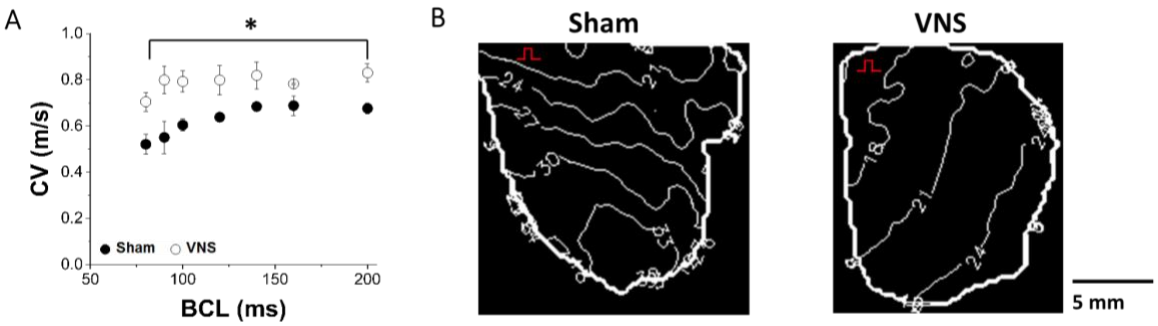


***Figure 3.5: Effects of VNS on and conduction velocity (CV).*** **A)** Mean CV values at different BCL values. **B)** Representative examples of LV action potential activation maps for the epicardial surfaces of Sham and VNS rats at BCL = 100 ms. Isochrones for activation time maps are shown 3 ms apart. The red marker denotes pacing site. *Statistical significance ($p < 0.05$).

### 3.4.5 VNS Prevents *Ex Vivo* Ventricular Arrhythmias

The anti-arrhythmic effects of VNS on healthy hearts were assessed by measuring the inducibility of the hearts to cardiac arrhythmias during *ex vivo* programmed electrical stimulation. As shown in **Fig, 3.6**, sustained VF/VT was observed in 3/4 Sham rats; whereas none (0/3) of the VNS rats developed VF or VT.

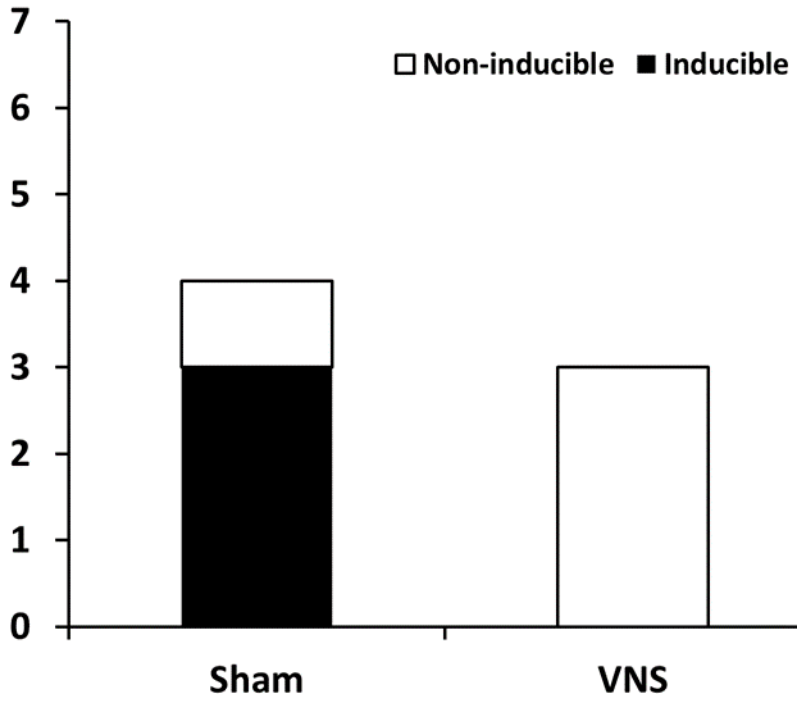


***Figure 3.6: Quantification of the number of rats exhibiting ex vivo ventricular fibrillation (VF) and tachycardia (VT) episodes during programmed stimulation.***

## 3.5 Conclusions and Discussion

In this study, we investigated the effects of chronic, cyclic VNS on healthy rat hearts. The main findings of this paper are as follows: 1) 10 weeks of intermittent VNS produced beneficial electrophysiological changes to the heart, including reduction of APD at larger BCLs and an increase of CV at all BCLs; 2) VNS did not induce any detrimental effects to the heart: neither affecting the LV function of the heart verified via

echocardiography nor increasing the spatial dispersion of APD (μ); 3) VNS significantly affected the restitution properties of the heart at the $APD_{50}$, but not at the $APD_{80}$, levels; 4) VNS had anti-arrhythmic effects of VNS that has been previously only reported for diseased hearts (Annoni et al., 2015; Beaumont et al., 2015). These results support the beneficial effects of VNS even in the absence of autonomic imbalance.

It is universally accepted that the autonomic nervous system, consisting of both the parasympathetic and sympathetic systems, plays an important role in regulating the function of the heart (De Ferrari and Schwartz, 2011; Hirsch et al., 1987; Schwartz and De Ferrari, 2011). In the last decades, an abundance of experimental and clinical evidence has shown that cardiovascular diseases are accompanied by an imbalance in the vagal-sympathetic outflow to the heart. It has been demonstrated that the autonomic balance can be potentially restored through the electrical stimulation of the vagus nerve (Annoni et al., 2015; Li et al., 2004; Premchand et al., 2015); however, not much is known about the effects of parasympathetic stimulation via VNS on healthy hearts where the sympathetic and parasympathetic nervous systems are in balance. This can be attributed to the early major belief that vagal fibers have sparse innervations and only play a limited role in ventricles. As histochemical evidence from several studies has now convincingly questioned this viewpoint (Coote, 2013; Hoover et al., 2004; Randall et al., 2003; Ulphani et al., 2010), it becomes increasingly important to gain a better and clearer understanding of the effects of VNS. This is especially true since VNS is now emerging as a promising neuromodulation therapy for HF due to positive results from multiple clinical trials, such

as the Autonomic Neural Regulation Therapy to Enhance Myocardial Function in Heart Failure (ANTHEM-HF) (Premchand et al., 2015).

Slowing of myocardial CV may increase the risk of cardiac arrhythmias (Gaztañaga et al., 2012). This is because a decrease in CV allows the creation of smaller wavelengths, thus facilitating the initiation and maintenance of reentry subsequent to creation of functional conduction block. Our data suggest that VNS is able to moderately increase CV. This increase can be attributed to the increase or further preservation of the gap junction protein, connexin-43 (Cx-43) expression in the myocardium (Sabbah, 2011). It has been shown in previous studies that VNS is able to preserve the expression of Cx-43 in a rat model of MI (Wu and Lu, 2011).

Prolongation of the ventricular APD is a hallmark of HF (Shah et al., 2005). In cases of HF, APD prolongation allows for the myocardium to preserve its contractility by prolonging calcium channel opening. However, this compensatory APD prolongation also causes intracellular calcium overload, increasing the propensity for triggered arrhythmias and increased T-wave alternans (Shimizu and Antzelevitch, 1999). Furthermore, this significant APD prolongation is typically associated with an increase in dispersion of repolarization (Wang and Hill, 2010). In other words, increases in both of these parameters have been shown to be able to create an arrhythmogenic substrate. Our results suggest that long-term intermittent VNS therapy decreases APD during programmed electrical stimulation and does not induce spatial APD dispersion, thereby rendering the hearts less vulnerable to inducible tachyarrhythmia as shown in Fig. 3-6.

Indeed, in the settings of HF with the characteristics of APD prolongation and CV slowing, which may promote reentrant arrhythmias, our observed effects of APD shortening and CV acceleration may be able to explain the beneficial effects of VNS. This, however, may be different in healthy hearts. In fact, it is important to note that APD shortening induced by activation of acetylcholine-activated potassium channels has been widely used as an arrhythmia model (Machida et al. 2011; Cho et al. 2014), and CV slowing has been an anti-arrhythmic feature of Class I anti-arrhythmic drugs (Cha et al. 1996; Kirchhof et al. 1998). APD shortening and CV acceleration have opposite effects on the wavelength for reentry, i.e. wavelength is the product of APD and CV which both are measured at a particular BCL. The wavelength can be used as an indicator of arrhythmia propensity in structurally normal hearts (Smeets et al. 1986; Pandit & Jalife 2013).

Finally, our results suggest that VNS may affect the restitution properties of the heart, specifically at the $APD_{50}$ level, which may suggest an increase in intracellular calcium handling. Our findings seem to support recent findings where VNS treatment activates the ryanodine receptor 2 (RyR2) channels (Li et al. 2015) and increases both sarcoplasmic reticulum $Ca^{2+}$ ATPase (SERCA2) and sodium-calcium exchanger (NCX1) protein expressions in a chronic HF rat model (Zhang et al. 2015). The activation of RyR2 channels increases calcium release from the sarcoplasmic reticulum (SR) (systole) which SERCA2 will pump the calcium back to the SR (diastole). Taken together, VNS is able to increase the expression levels of RyR2 and SERCA2; thus, enhancing excitation contraction coupling and improving cardiac pump function. Nonetheless, additional

experiments will need to be performed to specifically determine which myocyte membrane ion channels are up-or downregulated by chronic VNS.

There were limitations to this study. While we were able to demonstrate the effects of VNS on the electrophysiological properties of the healthy myocardium, no histochemical results from the ventricles were performed in parallel to confirm and/or investigate mechanisms. Another limitation is that an animal group with age-matched controls, i.e. that did not have an implanted stimulator and electrode, was not included in the present study. However, since the objective of our study was to directly investigate the effects of VNS, we removed the confounding factor of surgical procedure effects on electrophysiology by implanting non-functional stimulators in our Sham group. Hence, not including such a control group will not affect the interpretation of our results. The conclusions of our study are also limited by the small sample size of rats used.

In conclusion, we demonstrate that the administration of chronic intermittent VNS induces electrophysiological changes to a normal, healthy rat heart; thus, rendering the hearts less vulnerable to inducible arrhythmias. These results also suggest that VNS does not require the existence of autonomic imbalance to generate its positive effects.

# CHAPTER 4 CONTRIBUTIONS OF ATRIAL AND VENTRICULAR $M_2R$-$I_{KACh}$ SIGNALING PATHWAYS IN THE CHRONOTROPIC EFFECTS OF VNS

**(In Preparation for Manuscript Submission)**

S.W. Lee*, A. Anderson*, P.A. Guzman, A. Nakano, E.G. Tolkacheva, and K. Wickman, "Atrial GIRK channels mediate the effects of vagus nerve stimulation on heart rate dynamics and arrhythmogenesis." **(*Authors contributed equally to the study)**

## 4.1 Chapter Synopsis

Activation of the parasympathetic branch of the autonomic nervous system, carried primarily by the vagus nerve, slows heart rate (HR) and increases HR variability (HRV). Recently, vagus nerve stimulation (VNS) has gained attention as a potential neuromodulatory technique to therapeutically regulate cardiac physiology. Therefore, there is renewed interest in understanding the multiple downstream signaling pathways which may underlie these effects. Here, we investigated the impact of one such downstream effector, the G-protein-coupled inwardly-rectifying $K^+$ (GIRK) channel, on the chronotropic effects of acute VNS in mice. We collected *in vivo* electrocardiogram (ECG) recordings from mice lacking GIRK channels either globally or selectively in the atria or

ventricle during VNS. VNS induced bradycardia and increased HRV in wild-type mice and mice lacking GIRK in the ventricle. Global and atrial ablation of GIRK channels significantly blunted both HR and HRV responses to acute VNS. Additionally, both mice with either global or atrial ablation of GIRK channels were resistant to arrhythmic episodes induced by VNS. These data suggest that atrial GIRK channels are dominant mediators for VNS-induced dynamic changes in HR, HRV, and arrhythmogenesis in *in vivo* mice hearts.

## 4.2 Introduction

The autonomic nervous system is comprised of two main branches, parasympathetic and sympathetic, which work antagonistically to maintain cardiovascular homeostasis (Gordan et al., 2015). Autonomic dysregulation, characterized by excessive sympathetic activation and diminished parasympathetic response, is central to the pathogenesis of cardiovascular diseases, such as heart failure and hypertension (Bibevski and Dunlap, 2011; Schwartz and De Ferrari, 2011). Hence, autonomic modulation approaches to increase parasympathetic activity have emerged as a potential therapeutic strategy. As parasympathetic innervation to the heart is primarily carried by efferent fibers of the vagus nerve, vagus nerve stimulation (VNS) has shown promise in treating cardiovascular diseases (Beaumont et al., 2015; Premchand et al., 2015; Xie et al., 2014). As a result, VNS has gained significant popularity in recent years and there is renewed interest in understanding the downstream mechanisms of its actions in the heart..

Activation of the parasympathetic nervous system results in a decrease in heart rate (HR) and an increase in beat-to-beat variability, known as heart rate variability (HRV) (Ardell et al., 2015; Armour et al., 1975; Levy and Zieske, 1969; Libbus et al., 2017; Neely

and Urthaler, 1992; Thompson et al., 1998). Parasympathetic regulation of HR is mediated largely through the release of the neurotransmitter acetylcholine (ACh) which activates muscarinic $M_2$ receptors ($M_2R$), subsequently releasing inhibitory (Gi/o) G-proteins. Activation of these inhibitory G-proteins results in the dissociation of the $\alpha$ and $\beta\gamma$ subunits. The $G_\alpha$ subunit inhibits adenylyl cyclase activity which suppresses cAMP-dependent signaling, inhibiting both the HCN channel (pacemaker or "funny" current, $I_f$) and L-type $Ca^{2+}$ channel activity (DiFrancesco, 2010; DiFrancesco et al., 1989; DiFrancesco and Borer, 2007; Kozasa et al., 2018; Mangoni and Nargeot, 2008; Zaza et al., 1996). The $\beta\gamma$ subunit activates the atrial G-protein gated inwardly rectifying $K^+$ (GIRK) channel, often referred to as $I_{KACh}$. The GIRK channel is a heterotetramer composed of two distinct homologous GIRK channel subunits: GIRK1 ($K_{ir}3.1$) and GIRK4 ($K_{ir}3.4$) (Liang et al., 2014; Vorobiov et al., 2000; Wydeven et al., 2014). Activation of GIRK channels increases $K^+$ efflux, resulting in membrane hyperpolarization which ultimately contributes to the slowing of pacemaker activity and sinus rate (Anderson et al., 2018; Mesirca et al., 2016a; Wickman et al., 1998).

The direct contributions of cardiac GIRK channel activity to the acute chronotropic effects of VNS have yet to be fully elucidated. Previous work has suggested, through methoxamine-induced parasympathetic activation in *Girk4*$^{-/-}$ mice, that approximately 50% of bradycardia elicited is GIRK dependent, while the other 50% is likely mediated via $I_f$ or other currents (Wickman et al., 1998). Indeed, a recent study utilizing mice with knockdown of HCN4 show exaggerated responses to direct VNS (Kozasa et al., 2018). Since previous studies have shown that pharmacological manipulations do not consistently

recapitulate the effects of direct neuronal stimulation on cardiac electrophysiology (Mantravadi et al., 2007), the contributions of GIRK channel activation to the effects of direct VNS remain unclear. Here, we investigated the specific role of cardiac GIRK channels in mediating the chronotropic effects of VNS on the heart. This study is the first to evaluate the impact of GIRK channel ablation globally or selectively in the atrial or ventricular tissues on the chronotropic effects of direct VNS in mice *in vivo*.

## 4.3 Materials and Methods

All experiments were performed in accordance with the guidelines set forth by the National Institutes of Health *Guide for the Care and Use of Laboratory Animals* and were approved by the University of Minnesota Institutional Animal Care and Use Committee (IACUC).

### 4.3.1 Transgenic Murine Models

*Wild-type (C57BL/6J)* mice were purchased from The Jackson Laboratory (Bar Harbor, ME, USA). The generation of *Girk4*$^{-/-}$ and *MLC2VCre(+):Girk1*$^{fl/fl}$ mice was described previously (Anderson et al., 2018; Wickman et al., 1998). *Girk1*$^{fl/fl}$ mice were crossed with *SLNCre(+)* mice (Nakano et al., 2011) to generate the *SLNCre(+):Girk1*$^{fl/fl}$ line. All transgenic mouse lines were bred, validated, and provided by Allison Anderson and Dr. Kevin Wickman. All mice were housed in a quiet, temperature- and humidity-controlled room with a 12:12 hour light–dark cycle. Food and water were available ad libitum.

### 4.3.2 Vagus Nerve Bipolar Cuff Electrode Implantation

Mice were anesthetized with isoflurane (5% for induction and 1.5% for maintenance). After hair removal and skin cleaning, aseptic technique was used to make a

ventral midline incision in the neck, and the skin and muscles were retracted. After identifying and isolating the right vagus nerve, a custom helical lead bipolar cuff electrode (Cyberonics, USA) was implanted around the nerve. The electrode was then connected to the VNS pulse generator (Demipulse Model 103, Cyberonics, Inc., Houston, USA).

### *4.3.3 In vivo* ECG Recordings

Electrocardiograms (ECG) were recorded from each anesthetized mouse (IX-ECG-12, iWorx, USA). ECG electrodes were placed subcutaneously into the limbs. Mice were anesthetized with 1.5% isoflurane supplemented with an air mixture of 40% $O_2$/60% $N_2$ to sustain stable HR. Baseline ECG recordings were recorded for 2–10 min, at which point VNS was administered.

The six different groups of mice (n = 45, 2 – 3 months old) of approximately equal numbers of both sexes were used in the VNS experimental protocol (**Fig. 4.1**). After collecting baseline ECG recordings, VNS (0.25 mA, 10 Hz, 500 μsec) was then continuously delivered for 1 min. For each mouse, several (1-5) *stimulation runs* (see below) were performed. Afterwards, atropine (Sigma Aldrich, USA, 2.0 mg/kg) was administered via intraperitoneal (IP) injection, and after a 10 min waiting period, 1-2 *stimulation runs* were performed.

Each *stimulation run* consisted of the following *in-vivo* ECG recordings (**Fig. 4.1**):

(1) 1 min of baseline recording before VNS (**PRE**)

(2) 1 min of recording during continuous VNS (**ON**)

(3) 1 min of recording during recovery after VNS (**POST**)

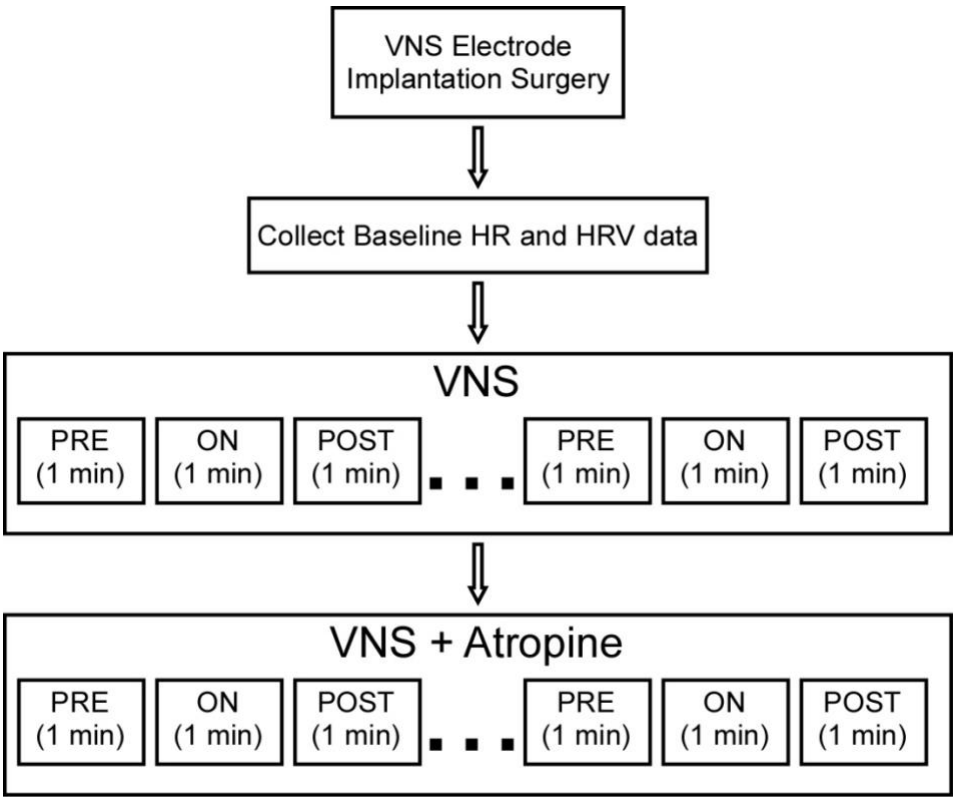


***Figure 4.1: Detailed schematic of the experimental stimulation run.*** VNS electrodes was placed around the cervical vagus nerve. VNS (0.25 mA, 10 Hz, 500 µsec) was administered continuously. Atropine (2.0 mg/kg) was injected IP to block the activity of the muscarinic receptors. Several (1-5) stimulation runs were collected which consists of **PRE** (baseline recording), **ON** (continuous VNS), **POST** (recovery).

### 4.3.4 Data Analysis for *In vivo* ECG Recordings

The *in-vivo* ECG recordings from all *stimulation runs* were used to quantify changes in the HR and HRV throughout the study using Kubios HRV 2.0 software (Tarvainen et al., 2014). All values were averaged over 1 min **PRE**, **ON**, and **POST** periods of VNS stimulation. Noisy data segments, premature atrial complexes (PACs), and arrhythmic episodes were excluded, and only steady-state data after initial adjustment of the HR to acute VNS were used for the analysis.

To account for variations in baseline HR, the chronotropic effect of VNS was determined by calculating a relative change in HR, $\Delta HR_{ON}$, as the following:

$$\Delta HR_{ON} = \left(\frac{HR_{ON} - HR_{PRE}}{HR_{PRE}}\right) * 100\%$$

where $HR_{ON}$ and $HR_{PRE}$ are the mean HR during the VNS **ON** and **PRE** periods, respectively.

To quantify the variation of beat-to-beat intervals, HRV was calculated as the ratio between the standard deviation of RR intervals to mean of RR intervals, as descried previously (McIntyre et al., 2014):

$$HRV = \left(\frac{SDRR}{Mean\ RR}\right) * 100\%$$

The number of mice that exhibited arrhythmic episodes were also quantified during both **PRE** and **ON**. An arrhythmic episode was defined as any of the following episodes: 1) skipped beats, 2) bigeminy, 3) bradycardia (at least 25 bpm less than the mean **PRE** or **ON** HR and lasted for more than 2 s), and 4) tachycardia (at least 25 bpm more than the mean **PRE** or **ON** HR and lasted for more than 2 s). PAC episodes were separated from all other arrhythmic events, as PACs can occur in healthy conditions and pose less threat to the heart than the other types of arrhythmias (Shindler and Kostis, 2009).

### 4.3.5 Statistical Analysis

All data are presented as mean ± SEM. A student's t-test, 2-way ANOVA with repeated measures, and Fisher's exact test were used as appropriate. For studies involving 2-way ANOVA analysis, interaction is reported if one was detected. *Post-hoc* analysis (Bonferroni multiple comparison) was used when appropriate. The level of significance was set at $P < 0.05$.

## 4.4 Results

### 4.4.1 Impact of GIRK ablation on basal regulation of HR and HRV

As functional GIRK channels are present in both atrial and ventricular tissue (Coote, 2013; Harvey and Belevych, 2003; Kurachi et al., 1986; Lomax et al., 2003; Ulphani et al., 2010), we aimed to distinctively assess and compare the relative contributions of tissue specific GIRK channel in mediating the bradycardic effects of VNS. Hence, in addition to the *SLNCre* mice line, we also included a recently developed ventricular GIRK knockout mouse line which was generated by crossing *Girk1*$^{fl/fl}$ mice with the *MLC2VCre* line (Anderson et al., 2018). Prior to VNS protocol initiation, we recorded baseline HR and HRV values to investigate the consequences of GIRK channel ablation on HR regulation *in vivo*. We did not observe a difference in baseline HR or HRV between wild-type and *Girk4*$^{-/-}$ mice (**Fig. 4.2(a,b)**). Similarly, there were no significant differences in baseline HR and HRV between *SLNCre(-):Girk1*$^{fl/fl}$ and *SLNCre(+):Girk1*$^{fl/fl}$ littermates (**Fig. 4.2(a,b)**). Lastly, *MLC2VCre(-):Girk1*$^{fl/fl}$ and *MLC2VCre(+):Girk1*$^{fl/fl}$ mice displayed comparable baseline HR and HRV values (**Fig. 4.2(a,b)**). These results indicate that GIRK channel ablation did not cause a significant difference in resting mean HR and HRV.

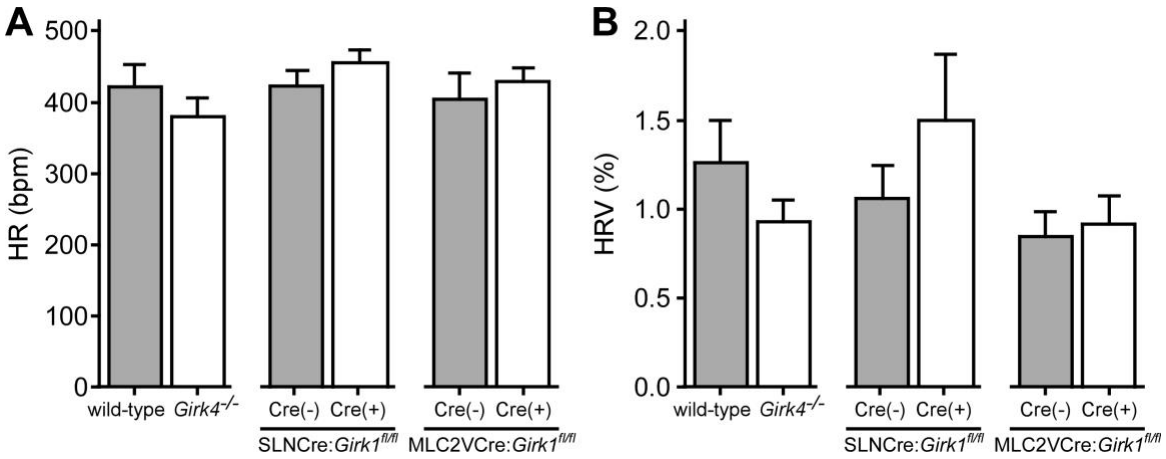


***Figure 4.2: Influence of GIRK channels on baseline HR and HRV.*** **A)** Summary of baseline HR data across genotypes. There were no significant differences between wild-type (n=10) and *Girk4*$^{-/-}$ (n=10) mice ($t_{18}$=1.0; *P*=0.32), *SLNCre(-):Girk1*$^{fl/fl}$ (n=6) and *SLNCre(+):Girk1*$^{fl/fl}$ (n=5) littermates ($t_9$=1.1; *P*=0.29), and *MLC2VCre(-):Girk1*$^{fl/fl}$ (n=6) and *MLC2VCre(+):Girk1*$^{fl/fl}$ (n=8) littermates ($t_{12}$=0.7; *P*=0.51). **B)** Summary of baseline HRV data across genotypes. There were no significant differences between wild-type (n=10) and Girk4-/- (n=10) mice ($t_{18}$=1.2; *P*=0.23), *SLNCre(-):Girk1*$^{fl/fl}$ (n=5) and *SLNCre(+):Girk1*$^{fl/fl}$ (n=5) littermates ($t_8$=1.1, *P*=0.32), and *MLC2VCre(-):Girk1*$^{fl/fl}$ (n=6) and *MLC2VCre(+):Girk1*$^{fl/fl}$ (n=8) littermates ($t_{12}$=0.32; *P*=0.76).

### 4.4.2 Contributions of GIRK channels to the acute effects of VNS on HR

We next sought to probe the consequences of GIRK channel ablation on the bradycardic effects of acute VNS by comparing the relative change in HR during VNS **ON** to **PRE** values ($\Delta HR_{ON}$). We observed pronounced VNS-induced bradycardia in wild-type mice (**Fig. 4.3(c)**). This dramatic HR decrease was significantly blunted in *Girk4*$^{-/-}$ (**Fig. 4.3(c)**). Similarly, *SLNCre(+):Girk1*$^{fl/fl}$ mice displayed minimal VNS-induced HR reduction as compared to *SLNCre(-):Girk1*$^{fl/fl}$ mice (**Fig. 4.3(a-c)**). On the other hand, the VNS-induced HR decrease was comparable between *MLC2VCre(+):Girk1*$^{fl/fl}$ and *MLC2VCre(-):Girk1*$^{fl/fl}$ mice (**Fig. 4.3(c)**). Regardless of genotype, VNS **POST** values returned back to baseline **PRE** values after the cessation of VNS (data not shown). Next, to investigate if the chronotropic effects of VNS were dependent on activation of muscarinic receptors, atropine (2.0 mg/kg) was administered before the VNS protocol was run again after a 10 min waiting period. In the presence of atropine, the negative chronotropic effects of VNS were suppressed regardless of genotype (**Fig. 4.3(d)**). Overall, our results show that bradycardia induced by VNS in the mouse is almost entirely dependent on muscarinic activation of atrial GIRK channels.

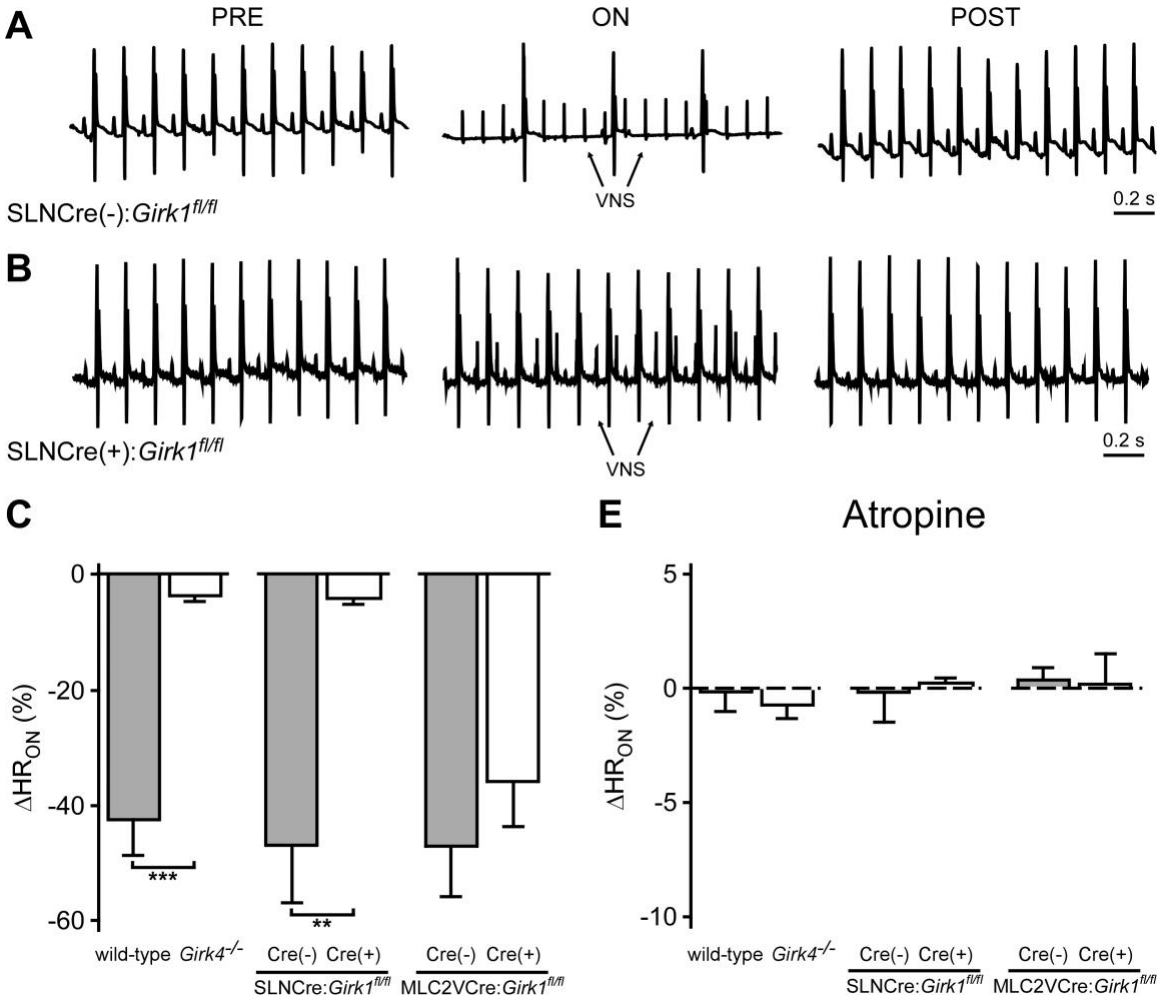


***Figure 4.3: Impact of GIRK channel ablation on the negative chronotropic effects of VNS.*** Representative raw ECG recording traces of anesthetized **A)** *SLNCre(-):Girk1*$^{fl/fl}$ and **B)** *SLNCre(+):Girk1*$^{fl/fl}$ mice at the following points of the VNS protocol: **PRE** (left) **ON** (middle) and **POST** (right). Note the presence of small spikes on the ECG traces during the **ON** periods corresponding to VNS stimulation artifacts. **C)** Relative change in HR drop during VNS **ON** ($\Delta HR_{ON}$) for all genotypes prior to atropine administration. There is a significant difference in HR drop observed between wild-type (n=9) and *Girk4*$^{-/-}$ (n=10) mice ($t_{17}$=6.5; $P$<0.001). Similarly, a significant difference in HR drop was observed between *SLNCre(-):Girk1*$^{fl/fl}$ (n=6) and *SLNCre(+):Girk1*$^{fl/fl}$ (n=5) littermates ($t_9$=3.9; $P$<0.01). No significant difference was detected between *MLC2VCre(-):Girk1*$^{fl/fl}$ (n=6) and *MLC2VCre(+)Girk1*$^{fl/fl}$ (n=8) littermates ($t_{12}$=0.95; $P$=0.36). Symbols: ***$P$<0.001 vs. wild-type; **$P$<0.01 vs. *SLNCre(-)Girk1*$^{fl/fl}$ mice. **D)** Relative change in HR drop during VNS **ON** ($\Delta HR_{ON}$) for all genotypes after atropine administration. There were no significant difference between wild-type (n=4) and *Girk4*$^{-/-}$ (n=6) mice ($t_8$=0.6; $P$=0.59), *SLNCre(-)Girk1*$^{fl/fl}$ (n=6) and *SLNCre(+)Girk1*$^{fl/fl}$ (n=4) littermates ($t_8$=0.2; $P$=0.82), and

*MLC2VCre(-):Girk1*$^{fl/fl}$ (n=6) and *MLC2VCre(+):Girk1*$^{fl/fl}$ (n=4) littermates ($t_8$=0.2, *P*=0.88).

### 4.4.3 Influence of GIRK channels to the acute effects of VNS on HRV

To assess how GIRK ablation impacts beat-to-beat variation in HR induced by VNS, we measured HRV during **PRE** and **ON** periods of VNS. During VNS **ON**, a significant increase in HRV was observed in wild-type mice (**Fig 4.4(b)**). This increase in HRV during VNS **ON** was significantly diminished in *Girk4*$^{-/-}$ mice (**Fig 4.4(b)**). Similarly, HRV increased during VNS **ON** in *SLNCre(-):Girk1*$^{fl/fl}$ control mice, but was absent in *SLNCre(+):Girk1*$^{fl/fl}$ mice (**Fig 4.4(a-b)**). HRV during VNS **ON** increased similarly in both *MLC2VCre(-):Girk1*$^{fl/fl}$ and *MLC2VCre(+):Girk1*$^{fl/fl}$ mice (**Fig 4.4(b)**). Notably, atropine blocked the VNS-induced increase in HRV in all genotypes, demonstrating the dependence of this effect on muscarinic receptor activation (**Fig 4.4(c)**). These results indicate that the VNS-induced increase in HRV in mice is primarily mediated through activation of atrial GIRK channels.

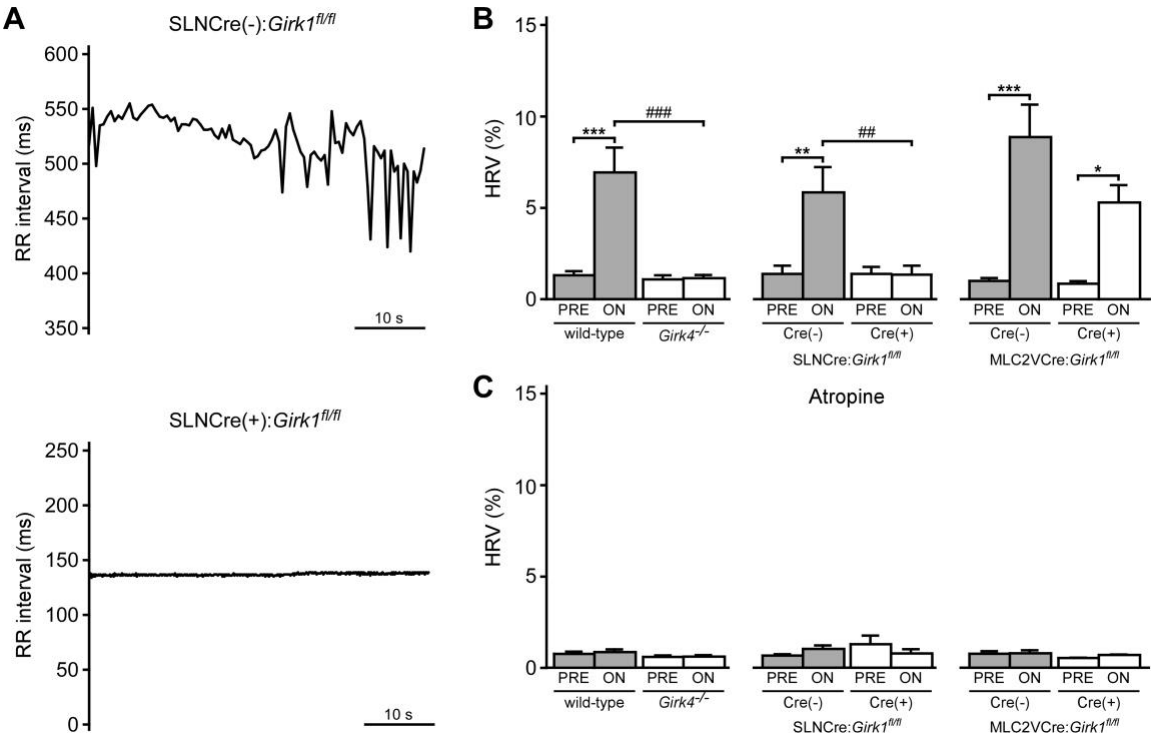


***Figure 4.4: Impact of GIRK channel ablation on VNS-induced HRV increase.*** **A)** Typical RR tachograms during VNS **ON**, comparing between the beat-to-beat changes in RR intervals between *SLNCre(-):Girk1*$^{fl/fl}$ (top) and *SLNCre(+):Girk1*$^{fl/fl}$ (bottom) mice. **B)** Summary of mean HRV data at **PRE** and **ON** VNS prior to atropine administration. Two-way ANOVA analysis revealed an interaction between genotype and treatment between wild-type (n=8) and *Girk4*$^{-/-}$ (n=10) mice ($F_{1,16}$=20.3; $P$<0.001), and between *SLNCre(-):Girk1*$^{fl/fl}$ (n=6) and *SLNCre(+):Girk1*$^{fl/fl}$ (n=5) littermates ($F_{1,9}$=12.8; $P$<0.01). There was a significant main effect of treatment ($F_{1,12}$=44.0; $P$<0.001) between *MLC2VCre(-):Girk1*$^{fl/fl}$ (n=6) and *MLC2VCre(+)Girk1*$^{fl/fl}$ (n=8) littermates, but no main effect of genotype ($F_{1,12}$=4.2; $P$=0.06) or interaction between genotype and treatment ($F_{1,12}$=3.2; $P$=0.10). Symbols: *,**,*** $P$<0.05, 0.01, and 0.001, respectively, vs. **PRE** (within genotype); $^{###}P$<0.001, **ON** wild-type vs. *Girk4*$^{-/-}$; $^{##}P$<0.01, **ON** *SLNCre(-):Girk1*$^{fl/fl}$ vs. *SLNCre(+):Girk1*$^{fl/fl}$. **C)** Summary of mean HRV data at **PRE** and **ON** VNS after atropine administration. There was no main effect of treatment or genotype ($F_{1,8}$=2.0, $P$=0.19), or interaction between genotype and treatment ($F_{1,8}$=3.2; $P$=0.11) between wild-type (n=4) and *Girk4*$^{-/-}$ (n=6) mice. There was no main effect of treatment ($F_{1,8}$=0.1, $P$=0.76) or genotype ($F_{1,8}$=0.53, $P$=0.49), and no interaction between treatment and genotype ($F_{1,8}$=3.5, $P$=0.1) between *SLNCre(-):Girk1*$^{fl/fl}$ (n=6) and *SLNCre(+):Girk1*$^{fl/fl}$ (n=4) littermates. There was no main effect of treatment ($F_{1,7}$=0.45, $P$=0.52 or genotype ($F_{1,7}$=0.79, $P$=0.40), and no interaction between treatment and genotype ($F_{1,7}$=0.3; $P$=0.62) between *MLC2VCre(-):Girk1*$^{fl/fl}$ (n=6) and *MLC2VCre(+)Girk1*$^{fl/fl}$ (n=4) littermates.

### 4.4.4 Impact of GIRK channels on VNS-induced arrhythmias

To explore the contributions of GIRK channels on VNS-induced arrhythmogenesis, we quantified arrhythmia occurrences (i.e., bigeminy, skipped beats, tachycardia, and bradycardia) during VNS **ON** (**Fig. 4.5(a)**). No mice displayed arrhythmic episodes prior to VNS (data not shown). However, arrhythmic episodes were commonly observed in wild-type, *SLNCre(-):Girk1$^{fl/fl}$*, *MLC2VCre(+):Girk1$^{fl/fl}$*, and *MLC2VCre(-):Girk1$^{fl/fl}$* mice during VNS **ON** (**Fig. 4.5(b)**). In contrast, both *Girk4$^{-/-}$ and SLNCre(+):Girk1$^{fl/fl}$* mice were resistant to VNS-induced arrhythmias (**Fig. 4.5(b)**). Similarly, these arrhythmic episodes were no longer observed after atropine administration during VNS **ON** (data not shown). No significant difference in the number of mice exhibiting PACs was observed **PRE** (data not shown) or **ON** (**Fig. 4.5(c)**) across all genotypes, suggesting that GIRK channels do not play a major role in the formation of PACs. Overall, these findings suggest that atrial GIRK channels play a critical role in the induction of arrhythmias via VNS.

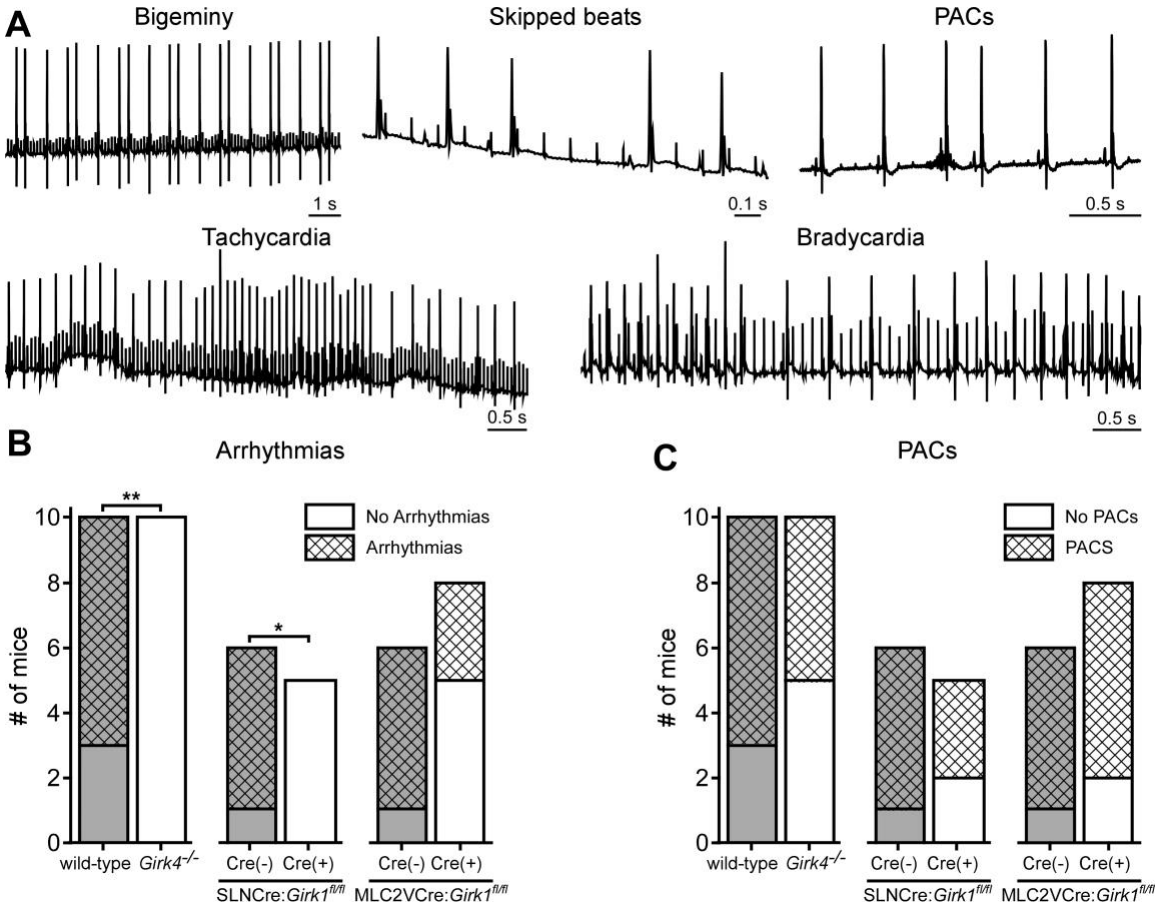


***Figure 4.5: Role of GIRK channels in VNS-induced arrhythmias*. A)** Representative examples of anesthetized raw ECG recordings of arrhythmic (i.e., bigeminy, skipped beats, bradycardia, and tachycardia) and PAC episodes during VNS **ON**. **B)** Total number of mice exhibiting arrhythmic episodes during VNS **ON**. Fisher's exact test revealed a significant difference in arrhythmia incidence between wild-type (n=10) and *Girk4*$^{-/-}$ (n=10) mice ($P$<0.01), and *SLNCre(-)Girk1*$^{fl/fl}$ (n=6) and *SLNCre(+)Girk1*$^{fl/fl}$ (n=5) littermates ($P$<0.05), but no difference between *MLC2VCre(-):Girk1*$^{fl/fl}$ (n=6) and *MLC2VCre(+):Girk1*$^{fl/fl}$ (n=8) littermates ($P$=0.14). Symbols: **$P$<0.01 vs. wild-type; *$P$<0.05 vs. *SLNCre(-)Girk1*$^{fl/fl}$. **C)** Total number of mice exhibiting PACs during VNS **ON**. Fisher's exact test revealed no significant differences in PAC incidence between wild-type (n=10) and *Girk4-/-* (n=10) mice ($P$=0.65), *SLNCre(-)Girk1fl/fl* (n=6) and *SLNCre(+)Girk1fl/fl* (n=5) littermates ($P$=0.55), or *MLC2VCre(-)Girk1*$^{fl/fl}$ (n=6) and *MLC2VCre(+)Girk1*$^{fl/fl}$ (n=8) littermates ($P$=1.0).

## 4.5 Conclusions and Discussion

VNS has received increased attention recently due to the potentially protective role it plays in various heart diseases (Beaumont et al., 2015; Premchand et al., 2015; Xie et al., 2014). Yet, the underlying mechanisms by which VNS affects the heart remain to be fully elucidated. Cardiac cholinergic signaling is a complex biological phenomenon involving the interactions of several ion channels following the activation of muscarinic receptors after the release of ACh. Several pharmacological and genetic studies have suggested that GIRK channels, voltage gated $Ca^{2+}$ channels, and the $I_f$ current are all downstream effectors of muscarinic activation, each contribute to parasympathetic regulation of the heart (DiFrancesco et al., 1989; DiFrancesco and Borer, 2007; Liang et al., 2014; Mangoni and Nargeot, 2008; Mesirca et al., 2013; Vorobiov et al., 2000; Wickman et al., 1998; Zaza et al., 1996). However, the relative contributions of each of these ion channels have not been distinctively investigated. This study is the first to apply VNS on transgenic GIRK-deficient mice, thereby specifically assessing the role of the muscarinic GIRK signaling pathway in mediating the chronotropic effects of VNS *in vivo*.

Previous reports have shown that *Girk4*$^{-/-}$ mice displayed blunted HR and HRV responses to the impact of pharmacological stimulation of the parasympathetic system (Mesirca et al., 2013; Wickman et al., 1998). Here, we observed that nearly all of the HR and HRV responses to electrical stimulation of the vagus nerve is absent in *Girk4*$^{-/-}$. Furthermore, the administration of atropine yielded similar results, demonstrating the muscarinic dependence of this response. Thus, these results highlight that muscarinic-GIRK channel signlaing plays a significant role in the negative chronotropic effects of

VNS. Notably, studies have shown that functional GIRK channels are not only exclusively located in atria, but rather are also present in the ventricles (Coote, 2013; Harvey and Belevych, 2003; Kurachi et al., 1986; Liang et al., 2014; Lomax et al., 2003; Ulphani et al., 2010). Hence, we used mouse lines by which GIRK channels were selectively ablated in the ventricles (Anderson et al., 2018) and in the atria. Mice lacking GIRK channels selectively in atrial tissue recapitulated the striking lack of HR and HRV responses to VNS observed in the *Girk4*$^{-/-}$mice. Taken together, our results strongly suggest that atrial GIRK channels are the main contributor in the parasympathetic regulation of HR induced by VNS.

Nonetheless, the finding that almost all the HR and HRV effects of acute VNS can be attributed to atrial GIRK as the downstream effector is surprising. Given that there are data suggesting that other effectors should also play a significant role in modulating the chronotropic effects of parasympathetic stimulation in addition to GIRK channel activity (Mesirca et al., 2015, 2016b; Verkerk and Wilders, 2014). This could be due to the fact that we applied "high-level" VNS with our set of stimulation parameters. In fact, DiFrancesco et al showed an ACh concentration-dependent effect in activating $I_f$ and $I_{KACh}$ in SA nodal cells: low doses of ACh in the nanomolar concentrations inhibits $I_f$ while a 20-fold higher concentrations are required to activate $I_{KACh}$ (DiFrancesco et al., 1989). Hence, additional studies are warranted to quantify and correlate the level of ACh release with a given a set of VNS parameters.

In addition to being used as a therapy to treat heart diseases (Beaumont et al., 2015; Premchand et al., 2015; Xie et al., 2014), VNS has also been used to induce and maintain

atrial fibrillation (AF) in large animal studies (Zhang and Mazgalev, 2011), and our results further highlight this pro-arrhythmic property. However, it is worth noting that there are important differences between the two applications. Both experimental and clinical VNS have been shown to be effective in treating heart failure when mild to moderate intensities are delivered, reducing HR by 10% or less (Zhang et al., 2009a). In contrast, VNS is arrhythmogenic when strong supra-threshold intensities are delivered, causing a significant HR reduction, as supported in this study (Akdemir and Benditt, 2016). In addition, this study further highlights the involvement of atrial GIRK channels specifically in mediating arrhythmia inducibility (Mesirca et al., 2016a), as none of our mice lacking GIRK both globally (*Girk4*$^{-/-}$) and selectively in atrial tissue (*SLNCre(+):Girk1*$^{fl/fl}$), exhibited arrhythmic episodes during VNS **ON**. Indeed, previous studies in mice have shown that *Girk4* ablation confers resistance to pacing-induced atrial fibrillation (Kovoor et al., 2001). Additionally, GIRK4 ablation has also been shown to restore normal cardiac rhythm in mouse models of sick sinus syndrome and AV block (Mesirca et al., 2016a, 2016b). This study further highlights the clinical potential of targeting GIRK channels for the management of supraventricular arrhythmias. Furthermore, future experiments should be conducted to investigate intensities that correlate to GIRK activation which may guide clinicians to select VNS parameters that will induce minor HR reduction and deliver therapeutic benefits without arrhythmogenic risk.

In summary, we conclude that muscarinic activation of atrial GIRK is a critical mediator in evoking the negative chronotropic and increased HRV effects of acute VNS in mice. Our findings also further highlight the role played by atrial GIRK in arrhythmia

inducibility and the potential of targeting this specific signaling pathway as a target for the management of atrial arrhythmias.

# CHAPTER 5 DEVELOPMENT AND CHARACTERIZATION OF STOCHASTIC VNS ON ACUTE HEART RATE DYNAMICS

**(Published)**

S.W. Lee, K. Kulkarni, E. M. Annoni, I. Libbus, B.H. KenKnight, and E.G. Tolkacheva. "Stochastic vagus nerve stimulation affects acute heart rate dynamics in rats." PLoS One. 2018 Mar 28:e0194910. doi: 10.1371/journal.pone.0194910.

## 5.1 Chapter Synopsis

Vagus nerve stimulation (VNS) is an approved therapy for treatment of epilepsy and depression. While also shown to be promising in several preclinical and clinical studies to treat cardiovascular diseases, optimal therapeutic stimulation paradigms are still under investigation. Traditionally, parameters such as frequency, current, and duty cycle are used to adjust the efficacy of VNS therapy. This study explored the effect of novel stochastic VNS (S-VNS) on acute heart rate (HR) dynamics. The effect of S-VNS was evaluated in Sprague Dawley rats by comparing the acute HR and HR variability (HRV) responses to standard, periodic VNS (P-VNS) across different frequencies (FREQs, 10 – 30 Hz). Our results demonstrate that both S-VNS and P-VNS produced negative chronotropic effects in a FREQ-dependent manner with S-VNS inducing a significantly smaller drop in HR at 10 Hz and 20 Hz compared to P-VNS ($p<0.05$). S-VNS demonstrated a FREQ-dependent drop in the SD1/SD2 ratio, a measure of HRV, which was absent in P-VNS, suggesting

that S-VNS may acutely modulate the nonlinear relationship between short- and long-term HRV. In conclusion, S-VNS is a novel stimulation procedure that may provide different physiological outcomes from standard P-VNS, as indicated by our analysis of HR dynamics. Our study provides a rationale for further detailed investigations into the therapeutic potential of S-VNS as a novel neuromodulation technique.

## 5.2 Introduction

In recent years, there has been an emergence of interest in using neuromodulation techniques to enhance or suppress activity of the nervous system for the treatment of various pathological conditions, including but not limited to systemic inflammation, obesity, spinal cord injuries, and neurological disorders. One such therapy is vagus nerve stimulation (VNS), which was approved by the FDA as a clinical therapy for the treatment of refractory epilepsy in 1997 and for the treatment of medication-resistant depression in 2005 (O'Reardon et al., 2006). As a result, VNS has become one of several non-pharmacological treatment options to control epileptic seizures worldwide.

The benefits of using VNS to treat cardiovascular diseases, including cardiac arrhythmias, heart failure (HF), hypertension, and myocardial ischemia, have been extensively explored in past decades, with several studies suggesting the therapy to be both safe and potentially effective as a long-term cardiac therapy (Annoni et al., 2015; Lee et al., 2016; Premchand et al., 2015; Xie et al., 2014). However, randomized clinical trials evaluating VNS in chronic HF patients have shown discrepant findings (Olshansky, 2016). While the INOVATE-HF and NECTAR-HF trials failed to demonstrate significant improvements, both ANTHEM-HF and the subsequent extension study (ENCORE)

yielded favorable and encouraging results including reduced HF symptoms and improved ventricular function (Gold et al., 2016; Nearing et al., 2016; Premchand et al., 2015; Zannad et al., 2015). In addition to different inclusion and exclusion criteria of HF patients, the different choice of stimulation parameters is another attributable factor for these mixed results.

Traditionally, the therapeutic intensity of VNS is selected to demonstrate engagement of the autonomic nervous system (typically via observed changes in heart rate (HR)) (Yoo et al., 2016). The stimulation parameters used to treat cardiac diseases, however, are highly variable depending on different models and studies (Annoni et al., 2015; Kong et al., 2012a; Li et al., 2004; Xie et al., 2014). Hence, there is an ongoing search for the optimal settings that will maximize the benefits of VNS. This can include the traditional approach of varying the stimulation frequency, current/voltage, and pulse width (Ardell et al., 2015; Kong et al., 2012a), as well as developing novel stimulation paradigms, such as the recently developed "microburst" VNS (Yoo et al., 2016). Typically, chronic periodic VNS (P-VNS) is applied, and its stimulation profile consists of administering periodic, repetitive electrical pulses with the level of stimulation (i.e. intensity) determined by a selected frequency, pulse duration, pulse amplitude, and duty cycle which all can be adjusted via radiofrequency communication link using a proprietary programming computer. In this study, we propose and evaluate an innovative stimulation technique: stochastic VNS (S-VNS). The version of S-VNS used in this study delivers electrical impulses to the nerve according to a Gaussian distribution of stimulation frequencies, instead of a constant frequency used in standard, P-VNS.

It is known that the cardiac beat-to-beat time intervals vary stochastically due to the inherent variability in HR (HRV). This variability can be attributed to many physiological factors including the influence of circadian rhythms, respiratory rhythms, temperature regulations, and others (Malik, 1996). In fact, it has been extensively reported that both increased HR and loss of HRV are associated with increased mortality in HF patients and are candidate markers for patients at risk of sudden cardiac death (Balasubramanian et al., 2017; Hori and Okamoto, 2012). An abundance of literature supports that acute P-VNS effectively decreases HR and improves HRV via the extensive innervation of the vagus nerve into the sinoatrial (SA) and atrioventricular (AV) nodes (Kapa et al., 2016; Shen and Zipes, 2014). Even though the exact mechanisms responsible for the coupling between VNS and HR and HRV remains unclear, it is postulated that it is mediated through muscarinic receptor activation via the neurotransmitter acetylcholine (ACh) released at parasympathetic nerve terminals (Harvey and Belevych, 2003). However, while P-VNS may effectively modulate HR dynamics, there may exist a 'physiological compensation mechanism' in which the vagus nerve and the central-peripheral nervous system can adapt to the periodicity of the stimulation, a phenomena which can be similar to pharmacological tolerance (Buschman et al., 2006; Lund et al., 2011; Samniang et al., 2016). We propose that S-VNS might help to avoid this potential adaptation, and therefore, the goal of our study is to evaluate the influence of acute S-VNS therapy on instantaneous HR and HRV by using *in-vivo* rat hearts, and compare it to the standard P-VNS.

## 5.3 Materials and Methods

Sprague-Dawley rats (n = 8, 250 – 400 g, Charles River Laboratories, Wilmington, MA) were used in this study. All experiments were performed in accordance with the guidelines set forth by the National Institutes of Health Guide for the Care and Use of Laboratory Animals and were approved by the University of Minnesota Institutional Animal Care and Use Committee (IACUC).

### 5.3.1 Vagus Nerve Bipolar Cuff Electrode Implantation

Rats were anesthetized with isoflurane (5% for induction and 1.5% for maintenance). After hair shaving and skin cleaning, aseptic technique was used to make a ventral midline incision in the neck, and the skin and muscles were retracted. After identifying and isolating the right cervical vagus nerve and common carotid artery bundle, a custom 1.5 mm diameter helical lead bipolar cuff electrode (Cyberonics, USA) was implanted around the bundle. The right vagus nerve was chosen for this study because it primarily innervates the atria and the sinoatrial node, and thus, right-side stimulation may induce significant change in cardiac rhythm (Muppidi et al., 2011). The electrode was then connected to a battery-driven, constant current stimulator (Stimulus Isolator, model A385, World Precision Instruments, USA). At the end of the study, the anesthetized rats were euthanized by thoracotomy followed by heart explantation.

### 5.3.2 VNS Protocols and Study Design

Both P-VNS and S-VNS were continuously delivered for 2 minutes at a pulse duration of 500 μsec and an output current of 1.0 mA (Annoni et al., 2015; Lee et al., 2016; Xie et al., 2014). The same number of stimuli was used for both P-VNS and S-VNS.

P-VNS was delivered at different frequencies (FREQ) of 10, 20, or 30 Hz that were kept constant throughout the 2 minutes of stimulation.

S-VNS was used with stochasticity (STOCH) of 10% or 20%. Three values of mean FREQ (i.e. 10, 20, and 30 Hz) were used similar to P-VNS, and STOCH (using a Gaussian distribution) was incorporated as:

$$\mathrm{FREQ}_{\mathrm{STOCH}} = \frac{\mathrm{FREQ}}{1 \pm [\mathrm{FREQ} * \delta(\mathrm{STOCH})]}$$

where δ(STOCH) is a random number with a mean of zero and a standard deviation of STOCH/FREQ. A custom LabView program was used to generate δ(STOCH) for each pulse.

The detailed study design is shown in **Fig. 5.1**. Briefly, the vagus nerve was first stimulated at FREQ = 20 Hz, starting with P-VNS (P-VNS #1) followed by S-VNS with STOCH = 20% after a 1-minute stabilization interval. After completion, a similar run was conducted for a FREQ = 30 Hz which was followed by a run at FREQ = 10 Hz. After a 10-minute stabilization interval, both P-VNS (P-VNS #2) and S-VNS with STOCH = 10% runs were conducted in the FREQ order of 20, 30 and 10 Hz. Each protocol for a certain FREQ consisted of the following stimulation:

(4) 2 minutes of baseline recording before VNS (**PRE**)

(5) 2 minutes of continuous VNS (**ON**)

(6) 2 minutes of recovery after VNS (**POST**)

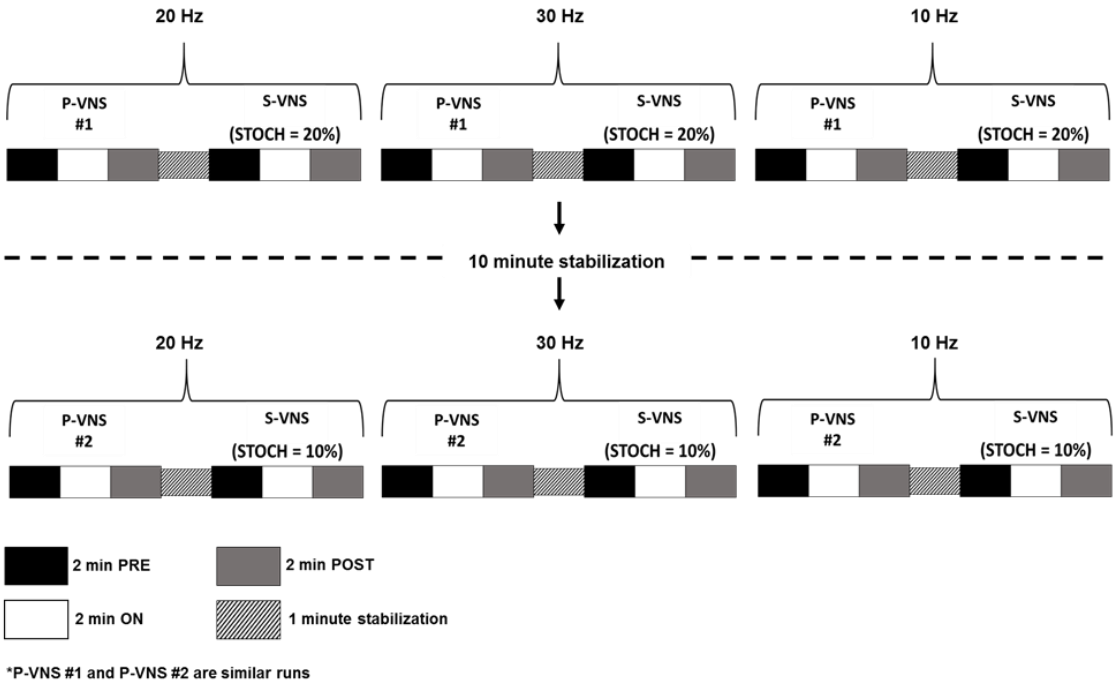


***Figure 5.1: Detailed schematic of the experimental VNS protocol.*** Standard P-VNS or S-VNS with different degree of stochasticity (STOCH, 10% and 20%) was administered across different frequencies (FREQ, 20, 30, and 10 Hz) with stabilization times between protocols and conditions. P-VNS, periodic vagus nerve stimulation; S-VNS, stochastic vagus nerve stimulation; STOCH, stochasticity; **PRE**, baseline recording; **ON**, continuous VNS; **POST**, recovery.

### 5.3.3 Data Analysis for *In Vivo* ECG Recordings

Electrocardiogram (ECG) was recorded from each anesthetized rat (IX-ECG-12, iWorx, USA). ECG electrodes were placed subcutaneously into the limbs. For both P-VNS and S-VNS, **PRE**, **ON**, and **POST** ECG data were recorded for 2 minutes. The *in-vivo* ECG recordings were used to quantify changes in the HR and HRV throughout the study using Kubios HRV 2.0 software (Tarvainen et al., 2014). Noisy data segments and ectopic beats were excluded and steady-state data after adjustment of the HR to acute VNS were used for the analysis. Hence, all runs of **PRE, ON,** and **POST** for all animals consisted of ~1-minute and 40 seconds interval for analysis.

To account for variations in baseline HR, the chronotropic effect of VNS was determined by calculating a relative change in HR, $\Delta HR_{ON}$, as the following:

$$\Delta HR_{ON} = \left(\frac{HR_{ON} - HR_{PRE}}{HR_{PRE}}\right) * 100\%$$

where $HR_{ON}$ and $HR_{PRE}$ are the mean HR during the VNS **ON** and **PRE** periods, respectively.

After the termination of VNS, we assessed the recovery of HR to $HR_{PRE}$ baseline value. Therefore, the HR post-VNS ratio ($HR_{POST\ Ratio}$) was calculated as

$$HR_{POST\ Ratio} = \left|\frac{\Delta HR_{POST}}{\Delta HR_{ON}}\right|$$

and

$$\Delta HR_{POST} = \left(\frac{HR_{POST} - HR_{ON}}{HR_{ON}}\right) * 100\%$$

where $HR_{POST}$ is the mean HR during the VNS **POST** period. A $HR_{POST\ Ratio} = 1$ means that the $HR_{POST}$ returned to the baseline $HR_{PRE}$ value. Whereas, if $HR_{POST\ Ratio} < 1$ (or > 1), then the $HR_{POST}$ was less (or greater) than the baseline $HR_{PRE}$ value.

To quantify HRV, Poincaré plots were used to provide a two-dimensional representation of the correlation between successive RR intervals, as described previously (Tarvainen et al., 2014). Briefly, *t*he spatial distribution of all points was fitted to an ellipse with the center coinciding with the average RR interval. The two dispersions (perpendicular (SD1) and parallel (SD2) to the line of identity y = x) and their ratio, SD1/SD2, were then calculated. Previously, it was established that SD1 is a measure of the

short-term HRV, while SD2 provides an assessment of both the short- and long-term HRV (Brennan et al., 2001; Tarvainen et al., 2014).

### 5.3.4 Statistical Analysis

All data are presented as means ± standard error. Statistical analyses were performed using Origin 9.1 software (Northampton, MA). Statistical comparisons were performed using a one-way ANOVA with repeated measures: 1) FREQ-dependent effect of P-VNS and S-VNS, 2) between S-VNS and P-VNS; 3) between the two P-VNS protocols, and 4) FREQ-dependent effect on SD1/SD2 for **PRE**, **ON**, and **POST**. A one sample *t*-test was performed to assess if the mean of the $HR_{POST\ Ratio}$ is equal to one. Values of $P < 0.05$ were considered to be statistically significant. If appropriate, post hoc comparisons with Tukey's test were performed, with *P*-values corrected for repeated comparisons.

## 5.4 Results

**Fig. 5.2** shows typical examples of ECG traces during P-VNS (Panel A) and S-VNS for STOCH = 10% and 20% (Panels B and C, respectively). Note the presence of small spikes on the ECG traces during the VNS **ON** periods corresponding to VNS stimulation artifacts, and the VNS-evoked decrease in HR. Furthermore, note the periodic, repetitive pattern of the VNS artifacts during P-VNS, and the absence of periodicity of the artifacts during S-VNS.

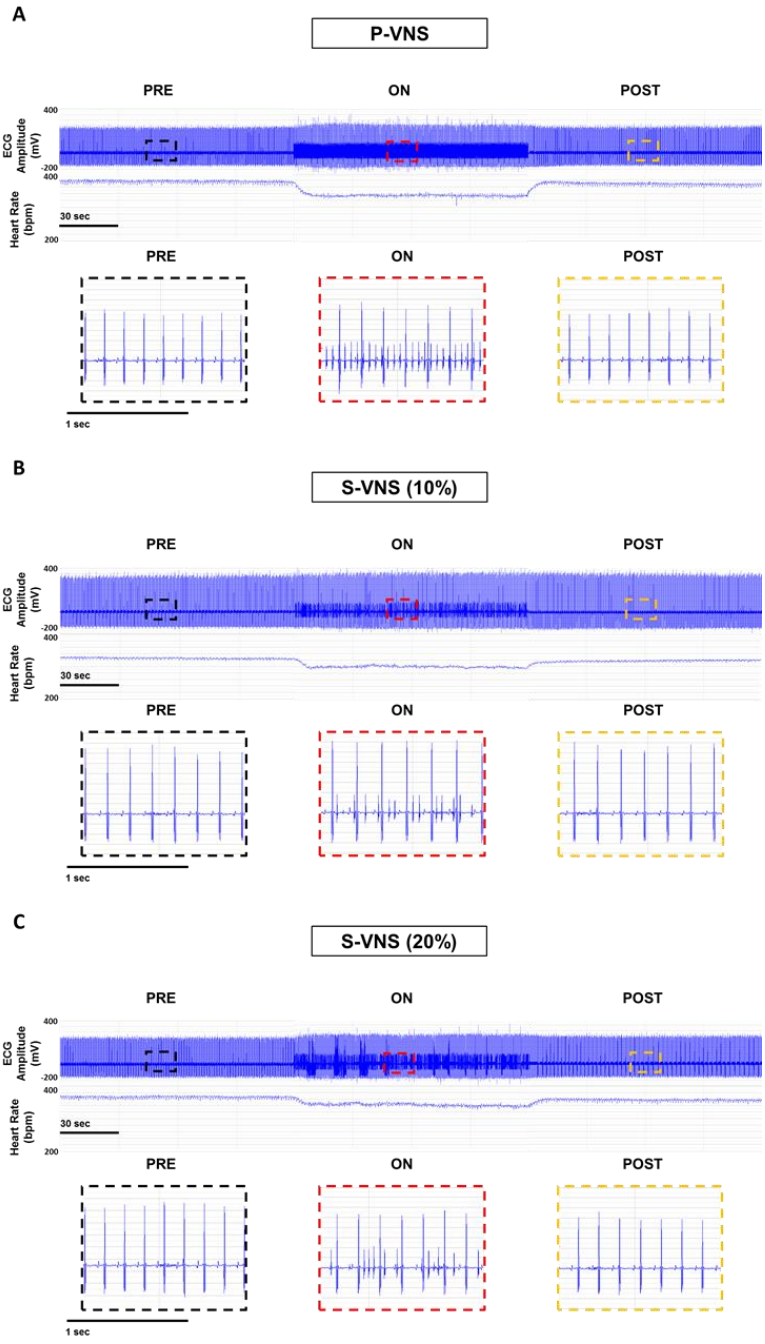


***Figure 5.2: ECG Recordings and Corresponding HR Responses.*** Representative segments of ECG recordings and corresponding heart rate (HR) response for an anesthetized rat for **PRE**, **ON**, and **POST** during **(A)** P-VNS, **(B)** S-VNS (10%), and **(C)** S-VNS (20%) of the right cervical vagus nerve. Zoomed-in snapshots of **PRE** (black), **ON** (red), and **POST** (yellow) highlights VNS artifacts during stimulation. Here, VNS was continuously delivered at 20 Hz, 500 µs pulse width, and 1.0 mA for 2 minutes.

### 5.4.1 FREQ-dependent Chronotropic Effects of P-VNS and S-VNS

The FREQ-dependent chronotropic effects of P-VNS and S-VNS are shown in **Fig. 5.3**. Note that the reported mean and SEM of the P-VNS protocols were averages of the P-VNS protocols (i.e., mean of the average of P-VNS #1 and P-VNS #2 protocols, n = 8). Relative changes in HR, $\Delta HR_{ON}$, in response to VNS across FREQ ranging from 10 to 30 Hz are shown for P-VNS (Panel A) and S-VNS (Panels B, C). For both P-VNS and S-VNS (both STOCH = 10% and 20%), no significant reduction in HR was observed as FREQ was increased from 10 Hz to 20 Hz. However, further increase of FREQ to 30 Hz produced a significant drop in HR.

It has been shown in several species such as dogs (Parker et al., 1984) and rats (Berntson et al., 1992) that VNS FREQ is linearly related to heart period, while the relation to HR is nonlinear. To account for this possibility, we also calculated the relative changes in heart period for both VNS protocols. **Fig. 5.3** (Panels D-F) indicate that FREQ-dependent chronotropic effect for heart period is similar to the one for HR (compare to Fig. **5.3**, Panels A-C).

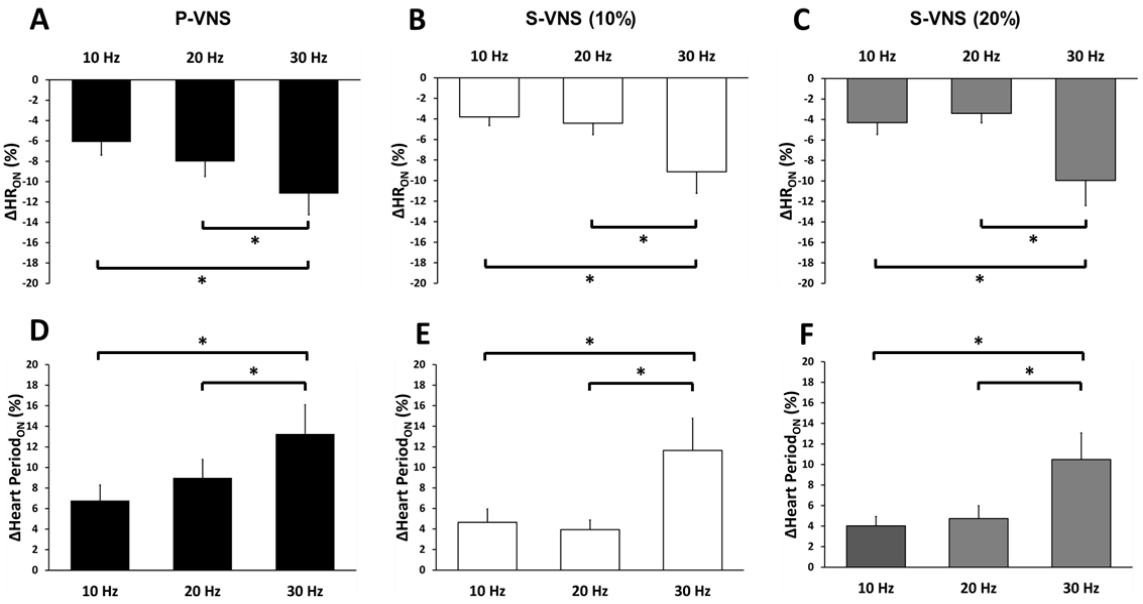


***Figure 5.3: Effects of VNS FREQ on HR and Heart Period.*** Mean percent drop in HR for **(A)** P-VNS, **(B)** S-VNS (10%), and **(C)** S-VNS (20%) at different FREQ. Mean percent drop in Heart Period for **(D)** P-VNS, **(E)** S-VNS (10%), and **(F)** S-VNS (20%) at different FREQ. Note data reported here for P-VNS is the mean and SEM of the average of P-VNS #1 and P-VNS #2 protocols (n=8). (*$p < 0.05$)

## 5.4.2 Effect of STOCH on HR and HRV

The relative changes in HR, $\Delta HR_{ON}$, in response to 10% (Panel A) and 20% S-VNS (Panel B), respectively, compared to its immediate preceding P-VNS at different FREQs are shown in **Fig. 5.4**. Overall, S-VNS had significantly smaller negative chronotropic effect relative to P-VNS at FREQ = 10 and 20 Hz. At 30 Hz, however, this reduced effect was eliminated as all the protocols exhibited similar relative drop in HR. Moreover, note that both P-VNS runs, P-VNS #1 and P-VNS #2, exhibited similar drop in HR at different FREQs, as indicated in Panel C, suggesting the stability of the experimental conditions over time. To investigate whether the order of application of P-VNS and S-VNS protocols contribute to the effects shown in Panels A and B, 20% S-VNS was compared to its

subsequent P-VNS #2 at different FREQs. **Fig. 5.4(d)** demonstrates similar effect in the relative change in HR responses when compared to Panels A and B, indicating that the effect is attributed to the S-VNS protocol itself, but not the different permutation of the two stimulation protocols.

Representative Poincaré plots of both P-VNS (Panel A) and S-VNS (Panel B) and their quantitative assessment, SD1/SD2 (Panel C) are shown in **Fig. 5.5**. While our results suggest that S-VNS did not significantly affect SD1/SD2 when compared to P-VNS (as indicated in **Fig. 5.5(c)**), we observed a FREQ-dependent effect. As shown in **Fig. 5.5(c)**, for P-VNS protocol, the SD1/SD2 values were similar for all FREQs for **PRE**, **ON**, and **POST** periods. Similarly, no significant difference in SD1/SD2 values was observed for S-VNS for **PRE** and **POST** periods. However, for VNS **ON** period, S-VNS showed significant reduction in SD1/SD2 values between FREQ = 10 Hz and 30 Hz. In addition to Poincaré analysis, we also evaluated HRV as a ratio of the standard deviation of RR interval (SDRR) to mean RR interval (mean RR), as described previously (McIntyre et al., 2014). From this approach, no significant difference was observed for all FREQs for PRE, ON, and POST periods for all VNS protocols (**Fig. 5.6**).

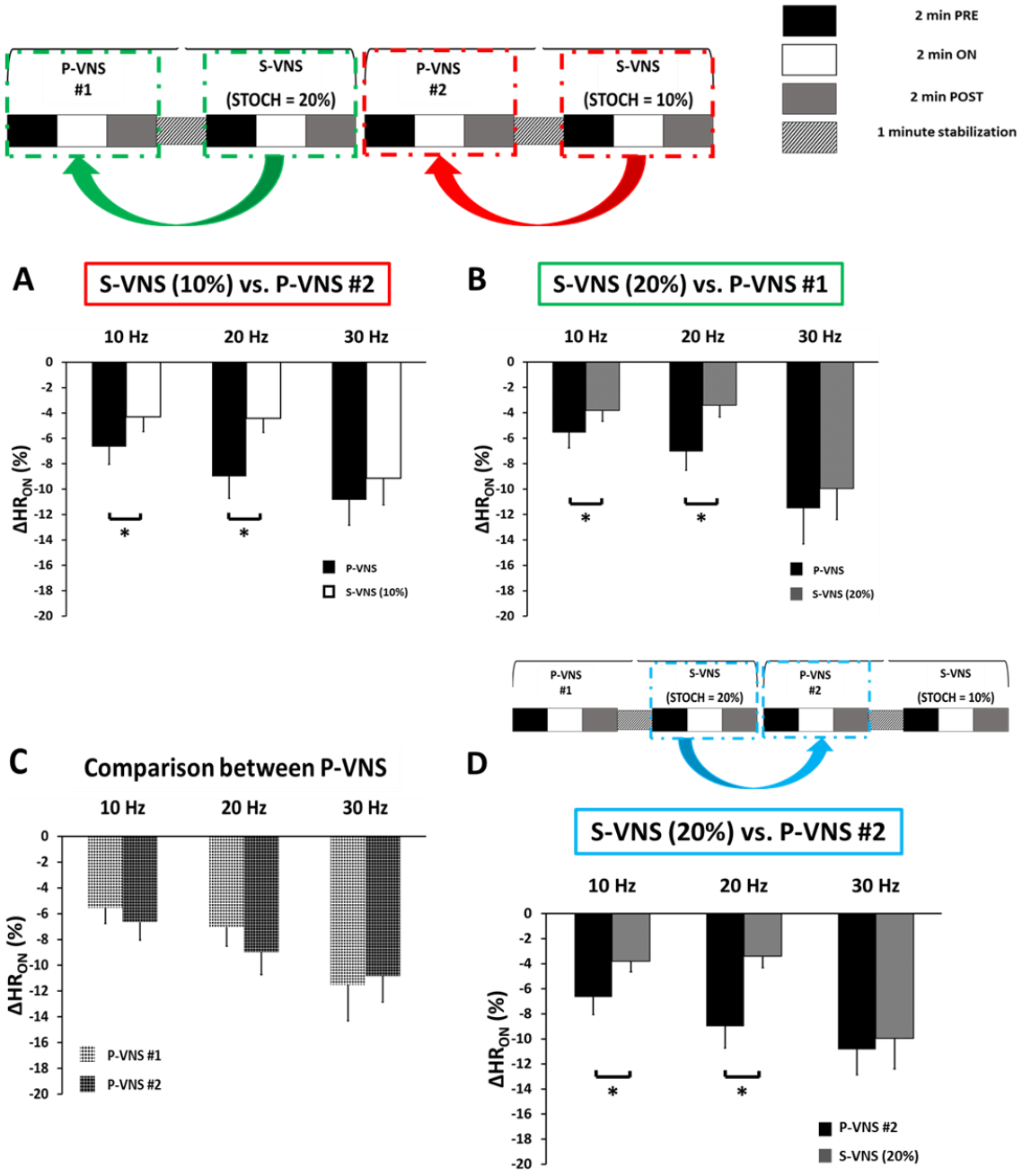


***Figure 5.4: Effects of STOCH on the chronotropic effects of VNS.*** Mean percent drop in HR for **(A)** S-VNS (10%) and **(B)** S-VNS (20%) being compared to its immediate preceding P-VNS protocol at different FREQ. **(C)** Comparison of mean relative drop in HR between P-VNS protocols and **(D)** S-VNS (20%) and its subsequent P-VNS protocol at different FREQ. (*$p < 0.05$)

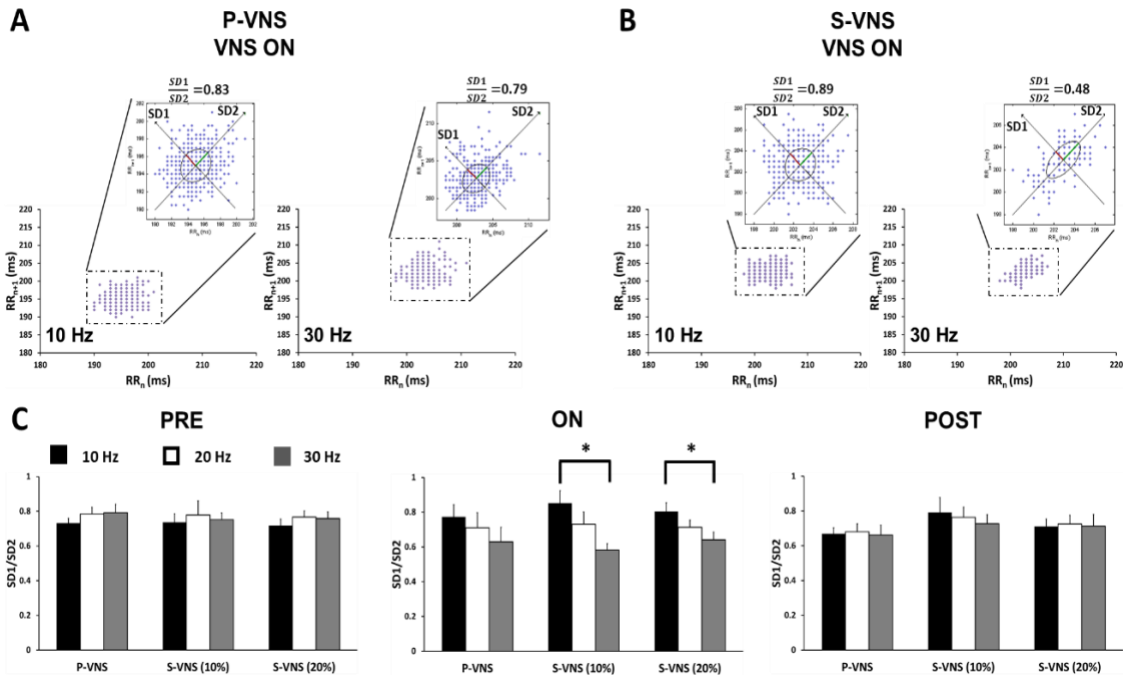


***Figure 5.5: Effects of VNS on HRV using Poincaré analysis.*** Representative Poincaré plots of **(A)** P-VNS and **(B)** S-VNS (10%) during VNS stimulation (**ON**) at 10 Hz and 30 Hz demonstrating the elliptical fitting of the beat-distribution cloud and the standard deviation of short-term (SD1) and long-term (SD2) variability. **(C)** Mean SD1/SD2 ratio for **PRE**, **ON** and **POST** across different FREQ. (*$p < 0.05$)

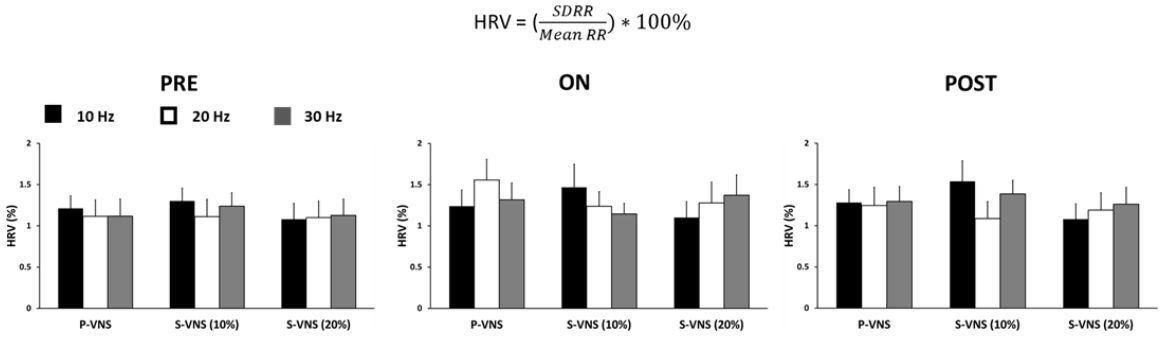


***Figure 5.6: Effects of VNS on HRV using Time-Domain analysis.*** HRV was calculated as a ratio of the standard deviation of RR interval (SDRR) to mean RR interval (mean RR), as described previously (McIntyre et al., 2014). From this approach, no significant difference was observed for all FREQs for **PRE**, **ON**, and **POST** periods for all VNS protocols.

To evaluate the recovery of HR to baseline values after VNS application, $HR_{POST\ Ratio}$ was calculated across different FREQs. Our results from Panels B-D in **Fig. 5.7** indicate that for FREQ = 30 Hz, the HR could recover back to its **PRE** value in S-VNS protocols. However, for FREQ = 10 or 20 Hz, the $HR_{POST\ Ratio}$ was less than 1, reflecting a persistent reduction in HR after the end of the VNS cycle.

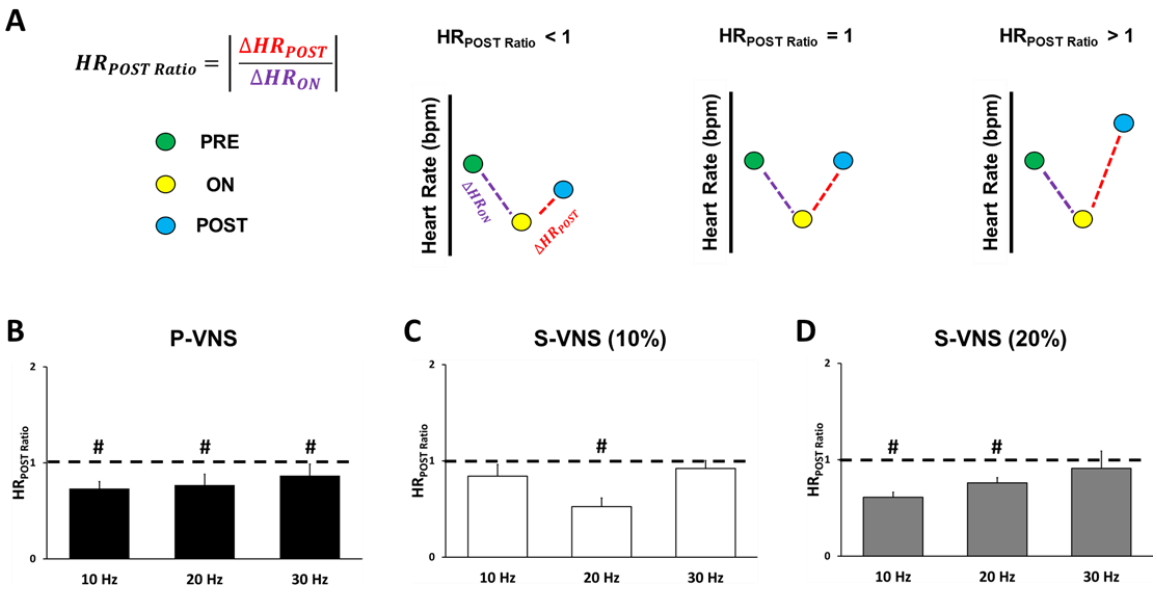


***Figure 5.7: Effects of VNS FREQ on HR recovery.*** **(A)** Schematic representation of different scenarios of HR recovery based on the value of $HR_{POST\ Ratio}$. Mean $HR_{POST\ Ratio}$ values for **(B)** P-VNS, **(C)** S-VNS (10%), and **(D)** S-VNS (20%) at different FREQ. # $p<0.05$ compared to a mean theoretical value of 1.

## 5.5 Conclusions and Discussion

The aim of the present study was to develop and test a new autonomic modulation stimulation protocol using stochastic stimulation (S-VNS), and compare it with traditional stimulation waveforms (P-VNS).

It has been well-established that an important feature of the adverse pathophysiological changes seen in HF is autonomic imbalance, characterized by sympathetic hyperactivation and parasympathetic withdrawal (De Ferrari et al., 2011). VNS has emerged as a promising therapy to normalize parasympathetic activation of cardiac control and restores normal levels of autonomic regulatory function. In fact, several animal studies suggest VNS exhibits both anti-arrhythmic and anti-inflammatory effects and attenuates myocardial damage and cardiac myocyte apoptosis (Annoni et al., 2015; Li

et al., 2004; Xie et al., 2014). Based on the encouraging results of the preclinical studies, several clinical VNS studies have been conducted. Both ANTHEM-HF and the subsequent extension study (ENCORE) yielded favorable and encouraging results as patients who received VNS experienced significant improvements in left ventricular (LV) structure and function, decreased HF symptom expression and decreased T-wave alternans, a measure of electrical instability (Nearing et al., 2016; Premchand et al., 2015). However, other randomized clinical trials, such as the INOVATE-HF and NECTAR-HF, failed to demonstrate significant improvements in clinical outcomes owing to imperfect inclusion/exclusion criteria and sub-therapeutic VNS dosing in significant (~30-50%) of the enrolled population (Gold et al., 2016; Zannad et al., 2015). Yet despite these and other studies, there still does not exist a universally accepted published prospective stimulation paradigm, which further highlights the importance and complexity of parameter optimization. Hence, to further optimize and improve VNS efficacy, this study introduced S-VNS, a novel technique that stimulates the vagus nerve stochastically since it is clinically well-established that healthy hearts have been associated with high HRV (Malik, 1996).

Our study demonstrated a FREQ-dependent reduction in HR as a result of VNS, which was previously shown in several studies asserting that increasing the stimulation FREQ alters the rate of propagation of action potential through the vagus nerve fibers (Ardell et al., 2015). However, we also observed that the drop in HR is significantly smaller for S-VNS as compared to P-VNS, even though mean FREQ was similar for both techniques. One of the possible reasons for this is that although the same number of stimuli were applied during both stimulation techniques, stimuli during S-VNS were distributed

more randomly. In P-VNS, there was a consistent number of stimuli being delivered between RR intervals, as highlighted in **Fig. 5.2**.

In order to determine the residual functional effects occurring after cessation of VNS, we calculated $HR_{POST\ Ratio}$. Our results show that the post HR of both S-VNS and P-VNS at certain FREQs did not return to baseline. This could be attributed to the fact that we applied continuous stimulation which is much longer than the typical intermittent VNS (e.g. duty cycle of 10% or 20%). Therefore, while other studies report a recovery to baseline at end of their intermittent stimulation (Ardell et al., 2015; Nearing et al., 2016), continuous stimulation may require more than the collected 2 minutes **POST** for the HR to return to baseline. Another possible explanation is that the cardiac effects of VNS may persist beyond the end of stimulation, and exhibit a "memory effect," a phenomenon similar to cardiac memory. Cardiac memory is an established property of paced cardiac myocytes to reflect the influence of pacing history and adapt and respond to novel stimuli. Several experimental studies and numerical simulations have shown that memory plays a role in modulating cardiac dynamics (Libbus and Rosenbaum, 2002; Tolkacheva, 2007). Indeed, in future studies, we will examine post-VNS recovery after a longer time delay.

In this study, we performed both linear and nonlinear approaches to evaluate the effects of VNS on HRV. Poincaré plots of RR intervals is a nonlinear approach used to monitor autonomic changes by means of SD1 and SD2. Physiologically, SD1 is an index of instantaneous recording of the beat-to-beat variability and reflects primarily the parasympathetic input to the heart, while SD2 is an index of long term variability which reflects the overall variability influenced by both the parasympathetic and sympathetic

contributions (Brennan et al., 2001; Libbus et al., 2017). Hence, their ratio (SD1/SD2) provides a measurement between both short term and long-term variability in the RR intervals. Libbus and colleagues recently reported that patients in the ANTHEM-HF trial who received chronic, right-sided intermittent P-VNS expressed an increase in the SD1/SD2 ratio, which suggested that right-sided VNS increases the balance in favor of parasympathetic dominance over sympathetic activity (Libbus et al., 2017). While our acute P-VNS did not induce any changes in SD1/SD2 ratio in rats, our experiments demonstrated that acute continuous S-VNS significantly decreased this ratio, specifically between 10 Hz and 30 Hz. We also observed no difference in SD1 and SD2 values with increase in stimulation FREQ across **PRE**, **ON**, and **POST** for P-VNS and S-VNS (**Fig. 5.8**). This data suggests that FREQ and STOCH not only play a role in the chronotropic effects of VNS, but also in the engagement of the autonomic nervous system via relative difference in ACh release between the two VNS techniques. Nonetheless, it is worth noting that brief changes in HRV, i.e. during VNS **ON** phase, may or may not have any significant effects on clinical outcomes, and will need to be further investigated. While Poincaré maps suggest a change in autonomic activity, our ratio of SDRR to mean RR saw no significant HRV difference induced by both S-VNS and P-VNS (S1 Fig). Indeed, there are several metrics to gauge autonomic activity which include time-domain (e.g. SDNN, RMSSD,…), frequency-domain (e.g. LF, HF, LF/HF,…), and nonlinear (Poincaré, sample entropy, detrended fluctuation analysis,…) methods (Shaffer and Ginsberg, 2017). Although previous studies have shown a possible correlation between the different measures (Guzik et al., 2007; Shaffer and Ginsberg, 2017), an exact equivalence has not been reported. It is

possible that Poincaré plots may detect abnormalities that are not as easily detectable with traditional time-domain measures, given that each parameter has different sensitivity to noise and other experimental conditions (Stapelberg et al., 2018). Hence, further investigations to fully uncover and understand the physiological relevance of these autonomic assessment methods are warranted in order to determine the efficacy of the different metrics in accurately quantifying autonomic activity.

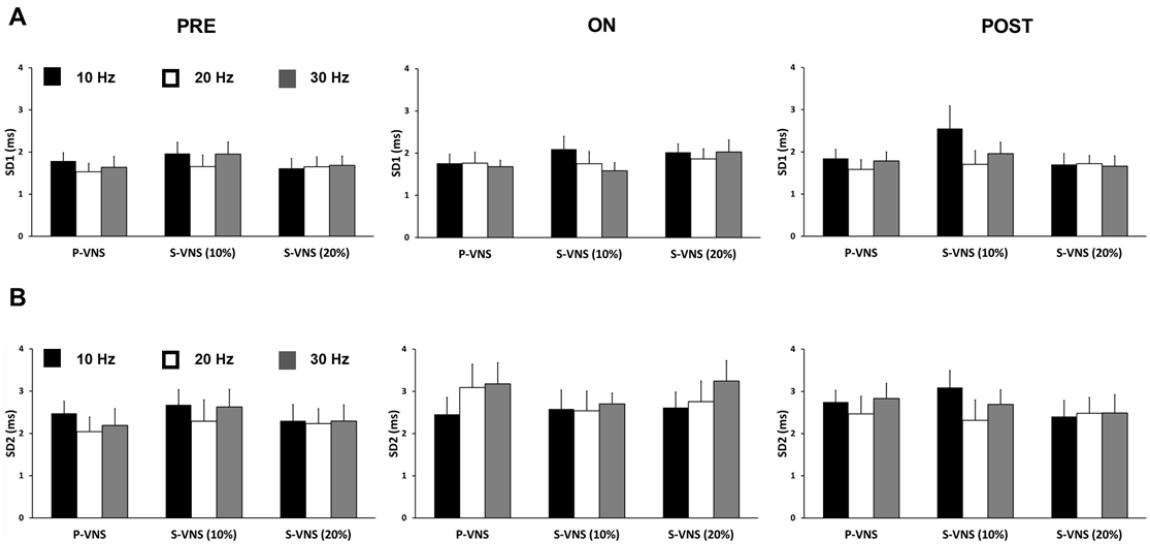


***Figure 5.8: Values of SD1 and SD2.*** Mean **(A)** SD1 and **(B)** SD2 values for **PRE, ON,** and **POST** across different FREQs. No significant difference in SD1 and SD2 values were observed with increase in stimulation FREQ across **PRE**, **ON**, and **POST** for P-VNS and S-VNS.

In the present study, we observed a smaller drop in HR and a reduction in SD1/SD2 ratio in S-VNS compared to P-VNS. From a physiological standpoint, this was a surprising finding since applying S-VNS does not necessarily correlate to stochastic release of ACh and stimulation of the muscarinic receptors of the cardiomyocytes. Rather, the efferent vagal fibers which are responsible for carrying descending information from the brain to the heart do not directly synapse with cardiomyocytes but rather with the intrinsic cardiac nervous system (ICNS), which acts as a buffer to register and send commands to the cardiomyocytes (Ardell et al., 2015). The ICNS is comprised of an intricate network of ganglia (and its neurons) that can independently act or communicate with its counterparts in the intrathoracic extracardiac, brain stem, spinal cord, and cortex to regulate intracardiac reflexes (Ardell et al., 2015). Although detailed studies will need to be performed to quantify the level of ACh release during the two stimulation protocols, we hypothesize that the observed minimal HR drop can be due to the fact that the temporal summation of ACh release is lower during S-VNS when compared to P-VNS protocol. This could be due to the fact that the instantaneous, effective FREQ of stimulation during S-VNS protocol is different (either less or more) from the corresponding FREQ of P-VNS protocol.

Phase response curves (PRC) detail how a system with its own intrinsic properties evolve with an external perturbation. The heart is an example of such dynamical systems that when given an external stimulus can cause either phase mismatch or entrainment. It has been well established that the chronotropic response to vagal stimulation is phase-dependent (Abramovich-Sivan and Akselrod, 1998). In fact, depending on the timing, duration, and magnitude of the vagal pulse, repetitive vagal stimulation has been shown to

be able to regulate the SA cells to beat at rates that are different from its intrinsic cycle length (Yang et al., 1984). Therefore, another possible explanation for our findings is that incorporating STOCH in our VNS may affect the level of entrainment between the vagal stimuli and the cycle length of the SA cells. Future additional studies should be conducted to understand how S-VNS may affect the intrinsic PRC.

There has been an emerging interest in using closed-loop neuro-stimulation to achieve targeted control of cardiac parameters (Ugalde et al., 2014). In fact, significant developments have been made in this area based on state transition models where an algorithm optimally selects the VNS parameters to regulate instantaneous HR synchronously with cardiac cycles (Romero Ugalde et al., 2017). We hypothesize that incorporating STOCH in closed-loop VNS may potentially lead to improved therapeutic efficacy. Physiologically, the heart rhythm is not deterministic and is known to exhibit beat-to-beat variability (HRV) caused by numerous physiological factors including the influence of circadian rhythms, respiratory rhythms, temperature regulations, and others (Dvir and Zlochiver, 2013). In fact, it has been associated that low HRV is a predictor for pathological cardiac conditions (Balasubramanian et al., 2017). Hence, we hypothesize that by recording real-time changes in HRV and then integrating this "inherent stochastic feedback" into the stimulation of the VNS through STOCH may lead to a more physiological stimulation of the vagus and increase the efficacy of VNS to treat cardiac disease. This will require a fully functional, implantable, and chronic version of the S-VNS system that has real-time monitoring capabilities

One of the limitations of our study is that we only investigated the differences between P-VNS and S-VNS with respect to HR and HRV, and used a healthy rat model. Furthermore, we only evaluated the acute effects. Beneficial effects have been observed when chronic P-VNS was applied in both healthy and diseased conditions (Annoni et al., 2015; Lee et al., 2016; Li et al., 2004; Nearing et al., 2016); therefore, additional chronic studies in both healthy and diseased conditions need to be performed in order to evaluate the full potential of S-VNS.

Moreover, our results suggest that S-VNS may enable some flexibility in nerve response by its ability to vary the stimulation intervals and providing a 'pseudo-intermittent' stimulation. Therefore, even though the same mean FREQ in both P-VNS and S-VNS were delivered, S-VNS had a smaller drop in HR. This could make S-VNS suitable for treatment of diseased conditions such as hypertension, where a controlled drop in blood pressure with a minimal change in HR are desired. This study suggests that incorporating STOCH may provide room for titration of other stimulation parameters (i.e. duty cycle and output current). In fact, in terms of treatment of brain disorders, non-periodic stimulation is currently being studied in the preclinical setting with promising results. Examples of stochastic neuromodulation techniques include but not limited to stochastic galvanic vestibular stimulation and transcranial random noise stimulation (Goel et al., 2015; van der Groen and Wenderoth, 2017). Therefore, there is the potential for S-VNS to induce changes in physiological parameters other than HR and HRV, making it a plausible candidate to improve current VNS treatment for epilepsy and depression, but this will require more in-depth investigation.

Furthermore, it is well accepted that the cervical vagus nerve is composed of both myelinated A and B fibers and unmyelinated C fibers (Yuan and Silberstein, 2016a), and our study does not address the question as to which fibers are indeed stimulated. Zagon et al have demonstrated that providing higher stimulation amplitudes, i.e. 200 μA, activates both unmyelinated and myelinated fibers in anesthetized rats (Zagon and Kemeny, 2000). Hence, this suggests that our stimulation current of 1 mA is sufficient to activate the whole thin vagal trunk of our rats. However, the discharge frequencies between afferent and efferent fibers may be different, and thus, future studies are needed to determine whether the mechanisms of both P-VNS and S-VNS occurs primarily through the afferent or efferent pathways.

Another limitation of our study is that the sequence testing was not randomized. However, we did not monotonically increase our FREQ from 10 Hz to 30 Hz. Instead the sequence order was 20 Hz, 30 Hz, and 10 Hz, but nonetheless, there may be the potential of order effects. Finally, the ECG recordings from rats were obtained with the use of general anesthesia, which is known to affect the HR of animals as compared to conscious animal ECG telemetry recordings. In fact, it has been reported that high-dose isoflurane can suppress the central cardiac parasympathetic activity in rats (Toader et al., 2011; Yang et al., 2014). As a result, we ensured that the dosage of isoflurane administered was low (~1.5%) and remained identical across all rats throughout the duration of the study; therefore, it should not affect the interpretation of our results.

Due to the long duration of the experimental procedures, we only tested the effect of STOCH values of 10% and 20% in this present manuscript. Additional experiments will

need to be performed to explore the full range of STOCH values. Furthermore, we also applied fixed values of current amplitude and pulse width. It is well accepted that VNS would elicit an immediate change in HR correlating with VNS current amplitude and pulse width (Nearing et al., 2016). Hence, while a different magnitude drop in HR value may be observed, our interpretation of the effects of incorporating STOCH should not be affected. In addition, while we only observed a difference of 2% HR drop between P-VNS and S-VNS which means extrapolating this to human may make these changes negligible, it is worth noting that the average HR of healthy rats is roughly 300 – 350 bpm which is about five times faster than the average resting HR of humans (Azar et al., 2011; Yang et al., 2014). Therefore, we propose these exploratory findings to first be confirmed in larger animal studies under both control and diseased conditions before being tested in humans. Nevertheless, we plan to further evaluate the robustness and efficacy of our proposed S-VNS in chronic future studies and on non-anesthetized murine models.

In conclusion, thethe evoked chronotropic response to P-VNS (delivered at a constant FREQ of 10, 20, or 30 Hz) were evaluated, and compared to S-VNS where stochastic variability was imposed in delivered FREQs with constraints for 10% or 20% around these three FREQs. The major findings of this study are as follows: (1) HR is reduced by both S-VNS and P-VNS in a FREQ-dependent manner. However, the negative chronotropic effect of S-VNS at 10 Hz and 20 Hz is significantly smaller than that of P-VNS and (2) S-VNS may acutely modulate the nonlinear relationship between short- and long-term HRV differently than P-VNS, as indicated by SD1/SD2 measurements. Overall, the results of our study suggest that acute S-VNS affects the dynamic changes in *in-vivo*

rat hearts, specifically HR and HRV in a different manner, when compared to traditional P-VNS. Hence, our study further supports the notion that different modes of stimulation provides different outcomes as measured by means of change in HR. We also highly suggest further investigations into characterizing the effects and elucidating the mechanisms of S-VNS as a novel neuromodulation technique under different diseased conditions.

# CHAPTER 6 CONCLUSIONS AND FUTURE STUDIES

This doctoral research applied principles of engineering and physiology as well fundamentals of cardiac electrophysiology to advance our understanding of vagus nerve stimulation (VNS) technology. This was accomplished by elucidating the mechanisms of action of VNS through 1) assessing atrial and ventricular electrophysiological properties after long-term VNS and 2) investigating the role of cardiac $M_2R$-$I_{KACh}$ signaling pathways in mediating the chronotropic effects of acute VNS. In addition, this research also 3) led to the development and evaluation of a novel stimulation paradigm.

## 6.1 Summary of Research Findings

VNS has emerged as a promising therapy to treat cardiovascular diseases, which has been characterized by autonomic dysregulation or specifically overdrive of the sympathetic nervous system and withdrawal of the parasympathetic nervous system. Being known to provide parasympathetic innervation of many vital visceral organs including the heart, stimulating the vagus nerve may potentially be able to normalize parasympathetic activation of cardiac control reflexes. Despite showing promising results in both preclinical and clinical research, the mechanism of action of VNS remains unclear. This dissertation aims to improve our knowledge of VNS and to elucidate the mechanism of action in order to further optimize and improve VNS efficacy.

First, it is without question that there are significant parasympathetic innervation in the atria (Coote, 2013; Hasan, 2013; Végh et al., 2016) and VNS has shown very promising

results to be able to treat heart failure (HF) and chronic myocardial-infarcted (MI) hearts (Beaumont et al., 2015; Kong et al., 2012a; Schwartz and De Ferrari, 2009; Uemura et al., 2010b). Surprisingly in spite of this, the effects of both chronic MI and VNS on the electrophysiological properties of the atrium was unclear and inconsistent (Li et al., 2000; Sridhar et al., 2009; Yeh et al., 2008). As demonstrated in **Chapter 2**, this dissertation work found that chronic MI had pro-arrhythmic effects on the heart via shortening of the action potential duration (APD) and increased spatial APD heterogeneity (μ). Long-term VNS increased APD values and restored them back to the healthy animal values, thus demonstrating and confirming the therapy's potential anti-arrhythmic and beneficial effects.

There currently is a gap in knowledge in regards to how VNS may be able to modulate ventricular function and electrophysiology especially since it has been heavily reported that VNS exhibits ventricular anti-arrhythmic effects (De Ferrari et al., 2011; Schwartz and De Ferrari, 2009; Wu and Lu, 2011). Particularly, since physiology textbooks state that parasympathetic postganglionic supply is limited to only the atria, and none into the ventricles (and if there are any innervations, they are sparse and should not have any influence on ventricular function) (Coote, 2013; Jungen et al., 2017). However this supposition has since been challenged by several researchers using a variety of immunohistochemical, histological, western blot, and other methods to demonstrate that there are indeed rich parasympathetic innervations in the ventricles (Akiyama and Yamazaki, 2001; Coote, 2013; Jacobowitz et al., 1967; Kawada et al., 2001; Kent et al.,

1974; Pauza et al., 2013; Pauziene et al., 2016; Taggart et al., 2011; Ulphani et al., 2010; Yasuhara et al., 2007; Zang et al., 2005; Zhan et al., 2013).

With this challenged supposition and confirming the beneficial effects of chronic low-level VNS in the atrium of diseased hearts in **Chapter 2**, I then investigated the effects of chronic low-level VNS on ventricular function and electrophysiological properties in **Chapter 3**. Based on the physiology dogma that there is minimal parasympathetic innervation into the ventricles, I would expect that administration of VNS would induce very minimal changes to the ventricles, but this study showed otherwise. Using hearts of healthy rats, I confirmed positive anti-arrhythmic effects of VNS even in the absence of autonomic imbalance as none of the VNS-treated hearts and 75% of the non-treated hearts developed ventricular arrhythmias during our *ex vivo* programmed electrical stimulation. This study showed that VNS induced changes in ventricular electrophysiological changes that were able to render the hearts less vulnerable to inducible arrhythmias. At the same time, VNS also did not induce any detrimental effects on cardiac function as no significant changes to ventricular ejection fraction (EF) and APD heterogeneity index μ was observed.

Now that my results from both **Chapters 2** and **3** suggest that the parasympathetic branch may indeed affect atrial and ventricular functions through stimulation of the vagus nerve, I then used novel transgenic mice to specifically investigate the role of $M_2R$-$I_{KACh}$ signaling pathway in mediating VNS effects. **Chapter 4** describes the experiments that applied acute VNS in mice in which the cardiac $I_{KACh}$ channel was ablated constitutively or selectively in the atria or ventricles. This study was the first to provide distinctive evidence that $M_2R$-$I_{KACh}$ signaling in the atria is required and plays the dominant role in

evoking the negative chronotropic and increased HRV effects of VNS. Our findings also further highlight the role atrial $I_{KACh}$ plays in arrhythmia inducibility and the potential of targeting this specific channel as a target for the management of atrial arrhythmias.

The aim of the study detailed in **Chapter 5** was to develop and test a new autonomic modulation stimulation protocol using stochastic stimulation (S-VNS) and compare it with traditional stimulation waveforms (P-VNS). Traditionally, the stimulation profile of VNS (P-VNS) consists of administering periodic, repetitive electrical pulses with the level of stimulation (i.e. intensity) determined by a selected frequency, pulse duration, pulse amplitude, and duty cycle which all can be adjusted via the radiofrequency communication link using a proprietary programming computer. The version of S-VNS developed and used in this study delivered electrical impulses to the nerve according to a Gaussian distribution of stimulation frequencies. The results suggest that acute S-VNS may indeed affect the dynamic changes in *in vivo* rat hearts, specifically HR and HR variability (HRV), in a different manner when compared to traditional P-VNS. This highlights the potential of S-VNS being used in the clinical setting as S-VNS may enable some flexibility in nerve response by its ability to vary the stimulation intervals and providing a 'pseudo-intermittent' stimulation. Specifically, even though the same mean FREQ in both P-VNS and S-VNS were delivered, S-VNS had a smaller drop in HR. This could make S-VNS suitable for treatment of diseased conditions in which a minimal change in HR is desired. Indeed, further investigations are absolutely necessary to characterize the effects and elucidate the mechanisms of S-VNS as a novel neuromodulation technique under different diseased conditions before being applied to humans.

**Collectively**, this work provides further evidence that the parasympathetic branch of the autonomic nervous system does indeed play a role in ventricular electrophysiology. Surprisingly, this work demonstrated that chronic VNS was able to prevent healthy hearts from having arrhythmias, even after applying a known arrhythmia-induced protocol. This anti-arrhythmic effect of VNS has always been reported in diseased hearts but not in healthy hearts where there is an absence of autonomic dysfunction. Hence, this dissertation suggests that VNS may not require sympathetic overdrive to induce its beneficial effects and is able to remodel the electrophysiological properties of the ventricles that makes the hearts less vulnerable to ventricular arrhythmias. Findings in this dissertation also contribute to current understanding of GIRK channel (specifically $M_2$-$I_{KACh}$) function in regards to VNS modulation in the heart. Furthermore, this work has set the stage for future studies to further investigate and analyze the role of the $M_2$R-$I_{KACh}$ signaling pathway in the atria and the ventricles, each in isolation, in mediating the beneficial effects of chronic VNS.

## 6.2 Future Work

While the work presented in this dissertation improves on the current knowledge on the development and mechanisms of VNS for cardiovascular diseases, further investigative works needs to be done to obtain a more complete mechanistic understanding.

### 6.2.1 Investigating VNS Effects on Calcium Dynamics

Results from **Chapter 3** suggest that chronic VNS is able to affect intracellular calcium dynamics as demonstrated in changes in the restitution properties at the $APD_{50}$ level. It has been previously reported that short-term VNS was beneficial to heart failure

(HF) rats through the improvement of excitation-contraction coupling by increased expression levels of ryanodine receptor 2 (RyR2) and sarcoplasmic reticulum $Ca^{2+}$ ATPase (SERCA2) (Li et al., 2015; Zhang et al., 2015). Additional experiments will be needed to determine which myocyte membrane ion channels are indeed up- or downregulated by chronic VNS.

Another approach to study how either acute or chronic VNS affects calcium dynamics is to use simultaneous optical mapping of voltage and intracellular $Ca^{2+}$. Specifically, this method can be used to investigate both membrane voltage and intracellular $Ca^{2+}$ simultaneously at each region of both VNS-treated and non-treated hearts, thereby allowing for the two parameters to be matched both spatially and temporally. Simultaneous optical mapping method has been previously developed and successfully implemented in Dr. Alena Talkachova's laboratory (Visweswaran et al., 2013).

### 6.2.2 How Does VNS affect CV?

Due to significant parasympathetic presence in the atria, it is well-accepted that VNS is able induce negative dromotropic effects in the atria. However, it remained unclear on how VNS may affect the conduction velocity (CV) in the ventricles. This dissertation suggests that chronic VNS is able to increase ventricular CV in the hearts of healthy rats. To investigate how VNS is able to modulate ventricular CV, I propose the following two investigative topics 1) gap junctions and 2) myocardial fiber orientation.

Previous studies have shown that intercellular electrical uncoupling plays an important role in arrhythmogenesis during MI (Saffitz et al., 1999; Smith et al., 1995). Intercellular electrical coupling mainly occurs through gap junctions that are formed by

connexins, and one of the most important connexins in the heart is connexin-43 (Dhein et al., 2002). Connexin-43 (Cx-43) is the main electrical coupling protein in the ventricles and it is well-established that the amount and distribution of Cx-43 are significantly altered during ischemia (Gutstein et al., 2001; Jiang et al., 2008; Lerner et al., 2000; Papp et al., 2007). It has been suggested that VNS is able to preserve Cx-43 in a MI rat model and improve ischemia-induced electrical instability (Ando et al., 2005; Wu and Lu, 2011). Nonetheless, this beneficial effect of Cx-43 preservation has only been shown in diseased hearts, but not in healthy hearts. I hypothesize that VNS may be able to increase ventricular CV by increasing the expression of Cx-43 and thus reduce the likelihood of ventricular arrhythmias, regardless of diseased or healthy hearts. Hence, I suggest future experiments to perform VNS in healthy animals, and then perform immunohistochemistry on sections of both VNS-treated and non-treated ventricular myocardium with anti-Cx-43 antibody to quantify level of Cx-43 expressions.

The architecture of myocardial fibers is known to play a role in electrical activation propagation (Kadish et al., 1988; Roberts et al., 1979). In fact, propagation is the fastest in the direction of myocardial fibers rather than across the fibers (Young and Panfilov, 2010). Therefore, another hypothesis I have to explain the increase in CV due to VNS is that chronic VNS is able to remodel the myocardial fibers in such a way that promotes smoother electrical propagation relative to non-treated VNS hearts. To investigate this hypothesis, I propose the use of optical methods such as optical coherence tomography (OCT) to acquire fiber orientation in heart tissues.

### 6.2.3 Identifying Peripheral Afferent and Efferent Neural Pathways Mediating the Therapeutic Effects of VNS

This dissertation work has largely focused and assumed on the efferent parasympathetic control of the heart. However, afferent parasympathetic pathways may also play a role in the therapeutic effects by reflexively inhibiting sympathetic nerve activity to the heart and other organs.

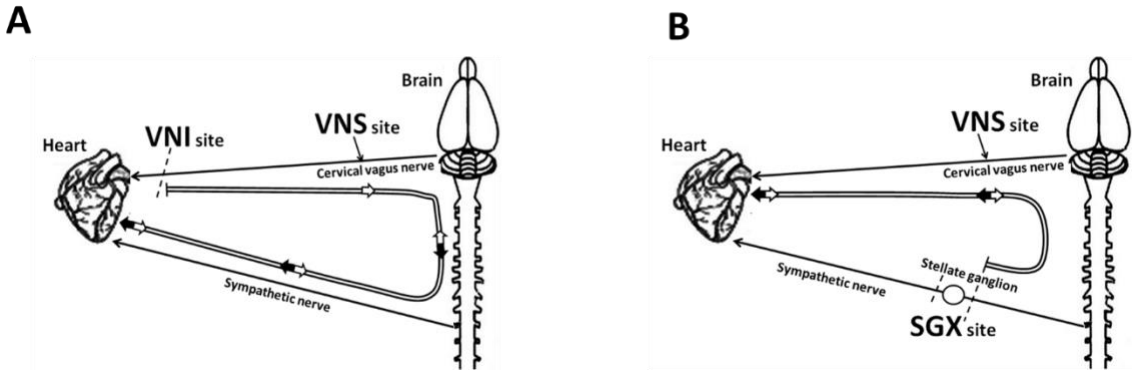


***Figure 6.1: Schematic Illustration of Propose Methods to Study Afferent vs. Efferent VNS.*** Schematic illustration of the proposed **(A)** vagus nerve isolation (VNI) and **(B)** bilateral stellate ganglionectomy (SGX) procedures to investigating peripheral afferent and efferent neural pathways mediating the therapeutic effects of VNS. White and black arrows illustrate the directions of afferent and efferent nervous pathways, respectively.

To test the hypothesis that the effects of VNS are mainly induced by vagal nerve *afferent* fibers rather than the direct stimulation of the heart through vagal efferent nerves, I propose to perform a vagus nerve isolation (VNI) surgical procedure. As shown in **Fig. 6.1(a)**, this surgical procedure involves isolating and transecting the vagal cardiac branch before it enters the heart to eliminate the contribution of efferent nerves to the effects of VNS. The vagal cardiac branch can be anatomically identified by its course from the thoracic vagus over the trachea toward the heart as described in (Rentero et al., 2002). The

VNI surgeries should be performed at the same time as the VNS stimulator implant procedure.

To test the hypothesis that VNS may be mediated by activation of vagal afferents which can reflexively decrease cardiac sympathetic efferent activity, I propose to perform the bilateral stellate ganglionectomy (SGX) surgical procedure which ablates cardiac sympathetic nerves, as shown in **Fig. 6.1(b)** and described in (Xie et al., 2011). This proposed study will help lead to a better understanding of the role of cardiac sympathetic nerves in mediating the response to VNS. In other words, successful SGX procedures will block the delivery of neurotransmitters to the heart through sympathetic nerves; thus, the observed VNS effects will be solely due to the parasympathetic innervation through the direct vagus efferent nerve bundles. The SGX surgeries should be performed at the same time as the VNS stimulator implant procedure.

### 6.2.4 Investigate S-VNS on Other Cardiac Responses and Miniaturization of VNS Pulse Generators

As demonstrated in **Chapter 5**, acute S-VNS induced dynamical changes in *in vivo* rat hearts that is different from standard acute P-VNS. Specifically, S-VNS produced minimal changes in HR compared to P-VNS. Hence, I hypothesize that S-VNS may be a suitable treatment for other diseased conditions such as hypertension where a controlled drop in blood pressure within a minimal change in HR are desired. For the study described in **Chapter 5**, however, I only investigated the differences between P-VNS and S-VNS with respect to HR and HRV, and used a healthy rat model. Therefore, the next step is to apply S-VNS in diseased hearts and look into other cardiac responses. Specifically, I propose to further investigate the potential of S-VNS to treat hypertension using

hypertensive rats and investigate its effects on blood pressure. To do so, a hypertension rat model can be generated by feeding Dahl-salt sensitive rats with a high salt diet. Blood pressure can be acquired through a pressure catheter placed in the femoral artery while HR can be collected through external ECG electrodes. Systolic and diastolic blood pressure, pulse pressure, and blood pressure variability can then be calculated from the pressure waveform. Then after confirming that acute S-VNS is able to reduce blood pressure in hypertensive rats, chronic S-VNS can then be applied by collaborating with LivaNova to develop a fully functional, implantable, and chronic version of the S-VNS system.

The VNS pulse generators that I used for this dissertation work typically have the following dimensions of 2.0 in x 2.0 in x 0.27 in and a weight of approximately 25 grams, as shown in Fig. 2-1. Therefore, putting in consideration the average weight of a healthy male wild-type C57BL/6J mouse is 27.7 grams at 12 weeks old (The Jackson Laboratory, 2017), implanting our relatively huge stimulator on mice for chronic studies is extremely difficult and raises ethical concerns. Hence, I propose that future investigators develop miniaturized pulse generators that can be implanted into mice in order to perform chronic studies, especially on genetically engineered mouse models to further investigate several VNS mechanisms

### 6.2.5 Determine the Optimal Time for the Onset of VNS

However, even though this dissertation work and several other studies strongly suggest that VNS therapy is beneficial, it still remains unclear as to when be the optimal time to begin VNS therapy to the injured heart. Based on literature, previous studies show an inconsistency as to the onset of VNS therapy to treat ischemic heart diseases (Kong et al., 2012b; Shinlapawittayatorn et al., 2013; Uemura et al., 2010a; Zhao et al., 2013). While

some studies begin stimulation 5-30 minutes prior to the cardiac injury, there are also those that begin stimulation at the onset of ischemia or during reperfusion. Therefore, I highly suggest for future studies to determine the most optimal time for the onset of VNS in order to achieve the maximal therapeutic benefits, specifically anti-inflammatory and anti-arrhythmic, to the injured heart.

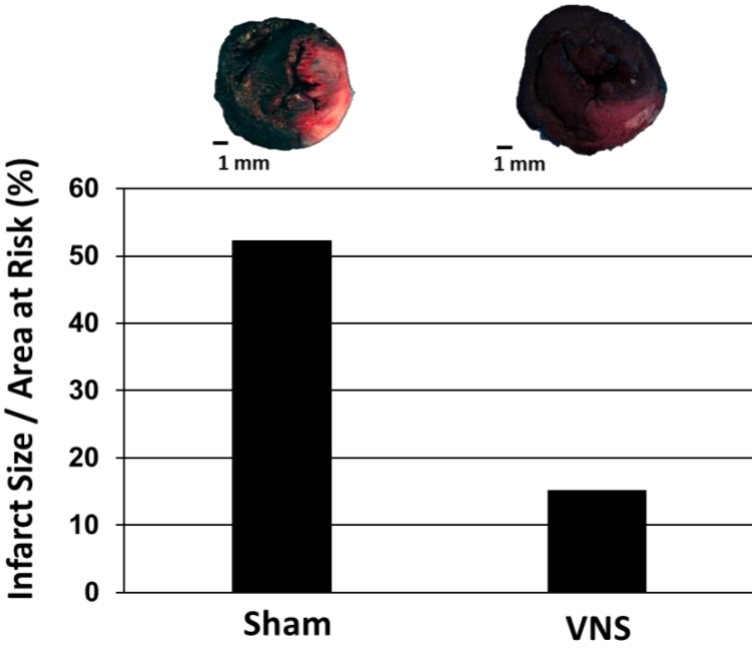


***Figure 6.2: Assessment of MI size.*** Sections of the hearts were photographed to identify the ischemic area at risk (AAR, uncoupled by Evan's blue dye), the MI size (unstained by TTC or the white region), and the non-ischemic zones (colored blue dye).

In fact, I have already begun these experiments and successfully established MI diseased rat models for Dr. Alena Talkachova's laboratory to pursue this avenue of research. Specifically, I have established both myocardial ischemia/reperfusion (I/R) and chronic MI rat models. From my most recent experiments, I have used a 30 minute ischemia and 24 hour reperfusion rat model and applied intermittent VNS (~12% duty cycle) therapy. VNS therapy was provided to the rat 30 minutes prior to MI and rats continued to receive the therapy throughout the 24-hour reperfusion period. Afterwards, I sectioned the hearts in order to assess 1) myocardial injury via scar size (i.e., area at risk and necrotic area using Evan's Blue Dye and Triphenyl tetrazolum chloride (TTC)), and 2) inflammatory response in the myocardium by quantifying the number of macrophages (via immunohistochemistry of a macrophage and nucleus marker (i.e., CD68 and DAPI)). These preliminary results are summarized in **Figs. 6.2 and 6.3**. From these experiments, I have shown that VNS was able to reduce the MI size by quantifying the area at risk and necrotic area and then expressing as a percentage **(Fig. 6.2**, n = 2 (n = 1 for Sham and n = 1 for VNS)). Note that I am unable to assess scar size and inflammatory response with the same hearts as the administration of Evan's blue dye and TTC will affect and make immunohistochemical staining difficult. To quantify the number of macrophages (n = 6 (n = 3 for Sham and n = 3 for VNS)), I analyzed the immunohistochemical slides (60X magnification). Panel A of **Fig. 6.3** shows sample immunohistochemical images of both Sham and VNS. Analysis was done using ImageJ and from each slide, counted the number of cells that express **both** CD68 and DAPI (i.e. excluding cells/area that either express only CD68). While the analysis suggest that our VNS therapy may not provide an anti-

inflammatory effect (**Fig. 6.3(b)**), I still strongly hypothesize that VNS has anti-inflammatory benefits but it will require some changes to the experimental protocol and further work to optimize the results. Suggested approaches include: 1) change the VNS therapy from intermittent to continuous stimulation and 2) in addition to macrophage counting, plan on performing cytokine analysis from blood draw and/or homogenization of myocardial tissue to gauge the inflammatory response. Results from this proposed study will be able to provide necessary information to guide therapeutic applications of VNS.

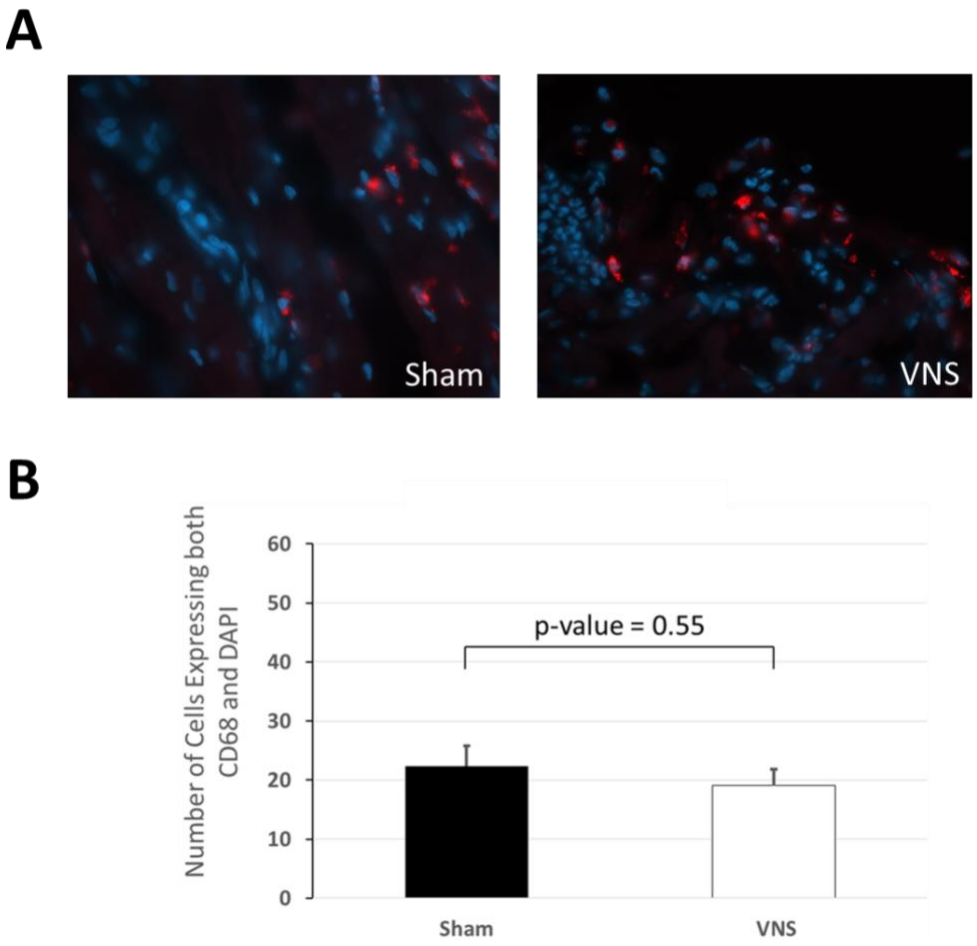


***Figure 6.3: Preliminary Assessment of Anti-inflammatory Effect of VNS.*** 30 minutes ischemia and 24 hours reperfusion was induced in rats (n = 6). VNS was provided 30 minutes prior MI. **A)** Sample images of both Sham and VNS treated rats. **B)** Mean

quantification of macrophages. Red represents CD68, one possible marker for macrophages, and blue stains for DAPI.

# REFERENCES


Abramovich-Sivan, S., and Akselrod, S. (1998). A Phase Response Curve Based Model: Effect of Vagal and Sympathetic Stimulation and Interaction on a Pacemaker Cell. *J. Theor. Biol.* 192, 567–579. doi:10.1006/jtbi.1998.0684.

AgostoniI, E., Chinnock, J. E., De Daly, M. B., and Murray, J. G. (1957). Functional and histological studies of the vagus nerve and its branches to the heart, lungs and abdominal viscera in the cat. *J. Physiol.* 135, 182–205. Available at: http://www.ncbi.nlm.nih.gov/pubmed/13398974 [Accessed October 30, 2017].

Akdemir, B., and Benditt, D. G. (2016). Vagus nerve stimulation: An evolving adjunctive treatment for cardiac disease. *Anatol. J. Cardiol.* 16, 804–810. doi:10.14744/anatoljcardiol.2016.7129.

Akiyama, T., and Yamazaki, T. (2001). Effects of right and left vagal stimulation on left ventricular acetylcholine levels in the cat. *Acta Physiol. Scand.* 172, 11–6. doi:10.1046/j.1365-201X.2001.00812.x.

Anderson, A., Kulkarni, K., Marron Fernandez de Velasco, E., Carlblom, N., Xia, Z., Nakano, A., et al. (2018). Expression and relevance of the G protein-gated K+ channel in the mouse ventricle. *Sci. Rep.* 8, 1192. doi:10.1038/s41598-018-19719-x.

Ando, M., Katare, R. G., Kakinuma, Y., Zhang, D., Yamasaki, F., Muramoto, K., et al. (2005). Efferent vagal nerve stimulation protects heart against ischemia-induced arrhythmias by preserving connexin43 protein. *Circulation* 112, 164–70. doi:10.1161/CIRCULATIONAHA.104.525493.

Annoni, E. M., Xie, X., Lee, S. W., Libbus, I., KenKnight, B. H., Osborn, J. W., et al. (2015). Intermittent electrical stimulation of the right cervical vagus nerve in salt-sensitive hypertensive rats: effects on blood pressure, arrhythmias, and ventricular electrophysiology. *Physiol. Rep.* 3. doi:10.14814/phy2.12476.

Ardell, J. L., Rajendran, P. S., Nier, H. A., KenKnight, B. H., and Armour, J. A. (2015). Central-peripheral neural network interactions evoked by vagus nerve stimulation: functional consequences on control of cardiac function. *Am. J. Physiol. Heart Circ. Physiol.* 309, H1740-52. doi:10.1152/ajpheart.00557.2015.

Armour, J. A., Murphy, D. A., Yuan, B. X., Macdonald, S., and Hopkins, D. A. (1997). Gross and microscopic anatomy of the human intrinsic cardiac nervous system. *Anat. Rec.* 247, 289–98. Available at: http://www.ncbi.nlm.nih.gov/pubmed/9026008 [Accessed December 16, 2015].

Armour, J., Randall, W., and Sinha, S. (1975). Localized myocardial responses to stimulation of small cardiac branches of the vagus. *Am. J. Physiol. Content* 228, 141–148. doi:10.1152/ajplegacy.1975.228.1.141.

Azar, T., Sharp, J., and Lawson, D. (2011). Heart rates of male and female Sprague-Dawley and spontaneously hypertensive rats housed singly or in groups. *J. Am. Assoc. Lab. Anim. Sci.* 50, 175–84. Available at: http://www.ncbi.nlm.nih.gov/pubmed/21439210 [Accessed December 26, 2017].

Balasubramanian, K., Harikumar, K., Nagaraj, N., and Pati, S. (2017). Vagus Nerve Stimulation Modulates Complexity of Heart Rate Variability Differently during Sleep

and Wakefulness. *Ann. Indian Acad. Neurol.* 20, 403–407. doi:10.4103/aian.AIAN_148_17.

Beaumont, E., Southerland, E. M., Hardwick, J. C., Wright, G. L., Ryan, S., Li, Y., et al. (2015). Vagus nerve stimulation mitigates intrinsic cardiac neuronal and adverse myocyte remodeling postmyocardial infarction. *Am. J. Physiol. Heart Circ. Physiol.* 309, H1198-206. doi:10.1152/ajpheart.00393.2015.

Ben-Menachem, E., Mañon-Espaillat, R., Ristanovic, R., Wilder, B. J., Stefan, H., Mirza, W., et al. Vagus nerve stimulation for treatment of partial seizures: 1. A controlled study of effect on seizures. First International Vagus Nerve Stimulation Study Group. *Epilepsia* 35, 616–26. Available at: http://www.ncbi.nlm.nih.gov/pubmed/8026408 [Accessed October 31, 2017].

Benjamin, E. J., Blaha, M. J., Chiuve, S. E., Cushman, M., Das, S. R., Deo, R., et al. (2017). Heart Disease and Stroke Statistics—2017 Update: A Report From the American Heart Association. *Circulation* 135, e146–e603. doi:10.1161/CIR.0000000000000485.

Bernstein, H. S., and Srivastava, D. (2012). Stem cell therapy for cardiac disease. *Pediatr. Res.* 71, 491–9. doi:10.1038/pr.2011.61.

Berntson, G. G., Quigley, K. S., Fabro, V. J., and Cacioppo, J. T. (1992). Vagal stimulation and cardiac chronotropy in rats. *J. Auton. Nerv. Syst.* 41, 221–6. Available at: http://www.ncbi.nlm.nih.gov/pubmed/1289386 [Accessed January 2, 2018].

Bibevski, S., and Dunlap, M. E. (2011). Evidence for impaired vagus nerve activity in heart failure. *Heart Fail. Rev.* 16, 129–35. doi:10.1007/s10741-010-9190-6.

Borovikova, L. V, Ivanova, S., Zhang, M., Yang, H., Botchkina, G. I., Watkins, L. R., et al. (2000). Vagus nerve stimulation attenuates the systemic inflammatory response to endotoxin. *Nature* 405, 458–62. doi:10.1038/35013070.

Brack, K. E., Coote, J. H., and Ng, G. A. (2011). Vagus nerve stimulation protects against ventricular fibrillation independent of muscarinic receptor activation. *Cardiovasc. Res.* 91, 437–46. doi:10.1093/cvr/cvr105.

Brennan, M., Palaniswami, M., and Kamen, P. (2001). Do existing measures of Poincare plot geometry reflect nonlinear features of heart rate variability? *IEEE Trans. Biomed. Eng.* 48, 1342–1347. doi:10.1109/10.959330.

Buschman, H. P., Storm, C. J., Duncker, D. J., Verdouw, P. D., van der Aa, H. E., and van der Kemp, P. (2006). Heart Rate Control Via Vagus Nerve Stimulation. *Neuromodulation Technol. Neural Interface* 9, 214–220. doi:10.1111/j.1525-1403.2006.00062.x.

Bush, N. R., Caron, Z. K., Blackburn, K. S., and Alkon, A. (2016). Measuring Cardiac Autonomic Nervous System (ANS) Activity in Toddlers - Resting and Developmental Challenges. *J. Vis. Exp.*, 53652. doi:10.3791/53652.

Byku, M., and Mann, D. L. (2016). Neuromodulation of the Failing Heart: Lost in Translation? *JACC. Basic to Transl. Sci.* 1, 95–106. doi:10.1016/j.jacbts.2016.03.004.

Calvillo, L., Vanoli, E., Andreoli, E., Besana, A., Omodeo, E., Gnecchi, M., et al. (2011). Vagal stimulation, through its nicotinic action, limits infarct size and the inflammatory response to myocardial ischemia and reperfusion. *J. Cardiovasc. Pharmacol.* 58, 500–7. doi:10.1097/FJC.0b013e31822b7204.

Castoro, M. A., Yoo, P. B., Hincapie, J. G., Hamann, J. J., Ruble, S. B., Wolf, P. D., et al. (2011). Excitation properties of the right cervical vagus nerve in adult dogs. *Exp. Neurol.* 227, 62–68. doi:10.1016/j.expneurol.2010.09.011.

Chen, P. S., and Tan, A. Y. (2007). Autonomic nerve activity and atrial fibrillation. *Heart Rhythm* 4, S61-4. doi:10.1016/j.hrthm.2006.12.006.

Chen, Y. J., Chen, S. A., Chen, Y. C., Yeh, H. I., Chang, M. S., and Lin, C. I. (2002a). Electrophysiology of single cardiomyocytes isolated from rabbit pulmonary veins: implication in initiation of focal atrial fibrillation. *Basic Res. Cardiol.* 97, 26–34. Available at: http://www.ncbi.nlm.nih.gov/pubmed/11998974 [Accessed June 4, 2014].

Chen, Y. J., Chen, Y. C., Yeh, H. I., Lin, C. I., and Chen, S. A. (2002b). Electrophysiology and arrhythmogenic activity of single cardiomyocytes from canine superior vena cava. *Circulation* 105, 2679–85. Available at: http://www.ncbi.nlm.nih.gov/pubmed/12045176 [Accessed May 31, 2014].

Coote, J. H. (2013). Myths and realities of the cardiac vagus. *J. Physiol.* 591, 4073–85. doi:10.1113/jphysiol.2013.257758.

Coronel, R., Wilders, R., Verkerk, A. O., Wiegerinck, R. F., Benoist, D., and Bernus, O. (2013). Electrophysiological changes in heart failure and their implications for arrhythmogenesis. *Biochim. Biophys. Acta* 1832, 2432–41. doi:10.1016/j.bbadis.2013.04.002.

De Ferrari, G. M., Crijns, H. J. G. M., Borggrefe, M., Milasinovic, G., Smid, J., Zabel, M., et al. (2011). Chronic vagus nerve stimulation: a new and promising therapeutic approach for chronic heart failure. *Eur. Heart J.* 32, 847–55. doi:10.1093/eurheartj/ehq391.

De Ferrari, G. M., and Schwartz, P. J. (2011). Vagus nerve stimulation: from pre-clinical to clinical application: challenges and future directions. *Heart Fail. Rev.* 16, 195–203. doi:10.1007/s10741-010-9216-0.

Dhein, S., Polontchouk, L., Salameh, A., and Haefliger, J. A. (2002). Pharmacological modulation and differential regulation of the cardiac gap junction proteins connexin 43 and connexin 40. *Biol. Cell* 94, 409–22. Available at: http://www.ncbi.nlm.nih.gov/pubmed/12566216 [Accessed April 29, 2014].

Dicarlo, L., Libbus, I., Amurthur, B., Kenknight, B. H., and Anand, I. S. (2013). Autonomic regulation therapy for the improvement of left ventricular function and heart failure symptoms: the ANTHEM-HF study. *J. Card. Fail.* 19, 655–60. doi:10.1016/j.cardfail.2013.07.002.

DiFrancesco, D. (2010). The Role of the Funny Current in Pacemaker Activity. *Circ. Res.* 106, 434–446. doi:10.1161/CIRCRESAHA.109.208041.

DiFrancesco, D., and Borer, J. S. (2007). The funny current: cellular basis for the control of heart rate. *Drugs* 67 Suppl 2, 15–24. Available at: http://www.ncbi.nlm.nih.gov/pubmed/17999560 [Accessed February 20, 2018].

DiFrancesco, D., Ducouret, P., and Robinson, R. B. (1989). Muscarinic Modulation of Cardiac Rate at Low Acetylcholine Concentrations. *Science (80-. ).* 243, 669–671. doi:10.2307/1703311.

Dvir, H., and Zlochiver, S. (2013). Stochastic cardiac pacing increases ventricular electrical

stability--a computational study. *Biophys. J.* 105, 533–42. doi:10.1016/j.bpj.2013.06.012.

Elger, G., Hoppe, C., Falkai, P., Rush, A. J., and Elger, C. E. (2000). Vagus nerve stimulation is associated with mood improvements in epilepsy patients. *Epilepsy Res.* 42, 203–10. Available at: http://www.ncbi.nlm.nih.gov/pubmed/11074193 [Accessed November 3, 2017].

Gaztañaga, L., Marchlinski, F. E., and Betensky, B. P. (2012). Mechanisms of Cardiac Arrhythmias. *Rev. Española Cardiol. (English Ed.* 65, 174–185. doi:10.1016/j.rec.2011.09.020.

Ghanem, T., and Early, S. V (2006). Vagal nerve stimulator implantation: an otolaryngologist's perspective. *Otolaryngol. Head. Neck Surg.* 135, 46–51. doi:10.1016/j.otohns.2006.02.037.

Goel, R., Kofman, I., Jeevarajan, J., De Dios, Y., Cohen, H. S., Bloomberg, J. J., et al. (2015). Using Low Levels of Stochastic Vestibular Stimulation to Improve Balance Function. *PLoS One* 10, e0136335. doi:10.1371/journal.pone.0136335.

Gold, M. R., Van Veldhuisen, D. J., Hauptman, P. J., Borggrefe, M., Kubo, S. H., Lieberman, R. A., et al. (2016). Vagus Nerve Stimulation for the Treatment of Heart Failure. *J. Am. Coll. Cardiol.* 68, 149–158. doi:10.1016/j.jacc.2016.03.525.

Gold, M. R., van Veldhuisen, D. J., and Mann, D. L. (2015). Vagal nerve stimulation for heart failure: new pieces to the puzzle? *Eur. J. Heart Fail.* 17, 125–127. doi:10.1002/ejhf.234.

Gordan, R., Gwathmey, J. K., and Xie, L.-H. (2015). Autonomic and endocrine control of cardiovascular function. *World J. Cardiol.* 7, 204–14. doi:10.4330/wjc.v7.i4.204.

Groves, D. A., and Brown, V. J. (2005). Vagal nerve stimulation: a review of its applications and potential mechanisms that mediate its clinical effects. *Neurosci. Biobehav. Rev.* 29, 493–500. doi:10.1016/j.neubiorev.2005.01.004.

Gutstein, D. E., Morley, G. E., Tamaddon, H., Vaidya, D., Schneider, M. D., Chen, J., et al. (2001). Conduction slowing and sudden arrhythmic death in mice with cardiac-restricted inactivation of connexin43. *Circ. Res.* 88, 333–9. Available at: http://www.pubmedcentral.nih.gov/articlerender.fcgi?artid=3630465&tool=pmcentrez&rendertype=abstract [Accessed April 29, 2014].

Guzik, P., Piskorski, J., Krauze, T., Schneider, R., Wesseling, K. H., Wykretowicz, A., et al. (2007). Correlations between the Poincaré Plot and Conventional Heart Rate Variability Parameters Assessed during Paced Breathing. *J. Physiol. Sci.* 57, 63–71. doi:10.2170/physiolsci.RP005506.

Harvey, R. D. (2012). "Muscarinic Receptor Agonists and Antagonists: Effects on Cardiovascular Function," in *Handbook of experimental pharmacology*, 299–316. doi:10.1007/978-3-642-23274-9_13.

Harvey, R. D., and Belevych, A. E. (2003). Muscarinic regulation of cardiac ion channels. *Br. J. Pharmacol.* 139, 1074–1084. doi:10.1038/sj.bjp.0705338.

Hasan, W. (2013). Autonomic cardiac innervation: development and adult plasticity. *Organogenesis* 9, 176–93. doi:10.4161/org.24892.

Heller Brown, J., and Laiken, N. (2012). "Chapter 15 – Acetylcholine and Muscarinic Receptors," in *Primer on the Autonomic Nervous System*, 75–78. doi:10.1016/B978-

0-12-386525-0.00015-9.
Hirsch, A. T., Dzau, V. J., and Creager, M. A. (1987). Baroreceptor function in congestive heart failure: effect on neurohumoral activation and regional vascular resistance. *Circulation* 75, IV36-48. Available at: http://www.ncbi.nlm.nih.gov/pubmed/2882866 [Accessed December 29, 2015].
Hoover, D. B., Ganote, C. E., Ferguson, S. M., Blakely, R. D., and Parsons, R. L. (2004). Localization of cholinergic innervation in guinea pig heart by immunohistochemistry for high-affinity choline transporters. *Cardiovasc. Res.* 62, 112–21. doi:10.1016/j.cardiores.2004.01.012.
Hori, M., and Okamoto, H. (2012). Heart rate as a target of treatment of chronic heart failure. *J. Cardiol.* 60, 86–90. doi:10.1016/j.jjcc.2012.06.013.
Howland, R. H. (2014). Vagus Nerve Stimulation. *Curr. Behav. Neurosci. reports* 1, 64–73. doi:10.1007/s40473-014-0010-5.
Ippolito, J., Xie, X., Kenknight, B. H., and Tolkacheva, E. G. (2014). Intermittent Vagus Nerve Stimulation Reflexively Modulates Heart Rate Variability in Rats With Chronic Ischemic Heart Failure. in *Journal of Medical Devices, Transactions of the ASME*.
Jacobowitz, D., Cooper, T., and Barner, H. B. (1967). Histochemical and chemical studies of the localization of adrenergic and cholinergic nerves in normal and denervated cat hearts. *Circ. Res.* 20, 289–98. Available at: http://www.ncbi.nlm.nih.gov/pubmed/6025610 [Accessed November 18, 2017].
Jiang, H., Hu, X., Lu, Z., Wen, H., Zhao, D., Tang, Q., et al. (2008). Effects of sympathetic nerve stimulation on ischemia-induced ventricular arrhythmias by modulating connexin43 in rats. *Arch. Med. Res.* 39, 647–54. doi:10.1016/j.arcmed.2008.07.005.
Johnson, M. D., Lim, H. H., Netoff, T. I., Connolly, A. T., Johnson, N., Roy, A., et al. (2013). Neuromodulation for Brain Disorders: Challenges and Opportunities. *IEEE Trans. Biomed. Eng.* 60, 610–624. doi:10.1109/TBME.2013.2244890.
Jungen, C., Scherschel, K., Eickholt, C., Kuklik, P., Klatt, N., Bork, N., et al. (2017). Disruption of cardiac cholinergic neurons enhances susceptibility to ventricular arrhythmias. *Nat. Commun.* 8, 14155. doi:10.1038/ncomms14155.
Kadish, A., Shinnar, M., Moore, E. N., Levine, J. H., Balke, C. W., and Spear, J. F. (1988). Interaction of fiber orientation and direction of impulse propagation with anatomic barriers in anisotropic canine myocardium. *Circulation* 78, 1478–94. Available at: http://www.ncbi.nlm.nih.gov/pubmed/3191601 [Accessed November 26, 2017].
Kalla, M., Herring, N., and Paterson, D. J. (2016). Cardiac sympatho-vagal balance and ventricular arrhythmia. *Auton. Neurosci.* 199, 29–37. doi:10.1016/j.autneu.2016.08.016.
Kapa, S., DeSimone, C. V, and Asirvatham, S. J. (2016). Innervation of the heart: An invisible grid within a black box. *Trends Cardiovasc. Med.* 26, 245–57. doi:10.1016/j.tcm.2015.07.001.
Karnovsky, M. J., and Roots, L. (1964). A "Direct-Coloring" Thiocholine Method for Cholinesterases. *J. Histochem. Cytochem.* 12, 219–221. doi:10.1177/12.3.219.
Kawada, T., Yamazaki, T., Akiyama, T., Shishido, T., Inagaki, M., Uemura, K., et al. (2001). In vivo assessment of acetylcholine-releasing function at cardiac vagal nerve

terminals. *Am. J. Physiol. Heart Circ. Physiol.* 281, H139-45. Available at: http://www.ncbi.nlm.nih.gov/pubmed/11406478 [Accessed November 18, 2017].

Kent, K. M., Epstein, S. E., Cooper, T., and Jacobowitz, D. M. (1974). Cholinergic innervation of the canine and human ventricular conducting system. Anatomic and electrophysiologic correlations. *Circulation* 50, 948–55. Available at: http://www.ncbi.nlm.nih.gov/pubmed/4430098 [Accessed November 18, 2017].

Klein, H. U., and Ferrari, G. M. De (2010). Vagus nerve stimulation: A new approach to reduce heart failure. *Cardiol. J.* 17, 638–44. Available at: http://www.ncbi.nlm.nih.gov/pubmed/21154273 [Accessed April 28, 2014].

Klocke, R., Tian, W., Kuhlmann, M. T., and Nikol, S. (2007). Surgical animal models of heart failure related to coronary heart disease. *Cardiovasc. Res.* 74, 29–38. doi:10.1016/j.cardiores.2006.11.026.

Koelle, G. B. (1955). The histochemical identification of acetylcholinesterase in cholinergic, adrenergic and sensory neurons. *J. Pharmacol. Exp. Ther.* 114, 167–84. Available at: http://www.ncbi.nlm.nih.gov/pubmed/14392585 [Accessed November 18, 2017].

Kong, S. S., Liu, J. J., Hwang, T. C., Yu, X. J., Zhao, M., Zhao, M., et al. (2012a). Optimizing the Parameters of Vagus Nerve Stimulation by Uniform Design in Rats with Acute Myocardial Infarction. *PLoS One* 7, e42799. doi:10.1371/journal.pone.0042799.

Kong, S. S., Liu, J. J., Yu, X. J., Lu, Y., and Zang, W. J. (2012b). Protection against ischemia-induced oxidative stress conferred by vagal stimulation in the rat heart: involvement of the AMPK-PKC pathway. *Int. J. Mol. Sci.* 13, 14311–25. doi:10.3390/ijms131114311.

Kovoor, P., Wickman, K., Maguire, C. T., Pu, W., Gehrmann, J., Berul, C. I., et al. (2001). Evaluation of the role of I(KACh) in atrial fibrillation using a mouse knockout model. *J. Am. Coll. Cardiol.* 37, 2136–43. Available at: http://www.ncbi.nlm.nih.gov/pubmed/11419900 [Accessed January 21, 2018].

Kozasa, Y., Nakashima, N., Ito, M., Ishikawa, T., Kimoto, H., Ushijima, K., et al. (2018). HCN4 pacemaker channels attenuate the parasympathetic response and stabilize the spontaneous firing of the sinoatrial node. *J. Physiol.* doi:10.1113/JP275303.

Krames, E., Hunter Peckham, P., Rezai, A., and Aboelsaad, F. (2009). "Chapter 1 – What Is Neuromodulation?," in *Neuromodulation* (San Diego, CA: Academic Press), 3–8. doi:10.1016/B978-0-12-374248-3.00002-1.

Krejcí, A., and Tucek, S. (2002). Quantitation of mRNAs for M(1) to M(5) subtypes of muscarinic receptors in rat heart and brain cortex. *Mol. Pharmacol.* 61, 1267–72. Available at: http://www.ncbi.nlm.nih.gov/pubmed/12021386 [Accessed November 19, 2017].

Kunze, D. L. (1972). Reflex discharge patterns of cardiac vagal efferent fibres. *J. Physiol.* 222, 1–15. Available at: http://www.pubmedcentral.nih.gov/articlerender.fcgi?artid=1331413&tool=pmcentrez&rendertype=abstract [Accessed April 25, 2014].

Kurachi, Y., Nakajima, T., and Sugimoto, T. (1986). Acetylcholine activation of K+ channels in cell-free membrane of atrial cells. *Am. J. Physiol.* 251, H681-4.

doi:10.1152/ajpheart.1986.251.3.H681.
Lee, S. W., Li, Q., Libbus, I., Xie, X., KenKnight, B. H., Garry, M. G., et al. (2016). Chronic cyclic vagus nerve stimulation has beneficial electrophysiological effects on healthy hearts in the absence of autonomic imbalance. *Physiol. Rep.* 4, e12786. doi:10.14814/phy2.12786.
Lemola, K., Chartier, D., Yeh, Y.-H., Dubuc, M., Cartier, R., Armour, A., et al. (2008). Pulmonary vein region ablation in experimental vagal atrial fibrillation: role of pulmonary veins versus autonomic ganglia. *Circulation* 117, 470–7. doi:10.1161/CIRCULATIONAHA.107.737023.
Lerner, D. L., Yamada, K. A., Schuessler, R. B., and Saffitz, J. E. (2000). Accelerated onset and increased incidence of ventricular arrhythmias induced by ischemia in Cx43-deficient mice. *Circulation* 101, 547–52. Available at: http://www.ncbi.nlm.nih.gov/pubmed/10662753 [Accessed April 29, 2014].
Levy, M. N., and Zieske, H. (1969). Autonomic control of cardiac pacemaker activity and atrioventricular transmission. *J. Appl. Physiol.* 27, 465–70. Available at: http://www.ncbi.nlm.nih.gov/pubmed/5822553 [Accessed August 4, 2017].
Li, D., Melnyk, P., Feng, J., Wang, Z., Petrecca, K., Shrier, A., et al. (2000). Effects of experimental heart failure on atrial cellular and ionic electrophysiology. *Circulation* 101, 2631–8. Available at: http://www.ncbi.nlm.nih.gov/pubmed/10840016 [Accessed June 4, 2014].
Li, M., Zheng, C., Sato, T., Kawada, T., Sugimachi, M., and Sunagawa, K. (2004). Vagal nerve stimulation markedly improves long-term survival after chronic heart failure in rats. *Circulation* 109, 120–4. doi:10.1161/01.CIR.0000105721.71640.DA.
Li, Y., Xuan, Y.-H., Liu, S.-S., Dong, J., Luo, J.-Y., and Sun, Z.-J. (2015). Short‐term vagal nerve stimulation improves left ventricular function following chronic heart failure in rats. *Mol. Med. Rep.* 12, 1709–16. doi:10.3892/mmr.2015.3597.
Liang, B., Nissen, J. D., Laursen, M., Wang, X., Skibsbye, L., Hearing, M. C., et al. (2014). G-protein-coupled inward rectifier potassium current contributes to ventricular repolarization. *Cardiovasc. Res.* 101, 175–84. doi:10.1093/cvr/cvt240.
Libbus, I., Nearing, B. D., Amurthur, B., KenKnight, B. H., and Verrier, R. L. (2017). Quantitative evaluation of heartbeat interval time series using Poincaré analysis reveals distinct patterns of heart rate dynamics during cycles of vagus nerve stimulation in patients with heart failure. *J. Electrocardiol.* doi:10.1016/j.jelectrocard.2017.06.007.
Libbus, I., and Rosenbaum, D. S. (2002). Remodeling of cardiac repolarization: mechanisms and implications of memory. *Card. Electrophysiol. Rev.* 6, 302–10. Available at: http://www.ncbi.nlm.nih.gov/pubmed/12114856 [Accessed July 24, 2017].
Linz, D., Ukena, C., Mahfoud, F., Neuberger, H.-R., and Böhm, M. (2014). Atrial Autonomic Innervation. *J. Am. Coll. Cardiol.* 63, 215–224. doi:10.1016/j.jacc.2013.09.020.
Liu, Y. H., Yang, X. P., Sharov, V. G., Nass, O., Sabbah, H. N., Peterson, E., et al. (1997). Effects of angiotensin-converting enzyme inhibitors and angiotensin II type 1 receptor antagonists in rats with heart failure. Role of kinins and angiotensin II type 2

receptors. *J. Clin. Invest.* 99, 1926–35. doi:10.1172/JCI119360.
Lomax, A. E., Rose, R. A., and Giles, W. R. (2003). Electrophysiological evidence for a gradient of G protein-gated $K^+$ current in adult mouse atria. *Br. J. Pharmacol.* 140, 576–584. doi:10.1038/sj.bjp.0705474.
Lund, C., Kostov, H., Blomskjøld, B., and Nakken, K. O. (2011). Efficacy and tolerability of long-term treatment with vagus nerve stimulation in adolescents and adults with refractory epilepsy and learning disabilities. *Seizure* 20, 34–37. doi:10.1016/j.seizure.2010.10.002.
Malik, M. (1996). Heart Rate Variability. *Ann. Noninvasive Electrocardiol.* 1, 151–181. doi:10.1111/j.1542-474X.1996.tb00275.x.
Mangoni, M. E., and Nargeot, J. (2008). Genesis and Regulation of the Heart Automaticity. *Physiol. Rev.* 88, 919–982. doi:10.1152/physrev.00018.2007.
Mantravadi, R., Gabris, B., Liu, T., Choi, B.-R., de Groat, W. C., Ng, G. A., et al. (2007). Autonomic nerve stimulation reverses ventricular repolarization sequence in rabbit hearts. *Circ. Res.* 100, e72-80. doi:10.1161/01.RES.0000264101.06417.33.
McCorry, L. K. (2007). Physiology of the autonomic nervous system. *Am. J. Pharm. Educ.* 71, 78. Available at: http://www.ncbi.nlm.nih.gov/pubmed/17786266 [Accessed October 11, 2017].
McIntyre, S. D., Kakade, V., Mori, Y., and Tolkacheva, E. G. (2014). Heart rate variability and alternans formation in the heart: The role of feedback in cardiac dynamics. *J. Theor. Biol.* 350, 90–7. doi:10.1016/j.jtbi.2014.02.015.
Mesirca, P., Bidaud, I., Briec, F., Evain, S., Torrente, A. G., Le Quang, K., et al. (2016a). G protein-gated IKACh channels as therapeutic targets for treatment of sick sinus syndrome and heart block. *Proc. Natl. Acad. Sci. U. S. A.* 113, E932-41. doi:10.1073/pnas.1517181113.
Mesirca, P., Bidaud, I., and Mangoni, M. E. (2016b). Rescuing cardiac automaticity in L-type Cav1.3 channelopathies and beyond. *J. Physiol.* 594, 5869–5879. doi:10.1113/JP270678.
Mesirca, P., Marger, L., Toyoda, F., Rizzetto, R., Audoubert, M., Dubel, S., et al. (2013). The G-protein-gated K+ channel, IKACh, is required for regulation of pacemaker activity and recovery of resting heart rate after sympathetic stimulation. *J. Gen. Physiol.* 142, 113–26. doi:10.1085/jgp.201310996.
Mesirca, P., Torrente, A. G., and Mangoni, M. E. (2015). Functional role of voltage gated Ca(2+) channels in heart automaticity. *Front. Physiol.* 6, 19. doi:10.3389/fphys.2015.00019.
Mihaylova, S., Killian, A., Mayer, K., Pullamsetti, S. S., Schermuly, R., and Rosengarten, B. (2012). Effects of anti-inflammatory vagus nerve stimulation on the cerebral microcirculation in endotoxinemic rats. *J. Neuroinflammation* 9, 183. doi:10.1186/1742-2094-9-183.
Mironov, S., Jalife, J., and Tolkacheva, E. G. (2008). Role of conduction velocity restitution and short-term memory in the development of action potential duration alternans in isolated rabbit hearts. *Circulation* 118, 17–25. doi:10.1161/CIRCULATIONAHA.107.737254.
Miyauchi, Y., Zhou, S., Okuyama, Y., Miyauchi, M., Hayashi, H., Hamabe, A., et al.

(2003). Altered atrial electrical restitution and heterogeneous sympathetic hyperinnervation in hearts with chronic left ventricular myocardial infarction: implications for atrial fibrillation. *Circulation* 108, 360–6. doi:10.1161/01.CIR.0000080327.32573.7C.

Monteiro, L. M., Vasques-Nóvoa, F., Ferreira, L., Pinto-do-Ó, P., and Nascimento, D. S. (2017). Restoring heart function and electrical integrity: closing the circuit. *npj Regen. Med.* 2, 9. doi:10.1038/s41536-017-0015-2.

Muppidi, S., Gupta, P. K., and Vernino, S. (2011). Reversible right vagal neuropathy. *Neurology* 77, 1577–9. doi:10.1212/WNL.0b013e318233b3a2.

Nakano, H., Williams, E., Hoshijima, M., Sasaki, M., Minamisawa, S., Chien, K. R., et al. (2011). Cardiac origin of smooth muscle cells in the inflow tract. *J. Mol. Cell. Cardiol.* 50, 337–45. doi:10.1016/j.yjmcc.2010.10.009.

Nattel, S. (2002). New ideas about atrial fibrillation 50 years on. *Nature* 415, 219–26. doi:10.1038/415219a.

Nearing, B. D., Libbus, I., Amurthur, B., KenKnight, B. H., and Verrier, R. L. (2016). Autonomic regulation therapy suppresses quantitative T-wave alternans and improves baroreflex sensitivity in patients with heart failure enrolled in the ANTHEM-HF study. *Hear. Rhythm* 13, 721–728. doi:10.1016/j.hrthm.2015.11.030.

Neely, B. H., and Urthaler, F. (1992). Quantitative effects of sympathetic and vagal nerve stimulations on sinus and AV junctional rhythms. *J. Auton. Nerv. Syst.* 37, 109–20. Available at: http://www.ncbi.nlm.nih.gov/pubmed/1607596 [Accessed February 19, 2018].

O'Reardon, J. P., Cristancho, P., and Peshek, A. D. (2006). Vagus Nerve Stimulation (VNS) and Treatment of Depression: To the Brainstem and Beyond. *Psychiatry (Edgmont).* 3, 54–63. Available at: http://www.ncbi.nlm.nih.gov/pubmed/21103178 [Accessed May 31, 2017].

Oda, Y. (1999). Choline acetyltransferase: the structure, distribution and pathologic changes in the central nervous system. *Pathol. Int.* 49, 921–37. Available at: http://www.ncbi.nlm.nih.gov/pubmed/10594838 [Accessed November 18, 2017].

Olshansky, B. (2016). Electrical Stimulation of the Vagus Nerve for Chronic Heart Failure: Is It Time to Pull the Plug? *J. Card. Fail.* 22, 643–645. doi:10.1016/j.cardfail.2016.05.005.

Papp, R., Gönczi, M., Kovács, M., Seprényi, G., and Végh, A. (2007). Gap junctional uncoupling plays a trigger role in the antiarrhythmic effect of ischaemic preconditioning. *Cardiovasc. Res.* 74, 396–405. doi:10.1016/j.cardiores.2007.02.021.

Park, H.-W., and Cho, J.-G. (2014). "Neural Mechanisms of Arrhythmia," in *Cardiac Arrhythmias* (London: Springer London), 61–64. doi:10.1007/978-1-4471-5316-0_6.

Parker, P., Celler, B. G., Potter, E. K., and McCloskey, D. I. (1984). Vagal stimulation and cardiac slowing. *J. Auton. Nerv. Syst.* 11, 226–31. Available at: http://www.ncbi.nlm.nih.gov/pubmed/6491162 [Accessed January 2, 2018].

Pauza, D. H., Saburkina, I., Rysevaite, K., Inokaitis, H., Jokubauskas, M., Jalife, J., et al. (2013). Neuroanatomy of the murine cardiac conduction system. *Auton. Neurosci.* 176, 32–47. doi:10.1016/j.autneu.2013.01.006.

Pauziene, N., Alaburda, P., Rysevaite-Kyguoliene, K., Pauza, A. G., Inokaitis, H.,

Masaityte, A., et al. (2016). Innervation of the rabbit cardiac ventricles. *J. Anat.* 228, 26–46. doi:10.1111/joa.12400.

Penry, J. K., and Dean, J. C. (1990). Prevention of intractable partial seizures by intermittent vagal stimulation in humans: preliminary results. *Epilepsia* 31 Suppl 2, S40-3. Available at: http://www.ncbi.nlm.nih.gov/pubmed/2121469 [Accessed October 31, 2017].

Premchand, R. K., Sharma, K., Mittal, S., Monteiro, R., Dixit, S., Libbus, I., et al. (2014). Autonomic regulation therapy via left or right cervical vagus nerve stimulation in patients with chronic heart failure: results of the ANTHEM-HF trial. *J. Card. Fail.* 20, 808–16. doi:10.1016/j.cardfail.2014.08.009.

Premchand, R. K., Sharma, K., Mittal, S., Monteiro, R., Dixit, S., Libbus, I., et al. (2015). Extended Follow-Up of Patients with Heart Failure Receiving Autonomic Regulation Therapy in the ANTHEM-HF Study. *J. Card. Fail.* doi:10.1016/j.cardfail.2015.11.002.

Randall, D. C., Brown, D. R., McGuirt, A. S., Thompson, G. W., Armour, J. A., and Ardell, J. L. (2003). Interactions within the intrinsic cardiac nervous system contribute to chronotropic regulation. *Am. J. Physiol. Regul. Integr. Comp. Physiol.* 285, R1066-75. doi:10.1152/ajpregu.00167.2003.

Rentero, N., Cividjian, A., Trevaks, D., Pequignot, J. M., Quintin, L., and McAllen, R. M. (2002). Activity patterns of cardiac vagal motoneurons in rat nucleus ambiguus. *Am. J. Physiol. - Regul. Integr. Comp. Physiol.* 283, R1327–R1334. doi:10.1152/ajpregu.00271.2002.

Roberts, D. E., Hersh, L. T., and Scher, A. M. (1979). Influence of cardiac fiber orientation on wavefront voltage, conduction velocity, and tissue resistivity in the dog. *Circ. Res.* 44, 701–12. Available at: http://www.ncbi.nlm.nih.gov/pubmed/428066 [Accessed November 26, 2017].

Romero Ugalde, H. M., Le Rolle, V., Bonnet, J.-L., Henry, C., Mabo, P., Carrault, G., et al. (2017). Closed-loop vagus nerve stimulation based on state transition models. *IEEE Trans. Biomed. Eng.*, 1–1. doi:10.1109/TBME.2017.2759667.

Rush, A. J., George, M. S., Sackeim, H. A., Marangell, L. B., Husain, M. M., Giller, C., et al. (2000). Vagus nerve stimulation (VNS) for treatment-resistant depressions: a multicenter study. *Biol. Psychiatry* 47, 276–86. Available at: http://www.ncbi.nlm.nih.gov/pubmed/10686262 [Accessed November 3, 2017].

Sabbah, H. N. (2011). Electrical vagus nerve stimulation for the treatment of chronic heart failure. *Cleve. Clin. J. Med.* 78 Suppl 1, S24-9. doi:10.3949/ccjm.78.s1.04.

Saffitz, J. E., Schuessler, R. B., and Yamada, K. A. (1999). Mechanisms of remodeling of gap junction distributions and the development of anatomic substrates of arrhythmias. *Cardiovasc. Res.* 42, 309–17. Available at: http://www.ncbi.nlm.nih.gov/pubmed/10533569 [Accessed April 29, 2014].

Samniang, B., Shinlapawittayatorn, K., Chunchai, T., Pongkan, W., Kumfu, S., Chattipakorn, S. C., et al. (2016). Vagus Nerve Stimulation Improves Cardiac Function by Preventing Mitochondrial Dysfunction in Obese-Insulin Resistant Rats. *Sci. Rep.* 6, 19749. doi:10.1038/srep19749.

Sampaio, K. N., Mauad, H., Spyer, K. M., and Ford, T. W. (2003). Differential

chronotropic and dromotropic responses to focal stimulation of cardiac vagal ganglia in the rat. *Exp. Physiol.* 88, 315–27. Available at: http://www.ncbi.nlm.nih.gov/pubmed/12719756 [Accessed June 4, 2014].

Schauerte, P., Scherlag, B. J., Pitha, J., Scherlag, M. A., Reynolds, D., Lazzara, R., et al. (2000). Catheter ablation of cardiac autonomic nerves for prevention of vagal atrial fibrillation. *Circulation* 102, 2774–80. Available at: http://www.ncbi.nlm.nih.gov/pubmed/11094046 [Accessed June 4, 2014].

Schwartz, P. J., and De Ferrari, G. M. (2009). Vagal stimulation for heart failure: background and first in-man study. *Heart Rhythm* 6, S76-81. doi:10.1016/j.hrthm.2009.08.012.

Schwartz, P. J., and De Ferrari, G. M. (2011). Sympathetic-parasympathetic interaction in health and disease: abnormalities and relevance in heart failure. *Heart Fail. Rev.* 16, 101–7. doi:10.1007/s10741-010-9179-1.

Seki, A., Green, H. R., Lee, T. D., Hong, L., Tan, J., Vinters, H. V, et al. (2014). Sympathetic nerve fibers in human cervical and thoracic vagus nerves. *Hear. Rhythm* 11, 1411–7. doi:10.1016/j.hrthm.2014.04.032.

Shaffer, F., and Ginsberg, J. P. (2017). An Overview of Heart Rate Variability Metrics and Norms. *Front. Public Heal.* 5, 258. doi:10.3389/fpubh.2017.00258.

Shah, M., Akar, F. G., and Tomaselli, G. F. (2005). Molecular basis of arrhythmias. *Circulation* 112, 2517–29. doi:10.1161/CIRCULATIONAHA.104.494476.

Shen, M. J., Shinohara, T., Park, H.-W., Frick, K., Ice, D. S., Choi, E.-K., et al. (2011). Continuous low-level vagus nerve stimulation reduces stellate ganglion nerve activity and paroxysmal atrial tachyarrhythmias in ambulatory canines. *Circulation* 123, 2204–12. doi:10.1161/CIRCULATIONAHA.111.018028.

Shen, M. J., and Zipes, D. P. (2014). Role of the autonomic nervous system in modulating cardiac arrhythmias. *Circ. Res.* 114, 1004–21. doi:10.1161/CIRCRESAHA.113.302549.

Shimizu, W., and Antzelevitch, C. (1999). Cellular and Ionic Basis for T-Wave Alternans Under Long-QT Conditions. *Circulation* 99, 1499–1507. doi:10.1161/01.CIR.99.11.1499.

Shindler, D. M., and Kostis, J. B. (2009). "Chapter 13 – Electrocardiographic Technology of Cardiac Arrhythmias," in *Sleep Disorders Medicine*, 182–187. doi:10.1016/B978-0-7506-7584-0.00013-6.

Shinlapawittayatorn, K., Chinda, K., Palee, S., Surinkaew, S., Thunsiri, K., Weerateerangkul, P., et al. (2013). Low-amplitude, left vagus nerve stimulation significantly attenuates ventricular dysfunction and infarct size through prevention of mitochondrial dysfunction during acute ischemia-reperfusion injury. *Heart Rhythm* 10, 1700–7. doi:10.1016/j.hrthm.2013.08.009.

Shuchman, M. (2007). Approving the vagus-nerve stimulator for depression. *N. Engl. J. Med.* 356, 1604–7. doi:10.1056/NEJMp078035.

Smith, R. M., Velamakanni, S. S., and Tolkacheva, E. G. (2012). Interventricular heterogeneity as a substrate for arrhythmogenesis of decoupled mitochondria during ischemia in the whole heart. *Am. J. Physiol. Heart Circ. Physiol.* 303, H224-33. doi:10.1152/ajpheart.00017.2012.

Smith, W. T., Fleet, W. F., Johnson, T. A., Engle, C. L., and Cascio, W. E. (1995). The Ib phase of ventricular arrhythmias in ischemic in situ porcine heart is related to changes in cell-to-cell electrical coupling. Experimental Cardiology Group, University of North Carolina. *Circulation* 92, 3051–60. Available at: http://www.ncbi.nlm.nih.gov/pubmed/7586276 [Accessed April 29, 2014].

Sridhar, A., Nishijima, Y., Terentyev, D., Khan, M., Terentyeva, R., Hamlin, R. L., et al. (2009). Chronic heart failure and the substrate for atrial fibrillation. *Cardiovasc. Res.* 84, 227–36. doi:10.1093/cvr/cvp216.

Stapelberg, N. J. C., Neumann, D. L., Shum, D. H. K., McConnell, H., and Hamilton-Craig, I. (2018). The sensitivity of 38 heart rate variability measures to the addition of artifact in human and artificial 24-hr cardiac recordings. *Ann. Noninvasive Electrocardiol.* 23, e12483. doi:10.1111/anec.12483.

Swedberg, K., Cleland, J., Cowie, M. R., Nieminen, M., Priori, S. G., Tavazzi, L., et al. (2008). Successful treatment of heart failure with devices requires collaboration. *Eur. J. Heart Fail.* 10, 1229–35. doi:10.1016/j.ejheart.2008.09.015.

Taggart, P., Critchley, H., and Lambiase, P. D. (2011). Heart-brain interactions in cardiac arrhythmia. *Heart* 97, 698–708. doi:10.1136/hrt.2010.209304.

Tai, C. T., Chiou, C. W., Wen, Z. C., Hsieh, M. H., Tsai, C. F., Lin, W. S., et al. (2000). Effect of phenylephrine on focal atrial fibrillation originating in the pulmonary veins and superior vena cava. *J. Am. Coll. Cardiol.* 36, 788–93. Available at: http://www.ncbi.nlm.nih.gov/pubmed/10987601 [Accessed June 4, 2014].

Tarvainen, M. P., Niskanen, J.-P., Lipponen, J. A., Ranta-aho, P. O., and Karjalainen, P. A. (2014). Kubios HRV – Heart rate variability analysis software. *Comput. Methods Programs Biomed.* 113, 210–220. doi:10.1016/j.cmpb.2013.07.024.

Texas Heart Institute, T. H. C. (2016). Anatomy of the Heart. Available at: http://www.texasheart.org/HIC/Anatomy/anatomy2.cfm.

The Jackson Laboratory (2017). Body Weight Information for C57BL/6J (000664). Available at: https://www.jax.org/jax-mice-and-services/strain-data-sheet-pages/body-weight-chart-000664.

Thompson, G. W., Levett, J. M., Miller, S. M., Hill, M. R. ., Meffert, W. G., Kolata, R. J., et al. (1998). Bradycardia Induced by Intravascular Versus Direct Stimulation of the Vagus Nerve. *Ann. Thorac. Surg.* 65, 637–642. doi:10.1016/S0003-4975(97)01351-9.

Toader, E., Cividjian, A., and Quintin, L. (2011). Isoflurane suppresses central cardiac parasympathetic activity in rats: a pilot study. *Minerva Anestesiol.* 77, 142–6. Available at: http://www.ncbi.nlm.nih.gov/pubmed/21150849 [Accessed December 26, 2017].

Tolkacheva, E. G. (2007). The rate- and species-dependence of short-term memory in cardiac myocytes. *J. Biol. Phys.* 33, 35–47. doi:10.1007/s10867-007-9040-5.

Triposkiadis, F., Karayannis, G., Giamouzis, G., Skoularigis, J., Louridas, G., and Butler, J. (2009). The Sympathetic Nervous System in Heart Failure. *J. Am. Coll. Cardiol.* 54, 1747–1762. doi:10.1016/j.jacc.2009.05.015.

Uemura, K., Zheng, C., Li, M., Kawada, T., and Sugimachi, M. (2010a). Early short-term vagal nerve stimulation attenuates cardiac remodeling after reperfused myocardial

infarction. *J. Card. Fail.* 16, 689–699. doi:10.1016/j.cardfail.2010.03.001.

Uemura, K., Zheng, C., Li, M., Kawada, T., and Sugimachi, M. (2010b). Early short-term vagal nerve stimulation attenuates cardiac remodeling after reperfused myocardial infarction. *J. Card. Fail.* 16, 689–99. doi:10.1016/j.cardfail.2010.03.001.

Ugalde, H. R., Le Rolle, V., Bel, A., Bonnet, J.-L., Andreu, D., Mabo, P., et al. (2014). On-off closed-loop control of vagus nerve stimulation for the adaptation of heart rate. in *2014 36th Annual International Conference of the IEEE Engineering in Medicine and Biology Society* (IEEE), 6262–6265. doi:10.1109/EMBC.2014.6945060.

Ulphani, J. S., Cain, J. H., Inderyas, F., Gordon, D., Gikas, P. V, Shade, G., et al. (2010). Quantitative analysis of parasympathetic innervation of the porcine heart. *Heart Rhythm* 7, 1113–9. doi:10.1016/j.hrthm.2010.03.043.

Uthman, B. M., Wilder, B. J., Penry, J. K., Dean, C., Ramsay, R. E., Reid, S. A., et al. (1993). Treatment of epilepsy by stimulation of the vagus nerve. *Neurology* 43, 1338–45. Available at: http://www.ncbi.nlm.nih.gov/pubmed/8327135 [Accessed October 31, 2017].

van der Groen, O., and Wenderoth, N. (2017). Random Noise Stimulation of the Cortex: Stochastic Resonance Enhances Central Mechanisms of Perception. *Brain Stimul.* 10, e4. doi:10.1016/j.brs.2016.11.030.

Vanoli, E., De Ferrari, G. M., Stramba-Badiale, M., Hull, S. S., Foreman, R. D., and Schwartz, P. J. (1991). Vagal stimulation and prevention of sudden death in conscious dogs with a healed myocardial infarction. *Circ. Res.* 68, 1471–81. Available at: http://www.ncbi.nlm.nih.gov/pubmed/2019002 [Accessed April 25, 2014].

Végh, A., Duim, S., Smits, A., Poelmann, R., ten Harkel, A., DeRuiter, M., et al. (2016). Part and Parcel of the Cardiac Autonomic Nerve System: Unravelling Its Cellular Building Blocks during Development. *J. Cardiovasc. Dev. Dis.* 3, 28. doi:10.3390/jcdd3030028.

Verkerk, A. O., and Wilders, R. (2014). Pacemaker activity of the human sinoatrial node: effects of HCN4 mutations on the hyperpolarization-activated current. *Europace* 16, 384–95. doi:10.1093/europace/eut348.

Visweswaran, R., McIntyre, S. D., Ramkrishnan, K., Zhao, X., and Tolkacheva, E. G. (2013). Spatiotemporal evolution and prediction of [Ca(2+) ]i and APD alternans in isolated rabbit hearts. *J. Cardiovasc. Electrophysiol.* 24, 1287–95. doi:10.1111/jce.12200.

Vonck, K., Boon, P., and Van Roost, D. (2007). Anatomical and physiological basis and mechanism of action of neurostimulation for epilepsy. *Acta Neurochir. Suppl.* 97, 321–8. Available at: http://www.ncbi.nlm.nih.gov/pubmed/17691318 [Accessed October 30, 2017].

Vorobiov, D., Bera, A. K., Keren-Raifman, T., Barzilai, R., and Dascal, N. (2000). Coupling of the muscarinic m2 receptor to G protein-activated K(+) channels via Galpha(z) and a receptor-Galpha(z) fusion protein. Fusion between the receptor and Galpha(z) eliminates catalytic (collision) coupling. *J. Biol. Chem.* 275, 4166–70. doi:10.1074/JBC.275.6.4166.

Wang, H., Han, H., Zhang, L., Shi, H., Schram, G., Nattel, S., et al. (2001). Expression of multiple subtypes of muscarinic receptors and cellular distribution in the human heart.

*Mol. Pharmacol.* 59, 1029–36. Available at: http://www.ncbi.nlm.nih.gov/pubmed/11306684 [Accessed November 19, 2017].

Wang, Y., and Hill, J. A. (2010). Electrophysiological remodeling in heart failure. *J. Mol. Cell. Cardiol.* 48, 619–32. doi:10.1016/j.yjmcc.2010.01.009.

Wickman, K., Nemec, J., Gendler, S. J., and Clapham, D. E. (1998). Abnormal Heart Rate Regulation in GIRK4 Knockout Mice. *Neuron* 20, 103–114. doi:10.1016/S0896-6273(00)80438-9.

Wu, W., and Lu, Z. (2011). Loss of anti-arrhythmic effect of vagal nerve stimulation on ischemia-induced ventricular tachyarrhythmia in aged rats. *Tohoku J. Exp. Med.* 223, 27–33. Available at: http://www.ncbi.nlm.nih.gov/pubmed/21187697 [Accessed April 29, 2014].

Wydeven, N., Marron Fernandez de Velasco, E., Du, Y., Benneyworth, M. A., Hearing, M. C., Fischer, R. A., et al. (2014). Mechanisms underlying the activation of G-protein-gated inwardly rectifying K+ (GIRK) channels by the novel anxiolytic drug, ML297. *Proc. Natl. Acad. Sci. U. S. A.* 111, 10755–60. doi:10.1073/pnas.1405190111.

Xie, X., Lee, S. W., Johnson, C., Ippolito, J., KenKnight, B. H., and Tolkacheva, E. G. (2014). Intermittent vagal nerve stimulation alters the electrophysiological properties of atrium in the myocardial infarction rat model. in *2014 36th Annual International Conference of the IEEE Engineering in Medicine and Biology Society* (IEEE), 1575–1578. doi:10.1109/EMBC.2014.6943904.

Xie, X., Visweswaran, R., Guzman, P. A., Smith, R. M., Osborn, J. W., and Tolkacheva, E. G. (2011). The effect of cardiac sympathetic denervation through bilateral stellate ganglionectomy on electrical properties of the heart. *Am. J. Physiol. Heart Circ. Physiol.* 301, H192-9. doi:10.1152/ajpheart.01149.2010.

Yamakawa, K., Matsumoto, N., Imamura, Y., Muroya, T., Yamada, T., Nakagawa, J., et al. (2013). Electrical vagus nerve stimulation attenuates systemic inflammation and improves survival in a rat heatstroke model. *PLoS One* 8, e56728. doi:10.1371/journal.pone.0056728.

Yang, C.-F., Yu-Chih Chen, M., Chen, T.-I., and Cheng, C.-F. (2014). Dose-dependent effects of isoflurane on cardiovascular function in rats. *Tzu Chi Med. J.* 26, 119–122. doi:10.1016/J.TCMJ.2014.07.005.

Yang, T., Jacobstein, M. D., and Levy, M. N. (1984). Synchronization of automatic cells in S-A node during vagal stimulation in dogs. *Am. J. Physiol.* 246, H585-91. Available at: http://www.ncbi.nlm.nih.gov/pubmed/6720914 [Accessed August 4, 2017].

Yasuhara, O., Matsuo, A., Bellier, J.-P., and Aimi, Y. (2007). Demonstration of choline acetyltransferase of a peripheral type in the rat heart. *J. Histochem. Cytochem.* 55, 287–99. doi:10.1369/jhc.6A7092.2006.

Yeh, Y.-H., Wakili, R., Qi, X.-Y., Chartier, D., Boknik, P., Kääb, S., et al. (2008). Calcium-handling abnormalities underlying atrial arrhythmogenesis and contractile dysfunction in dogs with congestive heart failure. *Circ. Arrhythm. Electrophysiol.* 1, 93–102. doi:10.1161/CIRCEP.107.754788.

Yoo, P. B., Liu, H., Hincapie, J. G., Ruble, S. B., Hamann, J. J., and Grill, W. M. (2016). Modulation of heart rate by temporally patterned vagus nerve stimulation in the

anesthetized dog. *Physiol. Rep.* 4, e12689. doi:10.14814/phy2.12689.

Young, R. J., and Panfilov, A. V (2010). Anisotropy of wave propagation in the heart can be modeled by a Riemannian electrophysiological metric. *Proc. Natl. Acad. Sci. U. S. A.* 107, 15063–8. doi:10.1073/pnas.1008837107.

Yuan, H., and Silberstein, S. D. (2016a). Vagus Nerve and Vagus Nerve Stimulation, a Comprehensive Review: Part I. *Headache J. Head Face Pain* 56, 71–78. doi:10.1111/head.12647.

Yuan, H., and Silberstein, S. D. (2016b). Vagus Nerve and Vagus Nerve Stimulation, a Comprehensive Review: Part II. *Headache J. Head Face Pain* 56, 259–266. doi:10.1111/head.12650.

Zagon, A., and Kemeny, A. A. (2000). Slow hyperpolarization in cortical neurons: a possible mechanism behind vagus nerve simulation therapy for refractory epilepsy? *Epilepsia* 41, 1382–9. Available at: http://www.ncbi.nlm.nih.gov/pubmed/11077451 [Accessed October 24, 2017].

Zang, W.-J., Chen, L.-N., and Yu, X.-J. (2005). Progress in the study of vagal control of cardiac ventricles. *Sheng Li Xue Bao* 57, 659–72. Available at: http://www.ncbi.nlm.nih.gov/pubmed/16344889 [Accessed December 3, 2015].

Zannad, F., De Ferrari, G. M., Tuinenburg, A. E., Wright, D., Brugada, J., Butter, C., et al. (2015). Chronic vagal stimulation for the treatment of low ejection fraction heart failure: results of the NEural Cardiac TherApy foR Heart Failure (NECTAR-HF) randomized controlled trial. *Eur. Heart J.* 36, 425–433. doi:10.1093/eurheartj/ehu345.

Zaza, A., Robinson, R. B., and DiFrancesco, D. (1996). Basal responses of the L-type Ca2+ and hyperpolarization-activated currents to autonomic agonists in the rabbit sino-atrial node. *J. Physiol.* 491 ( Pt 2, 347–55. Available at: http://www.ncbi.nlm.nih.gov/pubmed/8866859 [Accessed February 19, 2018].

Zhan, D.-Y., Du, C.-K., Akiyama, T., Sonobe, T., Tsuchimochi, H., Shimizu, S., et al. (2013). In vivo monitoring of acetylcholine release from cardiac vagal nerve endings in anesthetized mice. *Auton. Neurosci.* 176, 91–94. doi:10.1016/j.autneu.2013.02.014.

Zhang, Y., Chen, A., Song, L., Li, M., He, B., and Chen, Y. (2015). GW26-e2455 Vagal Nerve Stimulation Reverses Cardiac Dysfunction and Subcellular Calcium Handling in Heart Failure Rats After Myocardial Infarction. *J. Am. Coll. Cardiol.* 66, C35. doi:10.1016/j.jacc.2015.06.1162.

Zhang, Y., Ilsar, I., Sabbah, H. N., Ben David, T., and Mazgalev, T. N. (2009a). Relationship between right cervical vagus nerve stimulation and atrial fibrillation inducibility: Therapeutic intensities do not increase arrhythmogenesis. *Hear. Rhythm* 6, 244–250. doi:10.1016/J.HRTHM.2008.10.043.

Zhang, Y., and Mazgalev, T. N. (2011). Arrhythmias and vagus nerve stimulation. *Heart Fail. Rev.* 16, 147–61. doi:10.1007/s10741-010-9178-2.

Zhang, Y., Popovic, Z. B., Bibevski, S., Fakhry, I., Sica, D. A., Van Wagoner, D. R., et al. (2009b). Chronic vagus nerve stimulation improves autonomic control and attenuates systemic inflammation and heart failure progression in a canine high-rate pacing model. *Circ. Heart Fail.* 2, 692–9. doi:10.1161/CIRCHEARTFAILURE.109.873968.

Zhao, M., He, X., Bi, X. Y., Yu, X. J., Gil Wier, W., and Zang, W. J. (2013). Vagal stimulation triggers peripheral vascular protection through the cholinergic anti-inflammatory pathway in a rat model of myocardial ischemia/reperfusion. *Basic Res. Cardiol.* 108. doi:10.1007/s00395-013-0345-1.

# APPENDIX A: LIST OF OTHER PUBLICATIONS

## Appendix A.1 Pro-arrhythmic Effect of Heart Rate Variability during Periodic Pacing

**(Published)**

K. Kulkarni*, **S.W. Lee***, and E.G. Tolkacheva. "Pro-arrhythmic effect of heart rate variability during periodic pacing." Conf Proc IEEE Eng Med Biol Soc. 2016 Aug; 2016:149-152. doi: 10.1109/EMBC.2016.7590662. (***Authors contributed equally to the study**)

## Appendix A.2 Real-Time Closed Loop Diastolic Interval Control Prevents Cardiac Alternans in Isolated Whole Rabbit Hearts

**(Published)**

K. Kulkarni, **S.W. Lee**, R. Kluck, and E.G. Tolkacheva. "Real-Time Closed Loop Diastolic Interval Control Prevents Cardiac Alternans in Isolated Whole Rabbit Hearts." Ann Biomed Eng. 2018 Apr;46(4):555-566. doi: 10.1007/s10439-018-1981-2.

## Appendix A.3 Intermittent electrical stimulation of the right cervical vagus nerve in salt-sensitive hypertensive rats: effects on blood pressure, arrhythmias, and ventricular elctrophysiology

**(Published)**

E.M. Annoni*, X. Xie*, **S.W. Lee**, I. Libbus, B.H. KenKnight, J.W. Osborn, and E.G. Tolkacheva. "Intermittent electrical stimulation of the right cervical vagus nerve in salt-sensitive hypertensive rats: effect on blood pressure, arrhythmias, and ventricular electrophysiology." Physiol Rep. 2015 Aug;3(8). pii: e12476. doi: 10.14814/phy2.12476.

# Appendix A.4 Benchtop optical mapping approaches to study arrhythmias

**(Book Chapter)**

K. Kulkarni*, **S.W. Lee***, and E.G. Tolkacheva. "Benchtop optical mapping approaches to study arrhythmias." Advances and Challenges in the Field of Engineering and Medicine, Elsevier (ISBN: 9780128130681), September 1, 2018 (Published Date). **(*Authors contributed equally)**